

Real time cAMP dynamics in the vicinity of phospholemman in healthy and failing cardiomyocytes

Doctoral Thesis



In partial fulfillment of the requirements for the degree
“Doctor of Philosophy (Ph.D.)”
in the Molecular Medicine Study Programme
at the Georg-August University Göttingen

submitted by

Zeynep Baştuğ-Özel

born in Kassel, Germany

Göttingen, June 2016

Dedication

This dissertation is dedicated

*to my uncle Prof. Turgut Bařtuđ, who always inspired me by
broadening my horizons*

and

*to my beloved parents Hlyya and Ilyas Bařtuđ for their endless
support throughout my life.*

Members of the Thesis Committee

First member of the thesis committee/ supervisor:

Prof. Dr. Viacheslav Nikolaev
Institute of Experimental Cardiovascular Research,
University Medical Centre, UKE, Hamburg

Second member of the thesis committee:

Prof. Dr. Blanche Schwappach
Department of Molecular Biology
University Medical Centre, UMG, Goettingen

Third member of the thesis committee:

Prof. Dr. Walter Stühmer
Department Molecular Biology of Neuronal Signals
Max-Planck-Institute for Experimental Medicine, MPI, Goettingen

Date of Disputation: 15th July 2016

Affidavit

Here I declare that my doctoral thesis entitled

“Real time cAMP dynamics in the vicinity of phospholemman in healthy and failing cardiomyocytes”

has been written independently with no other sources and aids than quoted.

Zeynep Bařtuđ-Özel

Göttingen, June 2016

List of publications

Book chapter:

Zeynep Bastug and Viacheslav O. Nikolaev. Monitoring Real-Time Cyclic Nucleotide Dynamics in Subcellular Microdomains, Chapter 8: 135-146. **Cyclic Nucleotide Signaling (Methods in Signal Transduction Series)** edited by Xiaodong Cheng, May 12, 2015 by CRC Press. ISBN 9781482235562.

Manuscript in preparation:

Zeynep Bastug-Özel, Peter Wright, Davor Pavlovic, Jacqueline Howie, William Fuller, Julia Gorelik, Michael Shattock and Viacheslav O. Nikolaev. Heart failure leads to altered local β_2 -adrenoceptor/cAMP dynamics in the vicinity of phospholemman. 2016

Table of contents

List of Abbreviations	I
List of Figures	II
List of Tables	III
Abstract	IV
1. Introduction	1
1. 1 β -adrenergic signaling pathway.....	1
1. 1. 1 Subtype specific β -adrenergic signaling in the heart.....	1
1. 1. 2 cAMP - one second messenger with several functions	4
1. 1. 3 cAMP compartmentation in the heart - role of Phosphodiesterases and AKAPs..	5
1. 1. 4 Changes of local cAMP signaling and β -AR subtype modules in cardiac hypertrophy	10
1. 2 Differential regulation of the Na/K-ATPase by Phospholemman in the microdomain..	12
1. 2. 1 The cardiac sodium pump	12
1. 2. 2 Cardiac subunit expression and composition of the Na pump.....	13
1. 3 Kinase mediated control of Phospholemman over the Na/K-ATPase	14
1. 3. 1 Phospholemman- FXYP1 Protein.....	14
1. 3. 2 Kinase phosphorylation of Phospholemman	15
1. 4 Changes of PLM/ NKA complex in diseased heart.....	17
1. 5 Imaging local cyclic nucleotide dynamics	18
1. 5. 1 Fundamentals of Förster/Fluorescence resonance energy transfer	18
1. 5. 2 cAMP sensitive FRET Biosensors	19
1. 6 Aims of the project	21
2. Materials and Methods	22
2. 1 Materials	22
2. 1. 1 Cells	22
2. 1. 2 Plasmids.....	22
2. 1. 3 Bacteria strains.....	22
2. 1. 4 Animals	22
2. 1. 5 Oligonucleotides	23
2. 1. 6 Chemicals.....	24
2. 1. 7 Cell culture	26

2. 1. 8 Enzymes and Kits.....	26
2. 1. 9 Antibodies.....	27
2. 1. 10 Microscope devices and software	27
2. 1. 11 General devices and software	28
2. 1. 12 Other materials	28
2. 1. 13 Buffers and solutions	29
2. 2 Methods.....	31
2. 2. 1 Generation of the recombinant plasmids and adenoviral construction of E1-camps and PLM-E1 biosensors	31
2. 2. 2 PCR- Polymerase chain reaction.....	31
2. 2. 3 Gel electrophoresis, DNA purification and quantification.....	31
2. 2. 4 Gel electrophoresis, DNA purification and quantification.....	32
2. 2. 5 Ligation.....	32
2. 2. 6 Transformation of competent bacteria cells	33
2. 2. 7 Cloning the _{human} PLM-E1 FRET biosensor based on the pcDNA3 Epac1-camps construct	34
2. 2. 8 Cloning the _{canine} PLM-E1 FRET biosensor based on the PLM-YFP construct	34
2. 2. 9 Generation of the adenoviral constructs Epac1-camps, _{human} PLM-E1 and _{canine} PLM-E1	35
2. 2. 10 Calculating the multiplicity of infection and adenoviral transduction of ARVM ...	37
2. 2. 11 Cell culture and transfection of the HEK293A cell line	37
2. 2. 12 SDS-PAGE and Western Blot analysis	38
2. 2. 13 Co-immunoprecipitation.....	41
2. 2. 14 Cell surface biotinylation.....	42
2. 2. 15 Generation of a HEK293A cell line stably expressing PLM-E1.....	42
2. 2. 16 Ouabain sensitive ⁸⁶ Rb uptake measurements	43
2. 2. 17 Immunofluorescence	44
2. 2. 18 Heart failure rat model: Myocardial Infarction.....	44
2. 2. 19 ARVM Isolation by Langendorff perfusion.....	44
2. 2. 20 FRET measurements of ARVMs transduced with PLM-E1 and E1-camps.....	46
2. 2. 21 Statistics.....	47
3. Results	48
3. 1 Generation of the first version of the PLM-E1 FRET Biosensor.....	48
3. 1. 1 Expression and functional analysis	49
3. 1. 2 Localization analysis.....	50

3. 2	Generation of the optimized PLM-E1 FRET Biosensor and the adenoviral construct	.51
3. 2. 1	Sensor characterization - expression	52
3. 2. 2	Sensor characterization - localization	53
3. 2. 3	Sensor characterization - function	56
3. 3	Comparative FRET analysis of E1-camps and PLM-E1 transduced ARVMs	58
3. 3. 1	Effects of individual β -AR subtypes	58
3. 3. 2	PDE Profiles in PLM-E1 and E1-camps transduced ARVMs	59
3. 3. 3	ANP/cGMP mediated PDE3 response in the PLM/NKA microdomain	61
3. 3. 4	FRET measurements in PLM-E1 and E1-camps transfected ARVMs	63
3. 3. 5	Alterations in local PDE dependent cAMP regulation in the PLM/NKA microdomain	63
3. 3. 6	cAMP degrading PDE3 pools in the PLM/NKA microdomain are delocalized in the hypertrophied heart	65
4.	Discussion	67
4. 1	Challenges in generating novel PLM-E1 FRET biosensors with correct structural and functional properties	67
4. 2	Comparative FRET analysis of healthy ARVMs expressing adenoviral PLM-E1 and E1-camps biosensors reveal differentially regulated local β -adrenergic signaling	69
4. 2. 1	Restricted cAMP diffusion to the NKA/PLM complex via basal activity of phosphodiesterases	69
4. 2. 2	Locally confined β_2 -AR mediates cAMP signaling pathway proximal to the PLM/NKA complex	70
4. 2. 3	Critical PDE3-dependent regulation of β_2 -AR mediated cAMP in the vicinity of PLM	71
4. 3.	Alterations of β_2 -AR control over subsarcolemmal PLM microdomain through localized PDE2/PDE3 subsets in ARVM with chronic heart failure	73
5.	Conclusion and Outlook	75
6.	Bibliography	77
7.	Acknowledgements	93

List of Abbreviations

AC	adenylyl cyclase
AKAP	A kinase anchoring protein
Akt	protein kinase B
AMC	aged matched control
ANP	atrial natriuretic peptide
ARVM	adult rat ventricular myocyte
Bay	BAY 60-7550
β -Arr	β -arrestin
β_1 -AR	β_1 -adrenergic receptor
β_2 -AR	β_2 -adrenergic receptor
Ca^{2+}	calcium ion
CaMKII	Ca^{2+} -calmodulin-dependent protein kinase
cAMP	3',5'-cyclic adenosine monophosphate
Cav	caveolin
CFP	cyan fluorescent protein
cGMP	3',5'-cyclic guanosine monophosphate
CGP	CGP-20-712A
CHF	congestive heart failure
Cilo	cilostamide
CNGC	cyclic nucleotide gated channel
CREB	cAMP response element binding (protein)
ECC	excitation contraction coupling
Epac	exchange protein directly activated by cAMP
FRET	Förster (fluorescence) resonance energy transfer
for	forward
FXVD	consensus motif Proline-Phenylalanine-x-tyrosine-Aspartic acid
GC	guanylyl cyclase
G_i	inhibitory G-protein
G_s	stimulatory G-protein
GFP	green fluorescent protein
GPCR	G-protein coupled receptor
GRK	G-protein coupled receptor kinase
GTPase	guanosine triphosphatase
HCN2	hyperpolarization-activated cyclic nucleotide-gated channel 2
HEK cell	human embryonic kidney cell
I-1	inhibitor-1

IBMX	3-Isobutyl-1-methylxanthine
ICI	ICI 118,551
IP3	inositol-1,4,5-triphosphate
Iso	isoproterenol/ isoprenaline
K ⁺	potassium ion
K _m	Michaelis-Menten constant
KO	knockout
LTCC	L-type calcium channel / Ca _v 1.2
MI	myocardial infarction
Na ⁺	sodium ion
NCX	sodium-calcium exchanger
NKA	sodium-potassium ATPase / sodium pump
NO	nitric oxide
PDE	phosphodiesterase
PI3Kγ	phosphoinositide-3 kinase gamma
PKA	Protein kinase A
PKC	Protein kinase C
PKG	cGMP dependent protein kinase
PLM	phospholemman
PLN	phospholamban
PLCε	phospholipase C epsilon
PP1	protein phosphatase 1
Rap	Ras-related protein
Rb	rubidium
rev	reverse
Roli	rolipram
RT	room temperature
RyR2	ryanodine receptor 2
Ser	serine residue
SERCA2a	sarcoplasmic/endoplasmic reticulum Ca ²⁺ ATPase 2a
SICM	scanning ion conductance microscopy
SR	sarcoplasmic reticulum
SU	subunit
Thr	threonine
Tnl	troponin I
V _{max}	maximal velocity (maximal reaction rate)
YFP	yellow fluorescent protein

List of Figures

Figure 1. Schematic representation of the cellular cAMP signaling cascade	2
Figure 2. Cartoon describing β_1 ARs and β_2 ARs signaling pathways in cardiomyocytes	3
Figure 3. Cartoon depicting the differential role of cardiac cAMP in confined microdomains leading to differential phosphorylation of PKA targets	5
Figure 4. A-kinase anchoring proteins (AKAPs) controlling subcellular cAMP microdomains in the heart	9
Figure 5. Alterations of local cAMP signaling in compensated hypertrophy and heart failure	12
Figure 6. NKA - an integral player in the 'fight-or-flight' response	12
Figure 7. Structure of the Na/K-ATPase	13
Figure 8. Amino acid sequence of currently known mammalian FXYD proteins	15
Figure 9. Phosphorylation of phospholemman regulates sodium pump activity	16
Figure 10. The principles of FRET instancing the CFP and YFP pair	19
Figure 11. Cartoon showing means to determine intracellular cAMP dynamics	20
Figure 12. The co-Immunoprecipitation method	41
Figure 13. Layout of the FRET imaging setup	47
Figure 14. PLM-E1 construct in pcDNA3.0 vector	48
Figure 15. Expression, function and localization of PLM-E1 in HEK 293 cells	49
Figure 16. Co-immunoprecipitation	50
Figure 17. Design of the optimized PLM-E1 biosensor construct	52
Figure 18. Expression of the PLM-E1 sensor	53
Figure 19. Cell surface biotinylation of PLM-E1 transduced ARVM	53
Figure 20. Co-localization of PLM-E1 with the sodium pump	54
Figure 21. Association of PLM-E1 with the sodium-potassium pump α_1 subunit	55
Figure 22. Inhibition of NKA activity by PLM-E1	56
Figure 23. Sensor function in PLM-E1 transduced ARVMs	56
Figure 24. Sensitivity of E1-camps and PLM-E1 to adrenergic stimuli	57
Figure 25. Predominant control of β_2 -AR over the PLM/NKA microdomain	59
Figure 26. Significant PDE2 contribution to basal cAMP degradation in the vicinity of PLM	60
Figure 27. PDE3 pool in the vicinity of PLM confines β_2 -AR mediated cAMP signals to the PLM/NKA microdomain	61

Figure 28. Co-localization of the PDE3A isoform with the PLM microdomain	62
Figure 29. ANP induced PDE3 inhibition in ARVM results in high levels of β_2 -AR/cAMP in the PLM/NKA microdomain	62
Figure 30. Contributions of individual PDEs to cAMP hydrolysis after β_2 -AR stimulation in AMC and MI cardiomyocytes	64
Figure 31. β_2 -AR effects in AMC vs. MI cells	65
Figure 32. Confocal microscopy analysis of PDE3 localization	66
Figure 33. Cartoon showing highly confined basal cAMP dynamics and a distinct β_2 -cAMP effect in the PLM microdomain of ARVMs	76
Figure 34. Cartoon demonstrating the change in local cAMP dynamics at the cardiac PLM microdomain	76

List of Tables

Table 1. Cardiac PDE enzyme specifications and kinetic properties	6
Table 2. Primary antibodies	27
Table 3. Secondary antibodies	27
Table 4. Ingredients of the used gels for Western Blot analysis at King's College London	39
Table 5. Ingredients of the used gels for Western Blot analysis in UMG, Göttingen	40
Table 6. Phenotyping of aged matched control and 16 weeks post MI hearts	63

Abstract

The ubiquitous second messenger 3',5'-cyclic adenosine monophosphate (cAMP) is a crucial regulator of cardiac function and disease. It is known that cAMP signaling is mediated by discrete functional microdomains each containing a specific subset of differentially localized receptors, protein kinases and specific phosphodiesterases (PDEs). Cardiac phosphodiesterases (PDE1-5; PDE8 and 9) hydrolyze cyclic nucleotides, each with different selectivity and affinity for their substrates cAMP and 3',5'-cyclic guanosine monophosphate (cGMP). In one of these microdomains, the phosphorylation of the FXVD1 protein called Phospholemman (PLM), the negative regulator of Na⁺/K⁺-ATPase (NKA), via PKA or PKC leads to an increase of NKA activity and its sodium affinity, thereby lowering intracellular sodium levels and hence limiting cardiac inotropy. By obstructing high sodium levels during adrenergic stimulation it simultaneously favors calcium extrusion via the sodium-calcium exchanger (NCX). This mechanism may prevent calcium-overload, hypertrophy and triggered arrhythmias during cardiac stress. Interestingly, PLM expression is known to be altered in cardiomyocytes from postinfarcted rat hearts which results in depressed NKA activity. However, knowledge about the dynamics of cAMP pool coupled to PLM phosphorylation and the interactions of β -adrenergic receptors (β -AR) with individual cardiac PDE subtypes forming this important microdomain as well as their alterations in cardiac disease is insufficient. To investigate these questions, we developed a Förster Resonance Energy Transfer (FRET)-based PLM targeted cAMP biosensor PLM-E1. It can be used to precisely measure cAMP dynamics and to understand the regulatory mechanisms behind a possible local restriction of β -AR mediated cAMP signals in the PLM/NKA microdomain of adult rat ventricular myocytes (ARVMs).

Using functional ⁸⁶Rubidium-flux measurements in a PLM-E1 expressing stable HEK cell line, co-immunoprecipitation analysis of PLM-E1 transfected ARVMs and confocal microscopy, we showed that the newly developed PLM-E1 biosensor is associated with the α_1 subunit (SU) of the NKA. The obtained FRET results were compared with measurements in the bulk cytosol performed using the cytosolic E1-camps sensor. It is well known that PDE2 activity constitutes a relatively low proportion of total cardiac PDE activity in the rat heart. However, our findings suggest that the actions of PDE2 regulate cAMP signals in the PLM microdomain in a compartmentalized manner at basal state (without prestimulation with β -AR agonists). Using the targeted FRET biosensor PLM-E1 in ARVMs we further analyzed the subtype specific β -AR control of cAMP in the PLM/NKA domain. Interestingly, the β_2 -AR showed a distinct control over the PLM microdomain during adrenergic stimulation. Local cAMP-FRET responses to PDE3 inhibition were well detectable in the PLM/NKA microdomain and showed a significant effect of this PDE in confining β_2 -AR signals to the

vicinity of PLM upon adrenergic stimulation. Focusing on β_2 -AR stimulated cAMP pools in the PLM/NKA microdomain, we observed alterations of FRET responses in ARVMs from animals with chronic heart failure induced by myocardial infarction. These failing cells showed a significant loss of the PDE3 responses upon β_2 -AR stimulation and an almost compensating increase in PDE2 dependent control of cAMP in the vicinity of PLM. Strikingly, in this disease model the overall response of β_2 -AR to adrenergic stimulation in the PLM microdomain was reduced to a level comparable to the bulk cytosol.

In this study, the efficiency of the targeted PLM-E1 biosensor and its potential for real time monitoring of compartmentalized cAMP signaling in adult rat ventricular myocytes was successfully demonstrated. In addition, the practicability of the tagged biosensor in ARVMs in a cardiac disease model was confirmed and analyzed. In particular, our data show that real time dynamics of cAMP in the PLM/NKA microdomain are significantly different from cytosolic cAMP in terms of local PDE regulation and direct receptor-mediated control of the microdomain. In heart failure, these mechanisms are seriously altered which might explain impaired regulation of PLM in disease, bringing out a potential therapeutic target.

1. Introduction

1. 1 β -adrenergic signaling pathway

1. 1. 1 Subtype specific β -adrenergic signaling in the heart

As classic members of heptahelical G protein-coupled receptors (GPCRs), β -adrenergic receptors (β -ARs) are important mediators of sympathetic nervous system control. They are functionally involved in various processes such as metabolic regulation¹, immune reactions², growth control³, vascular smooth muscle cell contraction and relaxation⁴ as well as cell survival and apoptosis⁵. The textbook paradigm for β -AR signaling in the heart is the regulation of cardiac function via their activation by catecholamines; the sympathetic stimulation increases heart rate (positive chronotropic effect), myocardial contractility (positive inotropic effect) and accelerates relaxation (positive lusitropic effect)⁶. There are three different types of β -ARs expressed in the mammalian heart: β_1 -, β_2 - and β_3 -ARs. The β_1 -AR is found primarily in the heart and comprises 75-80% of the cardiac β -ARs⁷. This receptor is coupled to stimulatory G-proteins (G_s) which in turn activate adenylyl cyclase (AC), an enzyme responsible for the generation of the second messenger 3'-5'-cyclic adenosine monophosphate (cAMP) from ATP. Increasing cAMP levels activate cAMP-dependent protein kinase (PKA)⁸, cyclic nucleotide gated channels (CNGCs)⁹ and the exchange protein directly activated by cAMP (Epac)^{10,11} (Figure 1). The latter seems to have prohypertrophic effects upon chronic β_1 -AR stimulation, being a PKA independent downstream effector of sympathetic stimulation. Epac expression is increased in heart failure, where Epac activates Rap (a small GTPase) and induces hypertrophy in a cAMP-dependent but PKA-independent manner¹². In the heart, cAMP signal transduction is mainly mediated through PKA with its two regulatory (R)- and two catalytic (C)-subunits⁸. When cardiac cAMP binds the R-subunits, the C-subunits dissociate from the R-subunits¹³, which leads to a phosphorylation of downstream targets critical for the regulation of excitation contraction coupling (ECC). During cardiac ECC downstream effector proteins such as troponin I, the L-type Ca^{2+} channel (LTCC), phospholamban (PLB)¹⁴ and phospholemman (PLM) as the inhibitory protein of the sodium potassium pump (NKA)¹⁵ serve as PKA substrates, resulting in greater contractility and acute cardiac performance thereby facilitating diastolic function of the heart.

Contraction force is primarily controlled by sympathetic stimulation via β_1 -AR cAMP and elevated intracellular Ca^{2+} levels upon phosphorylation of voltage-gated LTCC, whereas the lusitropic effect of PKA is mediated by increased Ca^{2+} reuptake into the sarcoplasmic reticulum (SR) consequent to PLB phosphorylation and increased SERCA2a activity¹⁶. As an important part of the sympathetic 'fight or flight' response the NKA pump activity is upregulated by the PKA phosphorylation of PLM when sodium is pumped out of the cell in

response to elevated intracellular Na^+ levels through the Ca^{2+} transient driven Na^+ entry via the $\text{Na}^+/\text{Ca}^{2+}$ exchanger (NCX)¹⁷ (see section 1. 2. 1). Supported by several investigations about the effects of Ca^{2+} /calmodulin-dependent protein kinase II (CaMKII) upon β -AR stimulation, there is a great possibility that excessive β -AR stimulation is detrimental because of CaMKII mediated hyperphosphorylation of Ca^{2+} handling proteins (e.g. ryanodine receptor, RyR2, phosphorylation leading to diastolic SR Ca^{2+} leak)¹⁸.

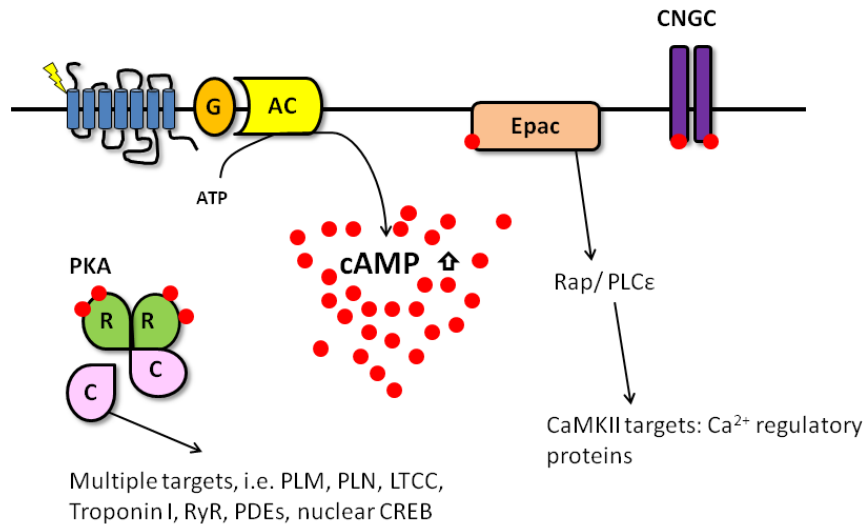


Figure 1. Schematic representation of the cellular cAMP signaling cascade. After stimulation of a GPCR, cAMP production is accelerated via G protein dependent AC activation. cAMP has three different downstream effectors: PKA, Epac and CNGCs. The catalytic (C) subunits of the PKA dissociate from the regulatory (R) subunits and phosphorylate several downstream targets such as PLM, PLN, LTCC, Troponin I, RyR, PDEs and CREB. Epac and the small GTPases Rap, in response to cAMP, activate CaMKII through phospholipase C ϵ (PLC ϵ) to regulate cardiac Ca^{2+} handling proteins. CNGCs show an increase in ion currents upon cAMP binding to these channels.

The β_2 -AR comprises 20–25% of cardiac β -ARs⁷ and is expressed in several other tissues such as in the lung¹⁹ and kidney²⁰. There is growing evidence for highly localized β_2 -AR dependent AC/cAMP/PKA signaling²¹. Previous studies in cardiac myocytes²²⁻²⁴ have shown an inotropic effect of β_2 -ARs mediated cAMP without having a direct influence on the phosphorylation status of PKA targets important for cardiac contraction, like PLB. It was suggested that β_2 -AR stimulation causes greater stimulation of the G_s -AC system and has a greater efficacy compared to the β_1 -AR²⁵⁻²⁷. Not only for this reason, cardiac β_2 -AR mediated cAMP signal transduction has been described to be quantitatively and qualitatively different from β_1 -AR induced signals²⁸ and markedly altered in heart failure²⁹. However, in addition to G_s , the β_2 -AR couples to pertussis toxin - sensitive inhibitory G protein (G_i)²².

Cehn-Izu et al. suggested, that the local β_2 -AR signaling character is G_i dependent; the joint signaling of β_2 -AR to both G_s - and G_i -proteins leads to a highly localized β_2 -AR signaling pathway to modulate sarcolemmal L-type Ca^{2+} channels in rat ventricular myocytes³⁰. Through the additional signaling pathway, the β_2 -AR-to- G_i branch might protect cells from

apoptosis induced by sustained sympathetic G_s mediated stimulation³¹. One theorized, that the switch of the β_2 -AR to G_i coupled survival pathway via phosphoinositide 3-kinase (PI3K)/Protein Kinase B (Akt) may be caused by PKA phosphorylation of the receptor and serve as a protective mechanism against catecholamine cardiotoxicity³². In heart failure, β_1 -ARs start to get desensitized via ligand stimulated phosphorylation by associated G protein-coupled receptor kinases (GRKs)³³. GRKs prepare the activated receptor for internalization via the recruitment of β -arrestin (β -Arr)³⁴, and the receptor loses its functional quality in addition to their desensitization by GRKs in spite of the increased circulation of catecholamines³⁵⁻³⁷. On the other hand, β_2 -ARs may support the failing/aging heart by enhancing myocardial contractility^{38,39} (Figure 2).

The β_3 -AR is found primarily in adipose tissue where it is coupled to G_s -proteins⁴⁰, and little in the heart. Previous studies in β_1/β_2 -AR-KO mice have suggested, that the Isoprenaline (non-selective β -AR agonist, Iso) induced β_3 -AR signaling leads to very modest cardiac contractility and seems to desensitize more rapidly than does signaling by either the β_1 AR or the β_2 AR⁴¹. Conversely, the cardiac-restricted overexpression of β_3 -AR in a transgenic mouse model showed enhanced cardiac contractility after treatment with a selective β_3 -AR agonist⁴². Reasons for disparities in β_3 -AR effects may be attributed to the use of different compounds and different transgenic animal models. It has been reported that β_3 AR couples to G_s - and G_i -proteins in diverse cell types^{43,44}. Recently, it was also demonstrated that cardiomyocyte expression of this receptor is increased in rodent and human failing heart and it might be cardioprotective by its coupling to G_i and nitric oxide synthase-dependent NO/soluble guanylyl cyclase/cGMP pathway^{45,46}.

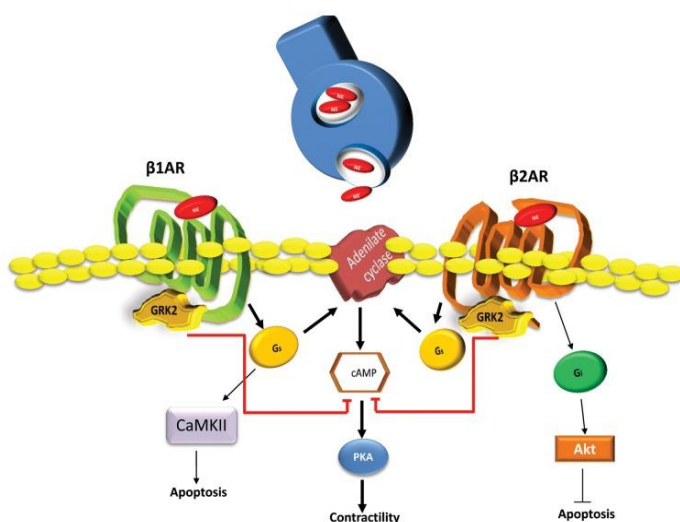


Figure 2. Cartoon describing β_1 -ARs and β_2 ARs signaling pathways in cardiomyocytes. G_s coupled β_1 -ARs activates PKA through the production of cAMP resulting in positive chronotropic and inotropic effects. Secondly, activated CaMKII can induce apoptosis with increased catecholamine stimulation. In contrast, anti-apoptotic signaling through Akt is mediated by G_i dependent β_2 -ARs. Both β -ARs are regulated by GRK2 leading to receptor down-regulation in case of chronic activation. Taken from Cannavo et al.²⁹.

1. 1. 2 cAMP - one second messenger with several functions

Discovered in 1958 by Earl W. Sutherland and co-workers⁴⁷ cAMP remains to be interesting for many researchers as a universal second messenger that produces different physiological effects depending on cell nature and composition. cAMP plays central roles in memory formation⁴⁸ and mid brain system⁴⁹, the secretion of insulin from pancreatic cells^{50,51}, regulation of gene expression⁵² and metabolism⁵³, immune reactions⁵⁴ and most important for this work: cardiovascular regulation⁵⁵. These effects can even be opposing in different cell types. For example, cAMP increases cardiac cell contractility but relaxes airway and vascular smooth muscle cells⁵⁶. Moreover, studies on rat ventricular myocytes provided first insights into the idea of the spatially segregated cAMP signals organized in microdomains containing several proteins as molecular components of the signaling pathway (see section 1. 1. 3). Briefly, cardiomyocytes stimulated by the β -adrenergic agonist isoprenaline (Iso) or by prostaglandine E₁ led to comparable amounts of synthesized cAMP resulting in PKA activation in both cases, but only Iso treated cells augmented cardiomyocyte contractility. The conclusion was that prostaglandine E₁ mediated cAMP showed no classical substrate phosphorylation (especially at cardiac troponin I) due to the activation of different pools of PKA within the cardiomyocyte⁵⁷. Likewise, cAMP signals elicited from glucagon receptors were demonstrated as not being involved in cardiac contractility in contrast to cAMP generated through β -ARs after Iso stimulation, which was another example of functionally distinct AC/cAMP/PKA microdomain⁵⁸. The idea that not all cAMP pools and its respective downstream effects in the heart are equal, was established and demonstrated in several other studies on cardiac myocytes^{23,59,60}. As mentioned above, there are differentially localized PKA subsets of PKA type I and PKA type II⁶¹, defined by their varying subunit isoforms and by differential binding to a variety of A-kinase anchoring proteins (AKAPs). This anchor proteins can also bind phosphodiesterases (PDEs), enzymes responsible for cAMP degradation, ensuring localized complexes and specific physiological responses to any given cAMP stimulus⁶². Next to the idea that cAMP has physical membrane barriers formed by different kind of organelles inside the cell^{63,64}, PDEs have a key role in shaping intracellular gradients of cAMP and disabling random cAMP diffusion⁶⁵.

Most studies were focused on comparing cAMP dynamics between soluble and particulate fractions^{66,67}, but it was also clear that the β -AR-AC-cAMP-PKA signaling pathway is not uniformly active at the plasma membrane either. For example, there are differences in lipid raft (cholesterin and sphingolipid rich planar domains) and non-lipid raft membrane domains^{10,68}. Caveolae (omega shaped membrane invaginations) represent a special type of cardiac lipid rafts, containing caveolin (Cav) proteins as main components. These membrane domains have been shown to harbor β -AR-cAMP pathway components important for Ca²⁺ cycling^{69,70} forming, for example, a macromolecular complex comprised of receptor and L-

type Ca^{2+} channel (LTCC) in the heart⁷¹. Furthermore, studies demonstrated that such gradients of cAMP specifically derived from β_2 -ARs²⁹ activate a subset of protein kinase A molecules anchored in proximity to T-tubules⁷² (large sarcolemmal invaginations at Z-lines of cardiomyocytes). Cardiac LTCCs are proposed to be a sarcolemmal substrates of PKA^{73,74} and presumably organized in cardiac T-tubules together with NKA and NCX⁷⁵⁻⁷⁸. There is an increasing body of evidence that PLM is a central player in the sympathetic response by kinase dependent inhibition of the NKA activity and indirect regulation of the cellular calcium load and inotropy of the heart¹⁵. In this context, elements important for the local tailoring of cAMP concentrations to distinct compartments and protection of possible substrates against inappropriate PKA phosphorylation within a cell are pointed out in the next section.

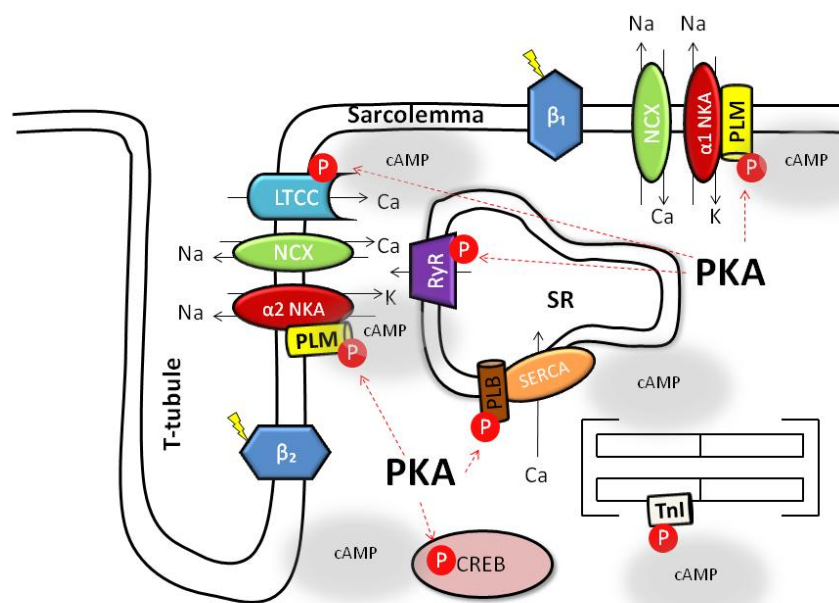


Figure 3. Cartoon depicting the differential role of cardiac cAMP in confined microdomains leading to differential phosphorylation of PKA targets. During the action potential, Ca^{2+} flows into the cell, which triggers Ca^{2+} dependent Ca^{2+} release from the SR facilitating Ca^{2+} binding to troponin I (TnI) at myofilaments and contraction¹⁵¹. The NKA is found in both sarcolemma and T-tubules regulating cellular Ca^{2+} and Na^{+} concentrations functionally linked to the NCX, which predominantly removes intracellular Ca^{2+} (forward mode)¹⁷² during diastole. Upon β -AR stimulation, cAMP activates PKA, which phosphorylates several downstream targets important for the cardiac excitation contraction coupling such as LTCC, RyR2, PLN, PLM and TnI, thereby increasing chronotropy, inotropy and lusitropy. The different Ca^{2+} and Na^{+} handling proteins are part of cAMP microdomains containing additional pools of PKA and PDEs (not shown here for simplicity).

1. 1. 3 cAMP compartmentation in the heart - role of Phosphodiesterases and AKAPs

The compartmentation of cAMP derived signals in functional microdomains and their specific effects are widely recognized and demonstrated in different kinds of cells over the years. Most remarkable attempt showing local PDE activity in distinct intracellular microdomains was by whole cell patch clamp recordings which indicated a local PDE dependant cAMP pool

involved in β -AR stimulation of LTCC currents in frog ventricular myocytes⁷⁰. Aberrant cAMP signals and changes in highly regulated microdomains may occur in diseased cells and contribute hypertrophy and heart failure⁷⁹. For this reason it is of extreme importance to maintain the architecture of positively and negatively cAMP modulating and scaffolding proteins in the given microdomains.

PDEs as cAMP degrading enzymes catalyze its hydrolysis and are critical for shaping the cAMP pools in mammalian cells^{65,80}. This enzyme superfamily is comprised of 11 families and 70 different isoenzymes, which are encoded by 21 genes⁸¹. Cardiac myocytes express several PDE families: PDEs 1-5, 8 and 9^{82,83}. PDEs are categorized in their affinity and catalytic rates, in which PDEs 1-3 can hydrolyze both cAMP and 3',5'-cyclic guanosine monophosphate (cGMP), while PDE4 and 8 are cAMP specific and PDE5 and 9 show a high selectivity for cGMP. Besides their kinetics, various PDE enzymes have differences in regulatory properties and sensitivity to inhibitors⁸⁴ (see Table 1).

Table 1. Cardiac PDE enzyme specifications and kinetic properties; Km = Michaelis-Menten constant, Vmax = maximal velocity (maximal reaction rate), - no information available; modified from Eiki Takimoto⁷³

PDE Isoenzyme		Km (μ M)	
		cAMP	cGMP
PDE1	Ca ²⁺ /CaM regulated, dual specificity	PDE1A: 73-120 PDE1B: 10-24 PDE1C: 0.3-1.2	PDE1A: 2.6-5 PDE1B: 1.2-5.9 PDE1C: 0.6-2.2
PDE2	cGMP stimulated, dual specificity	30-50	10-30
PDE3	cGMP inhibited, dual specificity	0.02-0.15	0.18
PDE4	cAMP-specific	2.9-10	-
PDE5	cGMP-specific	-	1.0-6.2
PDE8	cAMP-specific	0.15	-
PDE9	cGMP-specific	-	0.17-0.39

PDE inhibitors are commonly used to characterize subcellular contributions of PDEs to cAMP hydrolysis and spatio-temporal dynamics^{72,85}, dissecting their key roles in shaping intracellular microdomains (see section 1.4).

In particular, PDE1 has three subfamilies (PDE1A, PDE1B and PDE1C). PDE1 enzyme activity is increased via Ca²⁺/calmodulin binding at the regulatory domain in the N-terminus, PDE1 is also often referred to as the Ca²⁺/calmodulin stimulated PDE⁸⁶. Having different affinities for both cyclic nucleotides (dual substrate specificity), PDE1 isoenzymes are believed to be important in the crosstalk between the second messenger Ca²⁺ and cyclic nucleotide signaling⁸⁷. Albeit PDE1 has been suggested to play a role in cardiac disease^{88,89},

there is still a need for potent selective PDE1 inhibitors to better investigate a possible cardioprotective effect.

PDE2 is another dual specific enzyme family with three cardiac isoforms (PDE2A1-3). cGMP can enhance the catalytic activity of PDE2 through binding to a special regulatory domains at the N-terminus, referred to as GAF domains⁹⁰ (found in: cGMP-specific phosphodiesterases, Adenylyl cyclases and FhIA). Via an allosteric binding mechanism, this leads to a direct increase of cAMP hydrolysis (positive cGMP/cAMP crosstalk). Mongillo and co-workers have found that PDE2 is strongly involved in cGMP/cAMP interplay after β -adrenergic stimulation⁹¹. Using real time Fluorescence Resonance Energy Transfer (FRET)-based imaging in neonatal rat cardiomyocytes, they showed that 'cGMP activated' PDE2 modulation of cAMP was potentiated upon cGMP production via the β_3 -AR/NOS/cGMP pathway which exhibited a negative inotropic effect after beta-AR stimulation in neonatal rat cardiomyocytes⁹¹. Furthermore, studies in ventricular myocytes of guinea pigs⁹² and ARVMs⁹³ have supported their findings that PDE2 is highly membrane associated.

In contrast to PDE2, cGMP inhibits the hydrolyzing activity of PDE3 for both cyclic nucleotides. This competitive inhibition provides a means by which an increase in cGMP may lead to an increase in cAMP and its differential effects in spatially distinct subcellular domains (negative cGMP/cAMP crosstalk)⁹⁴. PDE3 comprises two subfamilies PDE3A and PDE3B. Although both are present in cardiomyocytes, PDE3A is the main subfamily⁹⁵ responsible for cardiac hypertrophy⁹⁶ and contractility which is typically augmented by PDE3 inhibition⁹⁷. PDE3 are described to be in the cytosolic fractions as well as membrane bound isoenzymes, depending on the isoform PDE3A1 (membrane and soluble), A2 or A3 (both are only membrane bound)^{98,99}. However, PDE3A is found mainly at the SR/endoplasmic reticulum rather than at the plasma membrane¹⁰⁰. PDE3 is a dual specific enzyme and displays high affinity for both cAMP and cGMP, having higher catalytic activity for cAMP than for cGMP¹⁰¹. A decrease in PDE3 expression is thought to have adverse effects on the heart as it promotes cardiomyocyte apoptosis and impairs cardiac dysfunction induced by chronic pressure overload¹⁰². PDE3 and PDE4 contribute the majority of the cAMP catabolism in cardiomyocytes⁶⁵.

PDE4, the cAMP specific PDE, is the most diverse PDE family with four encoding genes (PDE4A, B, C and D) and around 20 splice variants¹⁰³. In the mammalian heart, three out of four genes (PDE4A, B and D) encode for PDE4 isoenzymes^{102,104}. The N-terminal regulatory domain determines the subcellular localization of the PDE4 isoforms¹⁰⁵ and at the same time makes them essential players in cAMP compartmentation in cardiomyocytes. With the N-terminal regulatory/localization domain PDE4 variants are able to form local cAMP signaling hubs by binding to scaffolding proteins such as β -Arr or AKAPs and through direct interaction with β -AR receptors. For example, a fraction of PDE4B is colocalized with the LTCC along T-

tubules in the mouse heart, thereby controlling the β -AR stimulation of the L-type Ca^{2+} current and the phosphorylation of the LTCC via PKA¹⁰⁶. There is evidence that the PDE4D3 isoform and the PKA reside in the same signaling complex through their association with the muscle-selective A-kinase anchoring protein (mAKAP), which in turn enhances the PDE activity, forming a unique negative feedback control over rising of local cAMP in cardiomyocytes¹⁰⁷. Moreover, PDE4D3 was found in the cardiac RyR2/calcium-release-channel complex¹⁰⁸. Playing a key role in cellular desensitization mechanism for GPCRs (see section 1.1.1), PDE4D5 has been demonstrated to recruit β -Arr to the β_2 -AR upon receptor stimulation^{109,110}. The PDE4D8 isoform was reported to form signaling complexes with β_1 -ARs until binding of an agonist¹¹⁰. Phosphoinositide 3-kinase γ (PI3K γ) is another newly identified regulator of PDE action. It controls local β_2 -AR-cAMP responses by activation of the cardiac PDE4A, PDE4B and PDE3A isoforms through PKA. By doing this PI3K γ recruits the regulatory subunit of PKA to and the PDE isoforms, respectively, to the functional signaling complex. The absence of PI3K γ showed hyperphosphorylation of the L-type calcium channel ($\text{Ca}_v1.2$) and phospholamban which resulted in proarrhythmic changes¹¹¹. PDE5 is one of the most intensively studied enzymes for cGMP hydrolysis. PDE5 inhibitors show some benefits in hypertrophy and heart failure^{112,113}. There are clinically used PDE5 inhibitors officially approved for treatment of erectile dysfunction (PDE5A resides in the corpus cavernosum¹¹⁴) and pulmonary hypertension¹¹⁵. The three known isoforms PDE5A1-3 also contain a regulatory GAF domain with binding sites for cGMP like PDE2 does, but this leads to a stronger increase in cGMP catalytic activity in contrast to PDE2⁸⁴. One other difference between both cGMP hydrolyzing PDEs is the subcellular distribution (cGMP compartmentation); Castro et al. demonstrated that PDE5 controls cGMP originating from the particulate pool of guanylyl cyclase (GC), whereas PDE2 controls cGMP in the soluble fraction⁹³. PDE8 is another cAMP-specific PDE in the mammalian myocardium, which is encoded by two genes (PDE8A and PDE8B). PDE8A is highly expressed in testis and ovary of mouse and human cells^{116,117}, whereas PDE8B is found to be expressed specifically in thyroid glands¹¹⁸ in humans. PDE8 is distinguished from other cAMP specific proteins in the heart (PDE4) by its insensitivity to most of the PDE inhibitors including Isobutyl-1-methylxanthin (IBMX), however it can be inhibited by dipyridimole¹¹⁶. In the heart, PDE8A can be phosphorylated by the PKA holoenzyme¹¹⁹, similar to PDE4. Additionally, the same isoenzyme plays a regulatory role in the calcium transients during the ECC¹²⁰. The fifth PDE family PDE9 contain a cardiac PDE9A which is a high affinity cGMP-specific phosphodiesterase expressed at the mRNA level in healthy human but not in mouse heart¹²¹. This new phosphodiesterase is similar to PDE8A regarding its insensitivity to most of the commonly used inhibitors apart from zaprinast, a PDE5 inhibitor. Lee et al. demonstrated in

recent studies that unlike PDE5A, PDE9A can regulate cardiac cGMP signaling independent of the nitric oxide pathway and selective targeting of PDE9A could protect against sustained pressure-overload stress in cardiac diseases¹²².

A-Kinase Anchoring Proteins (AKAPs) are highly important in cardiac cAMP signaling amplitude and duration. Several cardiac AKAPs have been described as functionally essential scaffolding proteins, which selectively localize cAMP mediated PKA signaling to subcellular microdomains¹²³⁻¹²⁶ (Figure 4). At least 15 AKAPs were identified in cardiac cells, most of which are involved in recruiting PKA isoforms, PDEs and protein phosphatases (PPs) in order to confine relevant signaling complexes in the heart¹²⁷. AKAP18 α is found in association with the LTCC to facilitate the PKA-dependent phosphorylation of the channel at the sarcolemma⁷³. AKAP79/150 (in human/murine cardiomyocytes) assembles large signaling complexes with PKA, calcineurin, Cav-3 and AC at the T-tubular area, thereby facilitating PKA phosphorylation of LTCC, RyR2; and even PLB phosphorylation is AKAP150 dependent at its Cav-3 associated domains^{128,129}. Confinement of β -AR/cAMP signals, phosphorylation and dephosphorylation of PLB at the SERCA2 compartment is achieved through AKAP18 δ ^{130,131}. Additionally, PKA anchoring via AKAP9 (Yotiao) to the K⁺ channel is highly important in terms of rapid cardiac repolarization of cardiomyocytes¹³². PKA phosphorylation of the potassium channel is regulated by PDE4D3, also recruited by Yotiao, navigating cAMP effects on the K⁺ channel activity¹³³. As mentioned above, muscle-selective mAKAP mediate the dynamics of PKA activation within the RyR2 complex tightly regulated¹³⁴ by PDE4D3 and by AC5 activities¹³⁵, since both enzymes can directly bind to this anchoring protein. In this context, it has been demonstrated that mAKAP mediates PKA-induced phosphorylation of the RyR2 as a scaffold protein (Figure 4).

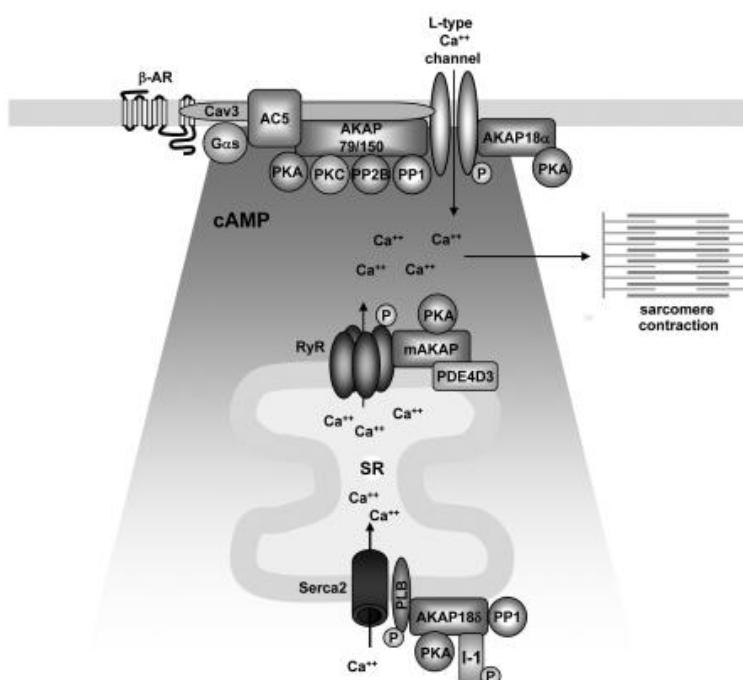


Figure 4. A-kinase anchoring proteins (AKAPs) controlling subcellular cAMP microdomains in the heart. Important AKAPs contributing to cAMP compartmentation and targeted PKA phosphorylation of key-regulatory proteins of the cardiac ECC. Taken from Diviani et al.¹⁰⁸.

1. 1. 4 Changes of local cAMP signaling and β -AR subtype modules in cardiac hypertrophy

Rat model of congestive heart failure (CHF) syndrome after myocardial infarction (MI) is the most commonly used experimental model to study the alteration and progression of cardiac physiology during progression to heart failure¹³⁶. By ligation of the left anterior descending artery, a method usually used for creating cardiac ischemia¹³⁷, irreversible myocardial injury and loss of cardiac myocyte function is observed in the infarct area. With ventricular remodeling and resulting hypertrophied cardiac muscle, the heart compensates for the diminished oxygen supply without losing much of its contractility¹³⁸ (compensated hypertrophy). This compensatory response is limited by the degree of infarct size; for example, if very large amounts of myocardium become necrotic, there is not enough hypertrophy to normalize myocardial volume. To sustain normal perfusion pressure, the renin-angiotensin-aldosterone system is activated promoting ventricular remodeling, progressive dilatation and deterioration in myocardial function^{139,140} (decompensated hypertrophy). The sympathetic activation of β -AR receptors is a critical component of the progression of heart failure, being a 'good' response under stress ("fight-or-flight" response) or for acute myocardial infarction to maintain cardiac performance, but is recognized as detrimental in a long-term view^{141,142}. As mentioned before, in response to accelerated release of catecholamines in progressive heart failure, there is desensitization and reduction of β -AR density in the myocardium^{37,143}.

Studies have shown that remodeling during the development of heart failure after MI starts at the cell membrane level, where the T-tubular network is altered^{144,145} leading to impairment of cAMP microdomains and subtype-specific β -AR signaling during heart failure. By combining scanning ion conductance microscopy (SICM) with the FRET based imaging technique, Nikolaev et al. have demonstrated a redistribution of β_2 -AR and normally highly confined β_2 -AR mediated cAMP signals from T-tubules to detubulated membrane areas^{29,146}. Impaired β_2 -AR regulation via PI3K γ controlled PDE3-dependent cAMP pools close to the plasma membrane was demonstrated to be a potential cause of ventricular arrhythmias which are often observed in heart failure¹¹¹.

During cardiac disease alterations in cAMP compartmentation and scaffolding by AKAPs and PDEs are observed. Several groups have shown that the PKA association with AKAPs is decreased in heart failure, for example due the pathological decrease in PKA-R subunit autophosphorylation¹⁴⁷, which in turn decreases cardiac troponin I phosphorylation in the failing human and animal heart^{148,149}. Disruption of the macromolecular complex of mAKAP/RyR/FKBP2.6/PDE4D3 leads to increased sensitivity to Ca²⁺ in failing human hearts. It has been demonstrated, that this can be either caused by distinct dissociation of FKBP2.6¹⁵⁰ (calstabin) from this complex due to RyR2 hyperphosphorylation¹⁵¹ or by

maladaptive changes of the cAMP sensitive PDE4D3 localization due to pathophysiological changes of the heart¹⁰⁸; both resulting in a 'leaky' RyR and consequent arrhythmogenesis by disturbed Ca^{2+} handling¹⁵². Interestingly, it has been suggested that mAKAP/RyR2 participates in early cardiac myocyte hypertrophy by adrenergic receptor signaling¹⁵³.

Evidence provided by several groups have proven that different stages of impaired cardiac performance, from early disease stage (compensated hypertrophy) to the stage of chronic heart failure, are reflected by changes of PDE microdomain action in terms of expression and localization. Using a transgenic mouse model of caveolin targeted FRET biosensor Perera et al. uncovered cGMP-sensitive PDE2 and PDE3 redistribution between β_1 -AR- and β_2 -AR-associated membrane microdomains with unaltered whole-cell PDE expression and activities in early cardiac disease (Figure 5B). Recent experiments by Sprenger et al., demonstrated local increase in cAMP dynamics at the PLB/SERCA2a due to PDE3 and especially PDE4 down-regulation in order to compensate for the loss of SERCA2a function in the early disease mouse model. Furthermore it was indicated that the decreased PDE4 effects are replaced by local PDE2 responses during sympathetic stimulation, which suggest protection of the heart and especially the SERCA2a compartment against elevated cAMP levels in hypertrophy¹⁵⁴.

Consistent with this notion, Mehel et al. showed that there is a significant PDE2 expression in human failing hearts, which constrains the effects of long-term β -AR stimulation on cardiomyocyte Ca^{2+} handling and contractility in HF¹⁵⁵.

By contrast, the expression and activity of other cAMP-hydrolyzing enzymes, PDE3 and PDE4, are significantly down-regulated^{102,156}. Under HF conditions, both the lower PDE3 levels promoting enhanced cardiomyocyte apoptosis and higher compensating PDE2 activity in late stage HF (Figure 5C) could be a consequence of increased cGMP, which is produced by guanylyl cyclase (GC) stimulated with increased levels of natriuretic peptides in hypertrophy.

PDE3A is suggested to be down-regulated in HF¹⁵⁷ which results in induction of a proapoptotic transcriptional repressor gene¹⁵⁶ in the PDE3 regulated cAMP-dependent nuclear microdomain. Treatment with PDE3 inhibitors (especially in congestive heart failure¹⁵⁸) improves cardiac contractility but increases mortality rate due to arrhythmias and sudden cardiac death¹⁵⁹.

Despite these detailed insights about alterations in global and local PDE effects (Figure 5)¹⁶⁰, there is little known about changes of individual subtype-specific β -AR dependent PDE regulation of cAMP signaling to the vicinity of the cardiac PLM-NKA complex. This topic amongst others is addressed in this project.

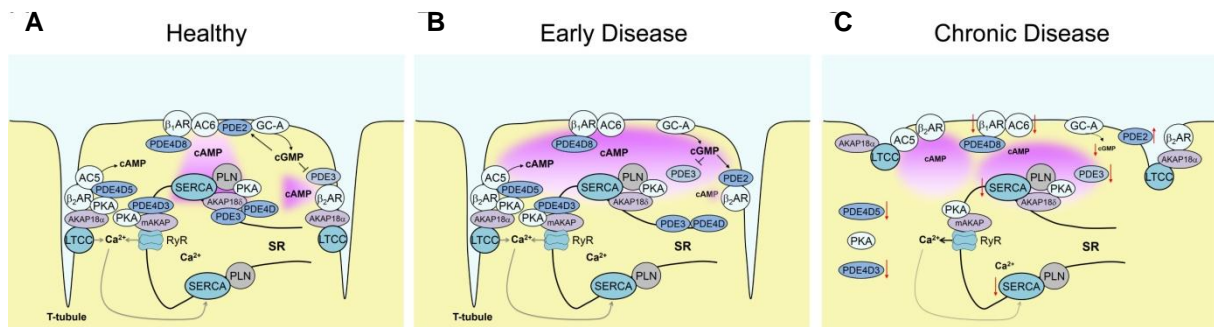


Figure 5. Alterations of local cAMP signaling in compensated hypertrophy and heart failure. (A) In healthy cardiomyocytes, cAMP is acting at major Ca^{2+} handling proteins, forming microdomains which contain local pools of PKA anchored to AKAPs and specific PDE isoenzymes. β_2 -AR signals are predominantly located around LTCC in the T-tubules, whereas β_1 -AR signals originate from the surface membrane producing far-reaching cAMP acting in subcellular microdomains (e.g. to SERCA2a) by means of scaffolding proteins. (B) In compensated hypertrophy (early stage of HF), the total PDE activities are unaltered, albeit local decreases at cAMP compartments (PDE3 at β_2 -AR and PDE3/PDE4 at SERCA) and specific relocations occur (e.g. PDE2 between β_1 - and β_2 -AR). (C) In heart failure (chronic cardiac disease), structural deformation of T-tubules and alterations in global and local PDE/PKA effects next to down-regulation and/or desensitization of β_1 -AR take place. There is a decrease in receptor-microdomain coupling and functional cAMP responses. Taken from Froese et al.¹⁴⁵.

1. 2 Differential regulation of the Na/K-ATPase by Phospholemman in the microdomain

1. 2. 1 The cardiac sodium pump

Discovered in 1957 by J.C. Skou the sarcolemmal sodium-potassium ATPase (NKA)¹⁶¹ is the predominant efflux source for cardiac sodium which maintains the transsarcolemmal sodium gradient and provides a rapid upstroke of action potential¹⁶². This gradient ensures proper ion homeostasis, critical for sodium dependent membrane transporters (for example, Na^+ /glucose cotransporter) and for normal cellular function¹⁶³. The action of the sodium pump regulates physiological electrical activity influencing the sodium-calcium exchanger (NCX) and cardiac contractility¹⁶⁴ (Figure 6). The NKA extrudes three sodium ions from the cytosol to the extracellular domain in exchange for two potassium ions particularly to restore the steady-state intracellular sodium concentration at 4-8 mM (10-15 mM in rat and mouse)¹⁶⁵ at the expense of metabolic energy driven from the hydrolysis of ATP¹⁶⁶. This ion exchange results in one net charge generating a membrane current. For the quantification of sodium pump mediated (i.e., ouabain-suppressible) transport the K^+ analogue ^{86}Rb (Rubidium) is often used as a tracer for K^+ and gives reliable results¹⁶⁷.

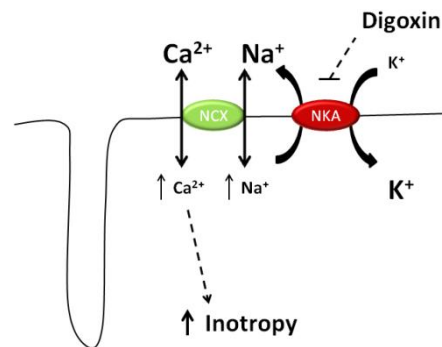


Figure 6. NKA - an integral player in the 'fight-or-flight' response. Enhancement of Na/K-ATPase activity limits the rise in intracellular Na^+ caused by the higher level of Na^+ influx during action potential. By doing so, NKA limits the rise in cellular and SR Ca^{2+} load by favoring Ca^{2+} extrusion via the Na/Ca exchanger. Inhibiting the NKA via cardiotonic steroids induces cardiac inotropy.

Upon action potential Na^+ and Ca^{2+} enter the cell through voltage gated ion channels, which triggers Ca^{2+} from the sarcoplasmic reticulum (SR). Elevated Ca^{2+} triggers cellular contraction in the systole, which is followed by diastolic Ca^{2+} extrusion mainly via the NCX in forward mode which in turn is promoted by the NKA pumping Na^+ out of the cell to keep the Na^+ levels constant¹⁶⁴. Hence, cellular Ca^{2+} levels, that are highly important for the regulation of the ECC, are linked to the NKA activity. Elevated intracellular sodium would favor reverse mode of NCX resulting in larger calcium transient and contractility¹⁶². Since the 18th century this mechanism is made use for cardiotoxic steroids. For example, digoxin as NKA inhibitor, induces acute cardiac inotropy and is used for treatment of heart failure¹⁶⁸. Several groups have shown that a small transmembrane protein called phospholemman (PLM) interacts with the NKA and modulates its activity, analogous to phospholamban (PLB) at SERCA¹⁶⁹, another P-type pump¹⁷⁰⁻¹⁷⁴. Upon β -adrenergic stimulation in the heart, PLM works against cardiomyocyte sodium and calcium overload primarily by disinhibiting the NKA (discussed below).

1. 2. 2 Cardiac subunit expression and composition of the Na pump

Solving of the crystal structure of the NKA in 2007¹⁷⁵⁻¹⁷⁷ revealed new insights about structure and composition of the cardiac sodium pump. In mammals, four α (α_1 , α_2 , α_3 , α_4) and three β (β_1 , β_2 , β_3) isoforms are recognized as minimum operative subunits (SUs)^{178,179}. Having binding sites for Na^+ , K^+ , ATP and cardiac glycosides the catalytic α -SU assembles with the β -SU, which is highly important for structural and functional maturation of the sodium pump¹⁸⁰, and one of the seven isoforms of the so called 'Fixid' proteins (FXYD), titled according to their conserved phenylalanine-X-tyrosine-aspartate motif^{181,182}. This functional multi-subunit enzyme (Figure 7) differs in tissue specific composition, proving that the sodium pump plays a key role in multiple regulatory mechanisms involving critical Na^+ transport under different physiological conditions. Predominant isoforms in the heart are α_1 , α_2 and β_1 having FXYD1 (PLM) as regulatory protein

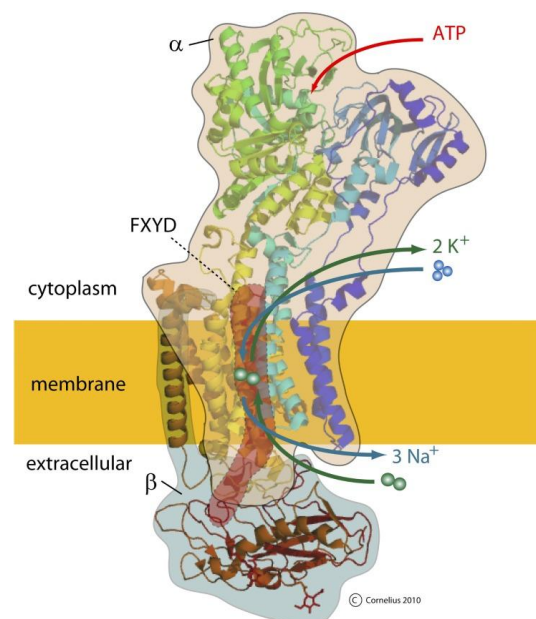


Figure 7. Structure of the Na/K-ATPase. The NKA consists of an intracellular α -SU (encircled in light brown) and extracellular β -SU (encircled in blue). The applied color on the quaternary changes gradually from the N-terminal (blue) to the C-terminal (red). Having a great transmembrane domain, the regulatory subunit of the pump (FXYD1-PLM) is red and associated with the α SU. The transmembrane domain contains binding sites for 3 Na^+ and 2 K^+ ions, respectively, which pass sequentially through the same cavity of the molecule. Taken from Clausen et al.¹⁵².

(see section 1. 3. 1)^{180,181,183}. It is proposed that the different α isoforms vary in subcellular distribution and function. Berry et al. have previously shown that, the NKA with the α_1 SU (NKA- α_1) is more to be found on surface membrane compartments and provides around 88% of the total Na^+ current. Even though the NKA- α_2 has a high functional T-tubular density being five times more present in the cardiac T-tubules than in the sarcolemma, the NKA- α_1 still generates at least 50% of cardiac T-tubular Na current in mice¹⁸⁴. Referring to their differential distribution in addition to their clear physical and functional association with the NCX¹⁸⁵⁻¹⁸⁷, the α_1 and α_2 -SUs are suggested to have different functional roles in cardiac myocytes: The NKA- α_1 is responsible for global Na^+ current, as it is the predominant isoform of the two, simultaneously it controls subsarcolemmal Na^+ microdomains together with the NKA- α_2 especially at the dyadic cleft located at the sarcoplasmic reticulum^{166,188}. Also, it is stated that the α_2 isoform preferentially regulates cardiac Ca^{2+} transients via the NCX¹⁸⁹⁻¹⁹¹. There is the intriguing idea of microdomains created by co-localization of ion transporters, where the NKA is regulated by PLM^{75,192,193}. It is supported by the fact that there is an indirect influence of the NKA isoforms on sub-sarcolemmal Na^+ controlled by the NCX which has already been suggested to be functionally linked to the NKA¹⁹². Additionally, it is stated that the cytoskeletal protein ankyrin B anchors NCX to the membrane actively forming a functional complex with the NKA and the IP3-receptor supports^{75,193}.

1. 3 Kinase mediated control of Phospholemman over the Na^+/K^+ -ATPase

1. 3. 1 Phospholemman- FXYD1 Protein

As stated above, the NKA is regulated by different cellular mechanisms, for example by sodium and potassium levels or membrane potential as well as factors like ATP availability and cardiac steroid binding. Next to this, it is regulated by FXYD1, a small membrane protein belonging to a family of proteins with 7 identified members (FXYD1-7) being firstly defined as regulators for ion transporters and named according to the aforementioned signature FXYD motif in the N-terminus¹⁸² (Figure 8). At least five of these proteins are described as auxiliary subunits regulating NKA activity in a tissue- and isoform-specific way¹⁹⁴. FXYD1, also known as phospholemman (PLM), is a 72 amino acids long single transmembrane protein, predominantly found in heart, skeletal and smooth muscle cells¹⁹⁵⁻¹⁹⁸. The N-Terminus with its 17 amino acid residues lies in the extracellular domain, whereas the C-Terminus resides in the cytosolic fraction with 35 amino acids. Bearing multiple phosphorylation sites at the COOH terminus PLM is phosphorylated at the Ser68 residue by PKA and PKC^{199,200}. The latter has additional phosphorylation targets at the Ser63 and Ser/Thr69 residues¹⁷⁴. Physical association of PLM was demonstrated by co-immunoprecipitation with the α -SU of the NKA⁷⁶ and supported by FRET experiments by Khafaga et al.²⁰¹. Worthy of comparison is PLB,

which is also a PKA substrate whereupon the SERCA2a is disinhibited, but PLB does not alter the maximum transport rate (V_{max}) of its pump like PLM does for NKA. Several laboratories have shown that PLM phosphorylation relieves the sodium pump by possibly increasing V_{max} ^{174,202-204} and K_m for Na^+ ions (increased Na^+ affinity)^{15,76,200,205,206}. Variation between studies regarding V_{max}/K_m showed discrepancies most likely due to different methodology performed in different labs.

Several other functional roles are ascribed to PLM in the heart¹⁶⁶. It is suggested that PLM modulates the gating of L-type Ca channels (Cav1.2) in an overexpression model²⁰⁷. Another study on cardiac cells revealed that PLM oligomerizes²⁰⁸, as originally proposed but instead of forming ion channels in *Xenopus* oocytes²⁰⁹ and regulating cell volume in cultures cardiac cells by forming taurine efflux channels²¹⁰, it is rather accepted to oligomerize¹⁹⁹ in order to generate a 'storage pool' to increase 'responsiveness' of a certain PLM-free NKA population in the heart to adrenergic stimulation, by as yet unidentified means¹⁶⁶.

Under catecholamine stress PLM works against of arrhythmogenesis although minimally causing negative inotropy by promoting Na extrusion^{211,212}. For this reason PLM expression and its phosphorylation may be important for protection against stress-induced arrhythmia.

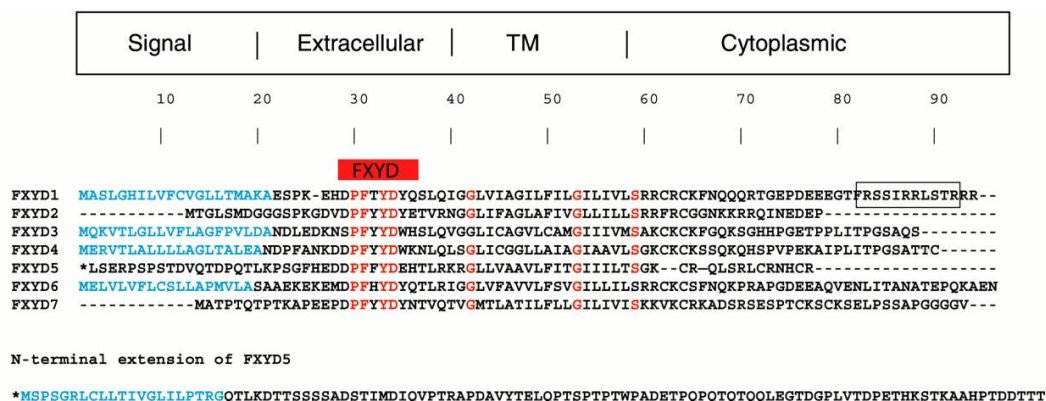


Figure 8. Amino acid sequence of currently known mammalian FXYP proteins.

Human FXYP sequence alignments showing seven known families with conserved residues (in red). The PKA/PKC phosphorylation domain of phospholemman is framed. Taken from Cornelius et al.¹⁸²

1. 3. 2 Kinase phosphorylation of Phospholemman

In 1985 PLM was identified as a PKA and PKC phosphorylatable protein in the heart^{213,214}. Initially, it was assumed that the NKA is regulated through phosphorylation of its α -SU via PKA, but it was strictly dependent on a detergent which makes the PKA phosphorylation site of the pump accessible²¹⁵. It is now generally accepted that phosphorylated PLM activates the cardiac sodium pump and tonically inhibits it at its basal state⁷⁶. Conclusive analysis of the Na^+ pump regulation was performed by whole cell voltage clamping of PLM-WT and

PLM-KO cardiomyocytes showing pump activity mechanisms under β -AR stimulated and non-stimulated conditions²¹⁶. The β -AR stimulation of PLM-WT cells increased Na^+ pump activity and Na^+ affinity to levels of NKA current of PLM-KO cells, where there was no inhibitory effect of PLM to the NKA enzyme. Additional experiments introducing a phosphorylated PLM peptide to

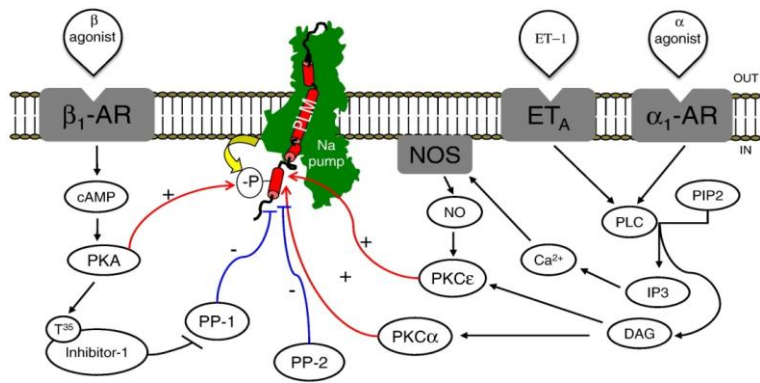


Figure 9. Phosphorylation of phospholemman regulates sodium pump activity. Signaling pathways mediating kinase and phosphatase activities involved in the PLM phosphorylation state. PKA and PKC phosphorylate PLM, hence stimulate the sodium pump, whereas PP-1 and PP2-A activity inhibit the pump by dephosphorylating PLM. ET-1, endothelin 1; ET_A, endothelin A receptor; NOS, nitric oxide synthase. Taken from Pavlovic et al.¹⁷³

cardiomyocytes of the same animals have indicated that Ser68 phosphorylation of PLM can even stimulate Na^+ pump current above basal levels, simultaneously indicating that the final 19 amino acids of PLM are sufficient to inhibit the NKA²⁰². Phosphorylation of PLM leads to a change in orientation, but the FXD1 protein remains physically associated to the α_1 -SU of the cardiac sodium pump, which is co-immunoprecipitated in several studies^{76,171,217,218}. It is widely known that similarly to PLM dependent PKA activation of the Na^+ pump, protein kinase C (PKC) mediated phosphorylation of PLM increases V_{max} with a change in Na^+ affinity of the NKA in some cases^{172,200}. There are speculations that PKC acts on a different pool of PLM predominantly associated to the α_2 isoform of the pump. The pump isoform specific effect of PLM phosphorylation via PKC is a theory demonstrated in several experiments from different labs^{172,205} which still remains questionable. It is supported by the fact that for instance PKC phosphorylation increases the maximum rate of the α_2 -NKA but not α_1 -NKA in genetically modified SWAP mice (where α_1 -NKA can be blocked by ouabain), and contradicted by FRET experiments showing no actual change between YFP-PLM and CFP- α_1 and $-\alpha_2$, respectively²⁰⁵. PLM phosphorylation at its multiple target residues by PKA and PKC turns out to be additive²⁰⁰, also in terms of NKA function. Investigations in ARVMs have shown high basal phosphorylation of PLM (~30% at Ser68 and ~50% at Ser63) mainly caused by the PKC activity, hence basal Ca^{2+} levels¹⁷⁴. Three PKC isoforms are identified in the heart (PKC α , δ , and ϵ)¹⁷⁴. Fuller et al. demonstrated that receptor-mediated PKC activation causes sustained phosphorylation of Ser63 and Ser68, but transient phosphorylation of Thr69, which leads to further stimulation of the sodium pump¹⁷⁴. There is evidence that exogenous/endogenous NO mediates PKC ϵ dependent PLM phosphorylation thereby limiting Na^+ and Ca^{2+} overload and related cardiac diseases²¹⁹.

The kinase phosphorylation of phospholemman, in particular during sympathetic stimulation is essential for the ECC¹⁷ where the phosphoprotein disinhibits NKA^{15,203} (Figure 9) while actively inhibiting the NCX^{173,220} thereby regulating intracellular Ca²⁺ concentration critical for cardiac function²²¹.

1. 4 Changes of PLM/ NKA complex in diseased heart

The importance of NKA function in the heart in terms of trans-membrane sodium gradient is demonstrated by several laboratories (see section 1. 2. 2). It is well known that Na⁺ overload contributes to cardiac diseases such as ischemia/reperfusion^{222,223} hypertrophy and heart failure (HF)²²⁴⁻²²⁶. Elevation in intracellular Na⁺ which occurs largely through several sodium influx pathways shown to be up-regulated in the failing myocardium^{227,228}, may contribute to the negative force-frequency relationship, slowed relaxation and arrhythmias¹⁹⁰. A large body of data suggests that this may be caused by a reduction of NKA activity and compromised Na⁺ extrusion via the pump in heart failure^{229,230}. Additionally, aberrant phosphorylation of PLM²³¹, the expression of NKA and its α subunits contribute to the disease pattern²¹⁷. There are different studies by groups focused on different stages of the disease process in human, canine and rat heart failure models^{226,232,233}. For example, Bossuyt et al. showed that the PLM fraction phosphorylated at Ser-68 was dramatically increased in a rabbit HF model²¹⁷. Comparable results were obtained in studies on murine cells 3 weeks post-MI by Mirza et al. This group observed a decrease in PLM expression, accompanied by an increase in the fraction of phosphorylated PLM in murine hearts 3 weeks post-MI²³⁴. Additionally, the enhanced NCX activity in PLM-KO-MI cells largely accounted for the improvement in cardiac and myocyte contractility compared to WT-MI hearts²³⁴. El-Armouche et al. reported significantly reduced PLM phosphorylation, which could possibly be involved in disease progression linked to an increase in Inhibitor-1 and Protein Phosphatase-1 (PP-1) activity, but there was no change in expression for total PLM or the α_1 -SU in failing human hearts²³¹. Similarly, data presented by Boguslavskyi et al. clearly indicate that the complete prevention of PLM phosphorylation sites via a PLM mutant knock-in mouse subjected to aortic constriction markedly exacerbates cardiac remodeling by further inhibiting the NKA²³⁰. Pointing out the aforementioned preferential role of the α_2 -NKA in EC coupling (section 1. 1. 2), the same group²³⁰ and others²³⁵ have revealed that the increase in α_2 -SU expression is a positive adaptive mechanism possibly allowing the normalization of ion, especially Ca²⁺, regulation in response to Na⁺ overload caused by hypophosphorylation of PLM in animals with induced hypertrophy.

1. 5 Imaging local cyclic nucleotide dynamics

1. 5. 1 Fundamentals of Förster/Fluorescence resonance energy transfer

As mentioned in section 1. 1. 3, it is widely accepted that spatial and temporal compartmentation of cAMP is important for targeting a range of proteins in functionally important subcellular locations. Measuring second messenger levels via biochemical assays such as radioimmunoassays directly detecting cAMP content in a cell pellet²³⁶⁻²³⁸ or indirect immunoblot analysis of phosphorylated proteins by the respective kinases (i.e. PKA) are alternative ways used to measure cAMP concentrations²³⁹. Offering poor spatial resolution, these classical methods do not enable to obtain results of physiological relevant free cAMP effects but rather total amounts of cAMP in lysed tissue, not focusing on single cells let alone cellular compartments. As most cellular activities appear in milliseconds, there was an urge to gain insights into cAMP dynamics at high temporal resolution.

Most commonly used live cell imaging techniques are based on the Förster resonance energy transfer (FRET) phenomenon, discovered by the German physicist Theodor Förster in 1948²⁴⁰. The Förster equation $E(FRET) = 1/[1 + (r/R_0)^6]$ describes the non-radiative energy transfer between two fluorophores in very close proximity (< 10 nm) which has provided a popular mean to detect protein-protein interaction and conformational change of proteins in living cells. More precisely, the donor fluorophore is excited with a specific wavelength of light matching its peak of absorption. The excited donor in turn transfers its emission energy to the acceptor fluorophore (Figure 10A). Therefore, a FRET pair should necessarily consist of two fluorophores, by which the donor fluorophore emission spectrum should overlap with the excitation spectrum of the acceptor fluorophore²⁴¹. The well-known Jablonski diagram (Figure 10B) demonstrates in detail the excited S_1 state of the donor electron and the its fall back to ground state S_0 via emission of fluorescence energy in form of a photon exciting the acceptor fluorophore on a energetically lower level²⁴². Similar to its donor pair, the excited acceptor electron emits fluorescent light when returning to its singlet ground state S_1 . According to the change in energy state, the donor fluorescence (emission) intensity is reduced and the acceptors emission is increased. For quantification of FRET occurring between the pair of fluorophores, the ratio acceptor emission intensity/donor emission intensity or vice versa is calculated, and a change in FRET can be observed during experiments²³⁹. FRET pairs often consist of green fluorescent protein (GFP) mutants, such as cyan fluorescent protein (CFP) as the donor protein and yellow fluorescent protein (YFP) as the acceptor protein. Tagged to sequences of proteins of interest, these fluorophores allow through optical recordings to monitor dynamic protein-protein interactions²⁴³ (Figure 10C)^{171,201}. FRET between CFP and YFP sandwiching cyclic nucleotide binding domains was introduced as a tool to detect cAMP and cGMP dynamics in several studies mentioned in the next section.

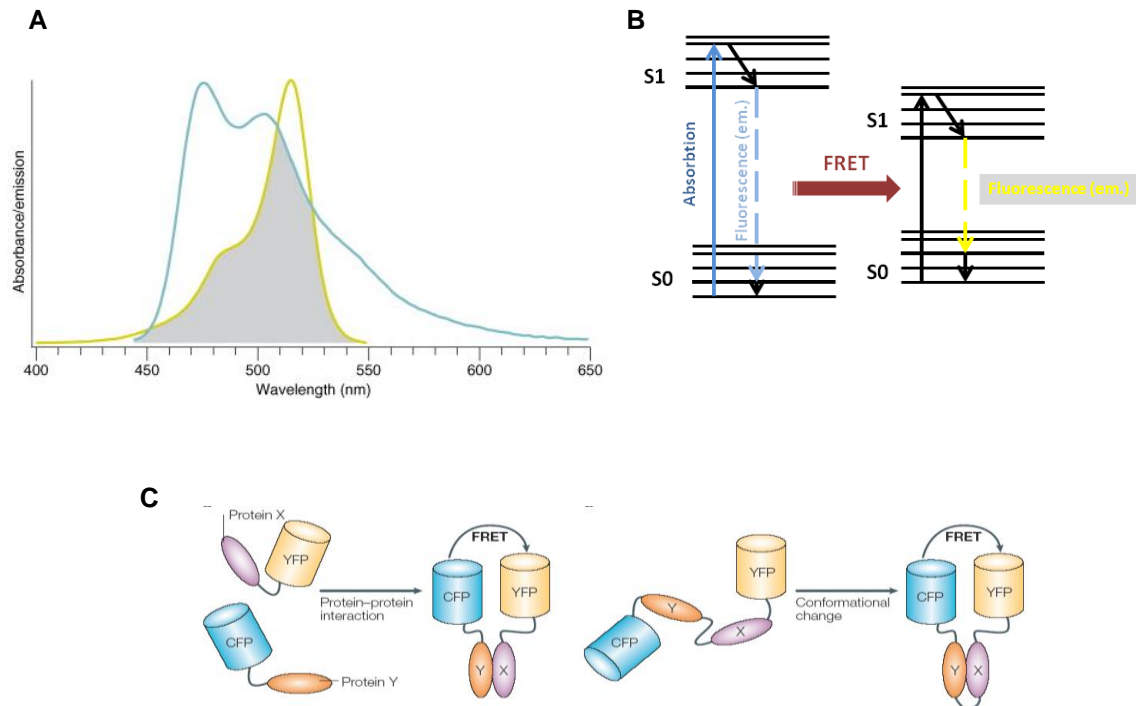


Figure 10. The principles of FRET instancing the CFP and YFP pair. (A) The prerequisite for FRET to occur is a spectral overlap between the donor and acceptor fluorophore. The emission spectrum (blue) of the donor fluorophore (CFP) overlaps with the excitation spectrum (yellow) of the acceptor fluorophore (YFP) and allows fluorescence resonance energy transfer (FRET). The overlapping spectral area is colored grey. Taken from Piston et al.²²⁵ (B) The schematic representation of the Jablonski-diagram describes the transfer of fluorescence energy from the donor to the acceptor fluorophore. Upon absorption of photon energy, the donor electron moves from a ground state (S0) to its excited state (S1). The donor fluorophore can partly transfer its energy from the lowest S1 state in form of fluorescent energy. The electrons of the acceptor fluorophore with a lower energetic excitation spectrum and close proximity is excited. Acceptor electrons are lifted from their S0 to the S1 state and yellow fluorescence light is emitted when the acceptor electrons “fall back” into their S0 state.²²⁶ (C) FRET is utilized for tracking dynamic protein-protein interactions and conformational changes within a single protein. Taken from Zhang et al.²²⁷

1. 5. 2 cAMP sensitive FRET Biosensors

Before starting to generate (targeted) cAMP sensitive FRET based biosensors, several groups have used the change in cAMP dependent LTCC⁷⁰ and CNGC^{102,244,245} currents as a readout for local cAMP dynamics and significantly contributed to characterization of β_2 -AR-cAMP pools shaped by PDEs (i.e. PDE3 and PDE4)²⁴⁶. Adams et al. created the first chemically labeled cAMP sensitive sensor called FliCRhR, utilizing the regulatory and catalytic subunits of the PKA holoenzyme. Injecting it to living cells, cAMP activity is monitored through PKA dissociation and loss of FRET²⁴⁷. The more practical genetically encoded PKA based biosensor was developed by Zaccolo et al., who fused CFP and YFP to the R and C subunits to detect cAMP changes close to the Z-lines in neonatal rat ventricular myocytes^{72,248}. It was the first attempt to monitor distinct PDE activities in subcellular microdomains. This sensor showed slow kinetics and probable interaction with endogenous PKA (Figure 11). Subsequently, several single cAMP binding site based sensors were

developed, which can monitor cAMP in the bulk cytosol. For example, the HCN2-camps sensor²⁸ contained the soluble C-terminal cAMP binding domain from the cyclic nucleotide-gated potassium channel 2 flanked with CFP and YFP sites enabling real time measurements of cAMP dynamics in the bulk cytosol. Additionally, either Epac1 or Epac2 based single chained biosensor with uniform cellular expression were widely used to detect rapid cAMP signals developing in the cytosol^{249,250}. Fused to CFP and YFP, a single cAMP binding domain changes its conformation upon cAMP leading to a decrease of the FRET signal. Epac1 and Epac2 based sensors differ in their cAMP affinity and FRET capacity. Despite its lower cAMP affinity, Epac1 based sensor E1-camps showed a larger FRET change, which is why it is used in this and other studies^{154,239,251}.

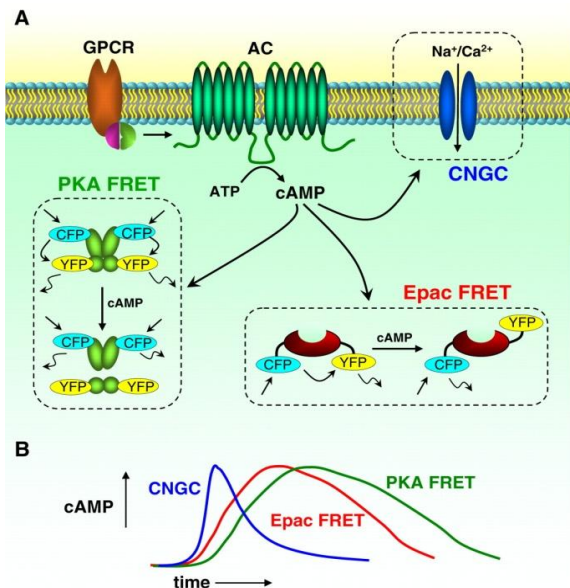


Figure 11. Cartoon showing means to determine intracellular cAMP dynamics. (A) Regulatory and catalytic subunits of PKA probes dissociate upon cAMP binding causing a decrease in the FRET signal. The Epac based FRET sensor has CFP and YFP in close proximity at basal state, after cAMP binds to the unimolecular sensor, there is a conformational shift and FRET-based YFP emission decreases. cAMP signals can be measured through determination of cyclic nucleotide gated channel currents by patch-clamp methods, or by imaging with a Ca^{2+} -sensitive dyes. (B) Compared with PKA-based probes, the Epac-based sensors exhibit an extended dynamic range and have better signal-to-noise ratio. FRET changes detected with the CNGC method are more transient and have a greater temporal resolution although they are restricted to the membrane. Taken from Willoughby et al.²²⁹

1. 6 Aims of the project

Previous studies have demonstrated that several cAMP-dependent PKA substrates important for the regulation cardiac ECC are organized in microdomains formed by scaffolding proteins and β -adrenergic receptor subtypes. However, the knowledge about the real time dynamics of cAMP in a microdomain coupled to PLM and NKA, its interaction with β -ARs and individual cardiac PDE families forming this important microdomain as well as their alterations in cardiac disease is insufficient.

Therefore, the aims of this work were:

1. To develop a FRET-based Phospholemman targeted cAMP biosensor PLM-E1 and to express it in ARVMs using an adenoviral expression system.
2. To perform real time monitoring of cAMP dynamics in the PLM/NKA compartment in order to understand the regulatory mechanisms behind a possible local restriction of β -AR mediated cAMP signals in the PLM/NKA microdomain.
3. To study microdomain-specific alterations of cAMP signaling at the PLM/NKA complex in a chronic heart failure disease model.

2. Materials and Methods

2. 1 Materials

2. 1. 1 Cells

HEK293A	Invitrogen
HEK293	Sigma Aldrich

2. 1. 2 Plasmids

pcDNA3.0	Invitrogen
Epac1-camps	Prof. Viacheslav Nikolaev
human ^{PLM}	Prof. Michael Shattock
canine ^{PLM-YFP}	Dr. William Fuller
human ^{PLM-E1 long linker}	this project
canine ^{PLM-E1 short linker}	this project
Gateway® pDONR™ 221	Invitrogen
Gateway® pAd/CMV/V5-DEST™	Invitrogen

2. 1. 3 Bacteria strains

One Shot® TOP10 chemically competent <i>E. coli</i>	Invitrogen
One Shot® OmniMax2T1	Invitrogen

2. 1. 4 Animals

Adult male 8-12 weeks old Wistar rats (250 - 300 g; Charles River) were held on site (Animal Care Facility, UMG Göttingen). They were maintained in compliance with the constitutional animal protection act (Tierschutzgesetz, TSchG). All animals were kept in containment rooms at room temperature. Between 4 and 6 rats were housed in each cage, allowing free access to food and water. All animal protocols were approved by the local University Medical Center Göttingen animal protection committee and all animal work was performed according to institutional and governmental guidelines.

Adult male 8 weeks old Sprague Dawley rats (~ 200 g) were used for introduction of the heart failure rat model and underwent heart isolation 16 weeks post MI, as described in sections 2. 2. 18 and 2. 2. 19. Aged matched control animals (AMC) were ordered both at our site in Göttingen (Janvier Labs) and at the Imperial College London in order to use for control experiments.

2. 1. 5 Oligonucleotides

The human PLM sequence was kindly provided by Prof. Michael Shattock, King's College London.

human PLM sequence

5'-ATGGCGTCTCTTGGCCACATCTTGGTTTTCTGTGTGGGTCTCTCACCATGGCCAAGGCAGAAAGTCCAAAGGAACACG
ACCCGTTCACTTACGACTACCAGTCCCTGCAGATCGGAGGCCTCGTCATCGCCGGGATCCTCTTTCATCCTGGGCATCCTCA
TCGTGCTGAGCAGAAGATGCCGGTGCAAGTTCAACCAGCAGCAGAGGACTGGGGAACCCGATGAAGAGGAGGGAACCTT
CCGCAGCTCCATCCGCGTCTGTCCACCCGCAGGCGG-3'

The canine PLM-YFP sequence with linker sequence (60 bp) was provided by Dr. William Fuller.

canine PLM-YFP

5'-ATGGCACCTCTCCACCACATCTTGGTTCTCTGTGTGGGTTTCTCACCACGGCCACCGCAGAAGCGCCACAGGAACA
CGACCCGTTCACTTACGACTACCAATCCCTGCGGATCGGAGGCCTCATCATCGCCGGGATCCTCTTTCATCCTCGGTATCCT
CATCGTCTGAGCAGAAGATGCCGGTGCAAATTCAACCAGCAGCAGAGGACTGGGGAACCTGATGAAGAGGAGGGAACCT
TCCGCAGCTCCATCCGCGTCTGTCCACCCGCAGGCGGAAAGAGATCTCGAGCTCAAGCTTCGAATTCTGCAGTCGACGGT
ACCCCGGTCGCCACCGGGGTGAGCAAGGGCGAGGAGCTGTTACCCGGGTGGTGCCCATCCTGGTCGAGCTGGACGGC
GACGTAACCGCCACAAGTTCAGCGTGTCCGGCGAGGGCGAGGGCGATGCCACCTACGGCAAGCTGACCCTGAAGTTCA
TCTGCACCACCGGCAAGCTGCCCGTGCCTGGCCACCCCTCGTGACCACCTTCGGCTACGGCCTGATGTGCTTCGCCCC
CTACCCCGACCATGAAGCAGCAGACTTCTTCAAGTCGCCATGCCCGAAGGCTACGTCCAGGAGCGCACCATCTTCTT
CAAGGACGACGGCAACTACAAGACCCGCGCCGAGGTGAAGTTCGAGGGCGACACCCTGGTGAACCGCATCGAGCTGAAG
GGCATCGACTTCAAAGAGGACGGCAACATCCTGGGGCACAAGCTGGAGTACAACAGCCACAACGTCTATATCATG
GCCGACAAGCAGAAGAACGGCATCAAGGTGAAGTTCAAGATCCGCCACAACATCGAGGACGGCAGCGTGCAGCTCGCCG
ACCACTACCAGCAGACACCCCATCGGCGACGGCCCGTGTCTGCTGCCGACACACTACTGAGCTACAGTCCGCC-3'

Which includes the canine PLM, the linker and the YFP sequences

All other oligonucleotides were purchased from MWG Biotech GmbH, eurofins Genomics, Ebersberg:

PLMHindIIIfor

5'-AAAAAGCTTACCATGGCGTCTCTTGG-3'

PLMNotIrev

5'-AAAGCTAGCAGATCCGGATCCCCGCCTGCGGGT-3'

YFPNotIfor

5'-AAAGCTAGCGTGAGCAAGGGCGAGG-3'

PLMYFPKpnfor

5'-AAAGGTACCCCGGTGCCACCGGGGTGAGCAAGGGCGAGG-3'

YFPEcoRIrev

5'-AAAGAATTCCTTGTACAGCTCGTCCATG-3'

pcDNA3attBfor

5'-GGGGACAAGTTTGTACAAAAAAGCAGGCTGACTCACTATAGGGAGACCC-3'

pcDNA3attBrev

5'-GGGGACCACTTTGTACAAGAAAGCTGGGTAGCGAGCTCTAGCATT-3'

attBPLMhundfor

5'-GGGG ACA AGT TTGTACAAAAAAGCAGGC TACGATGGCACCTCTCC-3'

attBYFPN1rev

5'-GGGGACAAGTTTGTACAAAAAAGCAGGCTCCGCGACTCTAGATCA-3'

2. 1. 6 Chemicals

Acrylamide (Rotiphoreses Gel 30)	(ROTH)
ANP	(Bachem)
Ampicillin	Roth, # K029.1
Ampuwa® water	Fresenius Kabi Deutschland GmbH
BAY 60-7550	Santa Cruz, # sc-205219
β-Mercaptoethanol	Sigma, # M3148
Bromphenol Blue sodium salt	Applichem, # A1120
8-Br-2'-O-Me-cAMP-AM	Biolog, # B028
2,3- Butanedione monoxime	Sigma, # B0753
Bumetanide	Sigma, #B3023-250MG
Calcium chloride	Sigma, # C4901-1KG-D
Calcium chloride dihydrat	Merck, # 17257
CGP-20712A methanesulfonate salt	Sigma, # C231
Cilostamide	Sigma, # C7971
Dimethyl sulfoxide DMSO	Sigma, # D2650
dNTPs	Promega, # U1240
EDTA	Roth, # 8040.3
Ethanol Rotipuran >99,8%	Roth, # 9065.1
EZ-Link™ Sulfo-NHS-SS-Biotin	Thermo Fischer, # 21331
Forskolin	Sigma, # F6886
GFP-Trap® A	Chromotech, # gta-10
Glucose	Sigma, # G7021
Glycerol	Sigma, # G8773
Glycine	Roth, # 3908.3
H-89 dihydrochloride hydrate	Sigma, # B1427
HEPES	Sigma, # H4034
Hydrochloride acid 37%	Sigma, # 84422
ICI-118.551 hydrochloride	Sigma, # I127
3-Isobutyl-1-methylxanthin	Applichem, # A0695
Isoproterenol hydrochloride	Sigma, # I6504
Laminin	Sigma, # L2020

LB- Agar powder Miller	Appllichem, # A0927
LB- Medium powder Miller	Appllichem, # A0954
Loading buffer DNA IV (for Agarose gels)	Appllichem, # A3481
Kanamycin	Appllichem, # A1493
Magnesium chloride	Sigma, # M8266-1KG
Magnesium chloride hexahydrate	Appllichem, # A1036
Magnesium sulfate heptahydrate	Sigma, # M2773
MDL-12,330A hydrochloride	Sigma, # M182
Methanol	Roth, # HN41.2
8-methoxymethyl-3-isobutyl-1-methylxanthine	Sigma, # M2547
Milkpowder	Roth, # T145.1
Monensin sodium salt	Sigma, # M5273-1G
<i>N</i> -Methyl-D-glucamine	Sigma, # 66930-100G
<i>N,N,N,N</i> -Tetramethylethylenediamine (TEMED)	Sigma, # T9281
Octaethylene glycol monododecyl ether	Sigma
Ouabain octahydrate	Sima, # O3125-1G
peqGOLD Universal Agarose	Peqlab, # 35-1020
PhosStop	Roche, # 04906837001
Ponceau S	Sigma, # P3504
Potassium bicarbonate	Sigma, # P7682
Potassium chloride	Sigma, # P5405
Potassium dihydrogen phosphate	Merck, # 4873
Protease Inhibitor Cocktail	Roche, # 11872580001
Protein G Sepharose 4 Fast Flow	GE Healthcare, #17-0618-01
Protein Marker V	Peqlab, #27-2211
Quick-Load® 100bp DNA ladder	Biolabs, # NO467S
Quick load® 1 kb DNA ladder	Biolabs, # NO468S
Rolipram	Sigma, # R6520
Rubidium-86 Radionuclide	Perkin Elmer, # NEZ072001MC
Sodium azide	Sigma, # S2002
Sodium bicarbonate	Sigma, # S5761
Sodium chloride	Sigma, # S5886
Sodium hydroxide	Roth, # 6771.3
Streptavidin Sepharose High Performance	GE Healthcare, # 17-5113-01
TAE-buffer (50x)	Appllichem, # A1691

Taurine	Sigma, # T8691
TRIS	Roth, # 4855.3
Triton-X® 100	Appllichem, # A1287.0025
Tween-20®	Sigma, # P1379
Vectashield® Mounting Medium	Vector Laboratories, # H-1000

2. 1. 7 Cell culture

Geneticin® Selective Antibiotic (G418 Sulfate) (50 mg/mL)	Thermo Fischer #10131027
DMEM, 4.5 % glucose	Biochrom, # F0445
FCS	Biochrom, # S0615
Glutamine	Biochrom, # K0283
Iscove Basal Medium	Biochrom, # FG 0465
Lipofectamine®2000 Reagent	Invitrogen, # 11668
Modified Medium 199	Sigma, #M7528
OPTI-MEM®	Gibco, # 11058
PBS Phosphate Buffered Saline (Dulbecco)	Biochrom, # L1825
Penicillin/Streptomycin	Biochrom, # A2213
Plaque GP Agarose	Biozym, # 850110
Trypsin/ EDTA solution	Biochrom, # L2143

2. 1. 8 Enzymes and Kits

Pfu DNA Polymerase (2-3 U/μL)	Promega, # M774B
Restriction enzymes for molecular cloning	New England Biolabs
Pierce BCA Protein Assay Kit	Thermo Scientific, # 23227
Plasmid Midi Kit	Qiagen, # 12945
Plasmid Mini Kit	Qiagen, # 12125
Proteinase K	Appllichem, # A3830-0500
QIAquick Gel Extraction Kit	Qiagen, # 28704
QIAquick PCR purification Kit	Qiagen, # 28104
T4 DNA Ligase	NEB, # M0202S

2. 1. 9 Antibodies

Table 2. Primary antibodies are used for Western Blot (WB) and immunofluorescence (IF) analysis. Antibodies for Western Blot analysis were diluted in the used blocking buffer (TBS + 1% Tween + 5% milk powder) and for immunofluorescence experiments in appropriate blocking buffer (PBS +10% FCS + 0.2% Triton-X-100).

Antibody	Dilution	Company
anti- α_1 mouse monoclonal C464.6	Western Blot: 1:10000 Immunofluorescence: 1:100	Millipore, # 05-369
anti-FXYD1 (PLM) rabbit polyclonal	Western Blot: 1:10000 Immunofluorescence: 1:100	Abcam, # ab76597
anti-GFP rabbit monoclonal	Western Blot: 1:10000	Abcam, # ab32146
anti-PDE3A goat polyclonal	Immunofluorescence: 1:100	Santa Cruz, # sc11834

Table 3. Secondary antibodies were diluted in buffers prepared for the used primary antibodies for WB and IH analysis.

Antibody	Dilution	Company
Alexa Fluor® 488 donkey anti-goat	Immunofluorescence: 1:500	Invitrogen, # A11055
Alexa Fluor® 633 goat anti-rabbit	Immunofluorescence: 1:500	Invitrogen, # A21070
Alexa Fluor® 488 goat anti-rabbit	Immunofluorescence: 1:500	Invitrogen, # A11034
Alexa Fluor® 633 rabbit anti-mouse	Immunofluorescence: 1:500	Invitrogen, # A21063
Immun-Star™ goat anti-mouse-HRP	Western Blot: 1:5000	Biorad, # 170-5047
Immun-Star™ goat anti-rabbit-HRP	Western Blot: 1:5000	Biorad, # 170-5046

2. 1. 10 Microscope devices and software

Attofluor® cell chamber	Invitrogen
AxioObserver A1 epifluorescence microscope	Carl Zeiss MicroImaging
Axiovert 200 microscope	Carl Zeiss MicroImaging
CFP/YFP filter set	Chroma Technology
CoolLED 440 nm	CoolLED
CoolSNAP-HQ CCD-camera	Visitron Systems
DualView filter slider	Photometrics
ImageJ Software	National Institutes of Health
Inverted fluorescent microscope	Nikon
710 NLO microscope	Carl Zeiss MicroImaging
Microsoft Office Picture Manager	Microsoft

Corporation Oil immersion 63x objective
ORCA-03G camera
ZEN 2010 Software

Carl Zeiss MicroImaging
Hamamatsu Photonics
Carl Zeiss MicroImaging

2. 1. 11 General devices and software

Alphamager® software
Biotek Reader (for BCA assay)
Centrifuges
MS-Excel
MS-PowerPoint
MS-Word
Multimage Light Cabinet
NanoDrop 2000
Powerpac HC
Thermocycler
ThermoMix compact
Ultracentrifuge L-70
iCycler
Mini-PROTEAN® Electrophoresis System
Mupid-One Gel Electrophoresis
Origin Pro 8.5 Software
pH meter
TRI-CARB 4910TR
Ultracentrifuge L-70
UV Table IL-350-M
Ventilator Minivent
X-Ray Film processor

ProteinSimple
BIOTEK Instruments
Thermo Scientific
Microsoft
Microsoft
Microsoft
Alpha Innotech Corporation
Thermo Scientific
Biorad
Sensoquest
Eppendorf
Beckman
Biorad
Biorad
Unit ADVANCE Co., Ltd.
OriginLab Corporation
Inolab
Perkin Elmer Inc., # A491000
Beckman
Bachofer
Hugo Sachs Electronic
SRX 101A Konica

2. 1. 12 Other materials

Dialysis Tubing for virus dialysis
Eppendorf tubes
Cryogenic Vials, Nunc
Falcon tubes
Fiber pads for Western blot
Filter Unit 0.2 RC Spartan 13 0.2 µm
(DNA filtration)

Medical International Ltd.
Eppendorf
Thermo Scientific, #5000-0012
BD Falcon
Bio Rad, #1703933

Whatman, # 10463040

Forene®	Abbott
21-gauge needle	BD Microlane
26-gauge needle	BD Microlane
Gauze	Th Geyer, # 9.068291
Glass Cover Slips 24 mm	Thermo Scientific, # 004710781
Heparin 25000 I.E./5 ml	Rotexmedica
Microscope Slides	Thermo Scientific, # J1800AMNZ
Medical X-Ray	Film Fujifilm, # 4014403 7
Pony Vial	Percin Elmer, Inc., # 6000292
Prolene suture 6-0	Ethicon
Protran Nitrocellulose Transfer Membrane	Whatman, # 4018650
Quickseal Centrifuge Tubes (virus centrifugation)	Beckmann, # 342413
Scintillation Liquid Lumasafe Plus	Lumac LSC, # 3097
Serological pipettes	Sarstedt
Slide-A-Lyzer Dialysis Cassettes, 10K MWCO	Thermo Scientific, # 66383 0.5ml
Spacer Plates for Western blot	Bio Rad, #1653311
Steriflips	Millipore, # SCGP00525
Short Plates for Western blot	Bio Rad, #1653308
Temgesic®	Essex Pharma GmbH
U-40 Insulin 30Gx1/2	Braun, # 40012525
U-40 Insulin Omnifix Solo	Braun, # 9161309v
Water bath	Julabo
6 Well Plates	Starlab, # CC7682-7506
12 Well Plates	Greiner Bio One, # 665180
96 Well Plates	Nunc, # 167008
96 Well Plate for MicroBeta	Perkin Elmer, Inc. #1450-401

2. 1. 13 Buffers and solutions

All buffers were prepared with deionized H₂O, if not indicated otherwise

<u>Name</u>	<u>Ingredients</u>
<u>Plasmid dialysis</u>	
EB Buffer in Ampuwa water	Tris-HCl 10 mM pH 8.5
TE Buffer in Ampuwa water	Tris-Cl 10 mM EDTA 1 mM pH 8.0

Transformation of component cells

5x KCM buffer	CaCl ₂	150 mM
	MgCl ₂	250 mM
	KCl	500 mM
LB Medium	LB medium powder	25 g/L
	Ampicillin	100 µg/mL
LB plates	LB agar powder	40 g/L
	Ampicillin	100 µg/mL

Transfection of HEK293A cells

2x BBS	Na ₂ HPO ₄	1.5 mM
sterile filtrated	BES	50 mM
	NaCl	280 mM
	pH	6.95 (NaOH)
CaCl ₂	CaCl ₂	2.5 M

Adenovirus purification

10x Sucrose buffer	Tris	24.22 g
	MgCl ₂ ·6H ₂ O	8.13 g
	D(+) Sucrose	800 g
	pH	8
	Aqua dest.	ad 2000mL

FRET measurements

FRET buffer	NaCl	144 mM
	KCl	5.4 mM
	MgCl ₂	1 mM
	CaCl ₂	1 mM
	HEPES	10 mM
	pH	7.3

2. 2 Methods

2. 2. 1 Generation of the recombinant plasmids and adenoviral construction of E1-camps and PLM-E1 biosensors

The development the cytosolic cAMP sensitive adenoviral biosensor was based on the already published DNA construct encoding for Epac1-camps²⁴⁹. This gene construct consists of a special nucleotide binding sequence (E157-E316) from the human Epac1 protein. We targeted the E1-camps biosensor to the PLM/NKA microdomain by using a special cloning strategy and thoroughly optimized the new PLM targeted FRET biosensor, which promised direct monitoring of cAMP dynamics in the vicinity of PLM. Following cloning strategies are used to produce reliable PLM-targeted biosensors and adenoviral constructs to monitor FRET changes in the vicinity of PLM (see sections 2. 2. 7-2. 2. 9).

2. 2. 2 PCR- Polymerase chain reaction

To amplify DNA sequence of interest and introduce restriction sites to DNA sequences during cloning, following PCR reaction was applied.

H ₂ O	81 µl
10x Pfu buffer	10 µl
dNTPs 10 mM	2 µl
for. Primer (25 µmol/L)	2.5 µl
rev. Primer (25 µmol/L)	2.5 µl
DNA sequence (200 ng)	1 µl
<i>Pfu</i> DNA Polymerase	1 µl

Following PCR protocol was applied:

(94°C for 5 min, 30 x (94°C for 30 s, 55°C for 30 s, 72°C for t), 72°C – 7 min) possible over night storage at 4 °C.

The elongation time (t) was dependent on the length of the desired PCR product and used enzyme (*Pfu* polymerase replicates 1 kb in 2 min).

2. 2. 3 Gel electrophoresis, DNA purification and quantification

A very important mean to analyze DNA sequences or to generate DNA segments for ligation and cloning, digestion with Type II restriction enzymes (New England Biolabs) was performed according to manufacturer's instructions. The available New England Biolabs buffer (NEBuffer) chart from the manufacturer simplified choosing the correct buffer for a digestion using a single or two enzymes. Following two protocols are applied in this project.

control digestion of DNA for 0.5 h at 37°C:

500 ng template (or 8 µL from a mini-preparation)

1.5 µL NEBuffer (suitable for both enzymes)

0.25 µL restriction enzyme 1 }
0.25 µL restriction enzyme 2 } or 0.5 of a single enzyme

ad 15 µL H₂O

The DNA segments were run on a 1% agarose gel and analyzed quantitatively using the Multi Image Light Cabinet Transilluminator (Alpha Innotech Corporation).

segmental digestion of DNA for cloning:

6–8 µg of vector plasmid or template DNA

5 µL NEBuffer

2.5 µL of restriction enzyme 1

2.5 µL of restriction enzyme 2

ad 50 µL H₂O

digestions were incubated over night at 37°C

DNA was isolated by gel electrophoresis (2. 2. 4), extracted and eluted in 50 µL EB-buffer (vector fragment) or 25 µL EB-buffer (insert).

2. 2. 4 Gel electrophoresis, DNA purification and quantification

Upon generating the PCR product or digestion with restriction enzymes, the DNA fragments were run on a 1% agarose gel (TAE buffer including 0.5 µg/ ml ethidium bromide) at 100-150 V. 1000 bp ladder (Quickload) was run in parallel, as DNA marker. Documentation of the results were prepared as a picture and printed out from the system. The DNA molecules were separated according to their size, DNA segment of interest were excised with a scalpel and extracted and purified using the QIAquick Gel Extraction Kit according to the manufacturer's protocol. The DNA was eluted in TE-buffer (or EB-buffer after BP and LR reaction). The Nanodrop device was utilized to determine the DNA concentration.

2. 2. 5 Ligation

Inserting DNA fragments into a vector plasmid with matching restriction ends requires the application of T4-DNA Ligase to connect the insert with the vector:

Ligation mix:

T4 DNA Ligase	1 μ L
vector (1 μ g)	1 μ L
digested insert(s)/or digested PCR product(s)	11.5 μ L
10x ligase reaction buffer	1.5 μ L

overnight incubation at 14°C

For a triple ligation, the different molecular masses of the used inserts are crucial to calculate vector-to-insert ratios. In this case, two insert samples are used in 11.5 μ L in a ratio adjusted to their molecular weights to provide equimolar amounts.

2. 2. 6 Transformation of competent bacteria cells

The generated plasmid DNA sequence was introduced into One Shot® TOP10 chemically competent *E. coli* or One Shot® OmniMax2T1 (for BP and LR reaction) incubating following reaction mix for 50-60 min at 37°C.

<i>E.coli</i> competent cells	100 μ L
Ligation Mix	15 μ L
H ₂ O	65 μ L
5x KCM Buffer	20 μ L (see 2.1.13)

The reaction mix was incubated on ice for 20 min followed by 10 min at RT. To simplify bacterial growth, 1 mL of LB medium (without antibiotics) was added to the mixture and incubated at 37°C in a ThermoMixer (700 rpm), pelletized and resuspended in 100 μ L of the aspirated supernatant (LB medium without antibiotics). Thereafter, the suspension was spread on ampicillin selective LB- medium plates (kanamycin selective plates are used after BP reaction) and colonies were grown overnight at 37°C and harvested in order to be raised in 4 mL LB medium with ampicillin (kanamycin) overnight at 37°C. The next day plasmid DNA was precipitated out of the bacteria using the Qiagen Plasmid Mini Kit for a 2 mL volume of bacterial suspension. Subsequent DNA restriction analysis demonstrated positive clones, which were used grown in 30 mL of LB medium with ampicillin over night at 37°C and plasmid DNA was extracted using the Qiagen Plasmid Midi Kit. The concentration of DNA was measured using the Nanodrop device, and plasmid DNA sequencing was performed at Eurofins Genomics.

2. 2. 7 Cloning the _{human}PLM-E1 FRET biosensor based on the pcDNA3 Epac1-camps construct

Our aim was to target the cytosolic cAMP sensor to the PLM microdomain via fusing it to the C-terminus of a full length human PLM sequence via a flexible linker GSGSAS. For this, the Epac1-camps plasmid was double digested with HindIII and EcoRI restriction enzymes to remove the N-terminal YFP sequence. The following two inserts were amplified by PCR: 1.) Full human PLM sequence without stop codon was amplified using the primers PLMHindIIIfor and PLMNhelrev; 2.) YFP sequence was amplified using YFPNhelfor and YFPEcoRIrev primers. The PCR products were run on an 1% agarose gel, purified and digested with HindIII/NheI and NheI/EcoRI, respectively, as described in 2 .2. 4. After DNA purification, both extracted and predigested DNAs of PLM and YFP were triple ligated with the HindIII/EcoRI digested pcDNA3-Epac1-camps vector sequence.

2. 2. 8 Cloning the _{canine}PLM-E1 FRET biosensor based on the PLM-YFP construct

After some initial experiments detailed in section 3. 1, an optimized sequence of the PLM-E1 biosensor was designed with the help of Dr. William Fuller, who kindly provided an alternative PLM-YFP sequence having a longer flexible linker between PLM and YFP. To retain this linker sequence KRSRAQASNSAVDGTTPVATG, 6 µg of the given PLM-YFP vector was double digested with KpnI and NotI. Two inserts were prepared by: 1.) PCR amplification of the YFP sequence using the pEYFP-N1 vector as a template with the primers PLMYFPKpnIfor and YFPEcoRIrev as described in 2. 2. 2. The PCR product was purified and digested with KpnI and EcoRI; 2.) 10 µg of the Epac1-camps plasmid were digested with EcoRI and NotI to obtain the second fragment which includes Epac1-CFP sequence. Both digested fragments and the vector were run on a 1 % gel and the DNA was extracted using the Qiaquick Gel Extraction Kit. To ligate the pEYFP N1 _{canine}PLM-linker vector, eluted in 50 µl elution buffer, with the YFP and Epac1-CFP fragments, each eluted in 25 µl elution buffer, following mix is prepared for an overnight ligation at 14°C:

pEYFP N1 _{canine} PLM-linker (~4200 bp)	1 µl
YFP (~700 bp)	6.5 µl
Epac1-CFP (~1200 bp)	5 µl
T4 Ligase buffer 10x	1.5 µl
T4 Ligase	1 µl

2. 2. 9 Generation of the adenoviral constructs Epac1-camps, _{human}PLM-E1 and _{canine}PLM-E1

The adenovirus generation is performed via the Gateway® Cloning system and in accordance with the manufacturer's instructions.

The sequence of interest embedded in the pcDNA3.0 or pEYFP-N1 vector was amplified by PCR using specially designed primers with flanking attB sequences.

Epac1-camps and _{human} PLM-E1		_{canine} PLM-E1	
H ₂ O	81 µl	H ₂ O	81 µl
10x Pfu buffer	10 µl	10x Pfu buffer	10 µl
dNTPs 10 mM	2 µl	dNTPs 10 mM	2 µl
pcDNA3attBFor (10 pmol/µl)	2.5 µl	attBPLMhundfor (10 pmol/µl)	2.5 µl
pcDNA3attBRev (10 pmol/µl)	2.5 µl	attBYFPN1rev (10 pmol/µl)	2.5 µl
pcDNA3 biosensor DNA (200 ng)	1 µl	pEYFP N1 PLM-E1 (200 ng)	1 µl
Pfu DNA Polymerase	1 µl	Pfu DNA Polymerase	1 µl

The PCR reaction was as follows:

94°C 5 min	} x 30
94°C 30 sec	
55°C 30 sec	
72°C 4 min 30 sec (4 min for Epac1-camps)	
72°C 7 min	

PCR product were separated on a 1% agarose gel and purified; the DNA concentration was determined with the Nanodrop system. Each of the constructs were introduced into the donor vector Gateway® pDONR™ 221 (attP) with in vitro recombination reaction (BP reaction) by means of the Gateway® BP Clonase™ II Enzyme Mix.

The cloned vector was transformed into One Shot®OmniMax2T1 bacteria and grown overnight at 37 °C on a kanamycin selective LB-medium plate. The grown colonies were selected and amplified, as described in 2. 2. 6. The control digestion was performed with EcoRI/EcoRV for Epac1-camps and _{human}PLM-E1 as well as with KpnI/NotI for _{canine}PLM-E1. To generate the virus expression vector containing the biosensor DNA construct, the BP reaction product was further recombined with pAd/CMV/V5-DEST™ through the LR-reaction overnight at 25°C. The LR product with the final recombinant adenoviral vector DNA was grown in One Shot®OmniMax2T1 cells and selected by using ampicillin instead of kanamycin LB-medium plates. The positive clone was identified by restriction enzymes EcoRI for Epac1-camps, NheI for _{human}PLM-E1 and XbaI for _{canine}PLM-E1.

Following mixtures are prepared and incubated overnight at 25°C.

BP reaction

PCR eluate	80 ng
pDONR™ 221 vector (150ng)	1 µL
TE-buffer	ad 8 µL
BP Clonase II Enzyme mix	2 µL

LR reaction

DNA	150 ng
pAd/CMV/V5-DEST™ (150ng)	1µL
TE-buffer	ad 8 µL
LR Clonase II Enzyme mix	2 µL

Before HEK293A transfection, Epac1-PLN adenoviral vector DNA was linearized as follows:

DNA	5 µg
10x buffer NEB1	2.5 µl
100x BSA	0.25 µl
Pacl	2 µl
H ₂ O ad	25 µl

Extraction of the DNA is achieved through ethanol precipitation of the digested vector. To initiate the precipitation by electrophilic interaction between negatively charged phosphate groups of the DNA and positively charged sodium ions in solution, 10 µl of 3 M sodium acetate solution was added to the digestion mix and incubated for 30 min at -20°C. At the same time, 70 µl of ice-cold 100 % ethanol was used as a less polar solvent than water to aid the functional groups to form stable ionic bonds and precipitate. After centrifugation for 10 min at 13.300 rpm, the generated DNA pellet was washed with 500 µl ice-cold 75% ethanol and centrifuged again for 5 min at 13.000 rpm. In order to solubilize the DNA pellet, 10 µl H₂O was added. The solution was used for transfection of a 10 cm plate with HEK-293A cells at 80% confluency by the Lipofectamine®2000 reagent (7 µL) in OPTI-MEM® (300 µL), incubated for 20 min at RT. After 7-14 days, virus production led to detachment of transfected HEK293A cells. The detached cells with virus were harvested by centrifuging for 5 min at 800 rpm. The supernatant was used for further HEK293A transduction and virus amplification in Iscove Basal Medium (5% FCS, 1% antibiotic, antimycotic). Performing a ultracentrifugation of the lysed virus containing supernatant of HEK293A cells (40.000 rpm overnight at 16 °C, Beckmann Rotor Ti90). The virus was concentrated in a cesium chloride gradient during centrifugation. The developed virus band was collected using a 21 gauge needle and dialyzed in 10 x sucrose buffer. To determine physical virus concentration, the optical density (OD₂₆₀) was measured. After diluting the virus solution 1:100 with sucrose buffer containing 10% of sterile glycerol, the aliquots were labeled and stored at -80°C. Using

a Plaque Assay (Cooper, 1961) the biological virus activity (plaque forming units per ml [pfu/mL]) was assessed. For this purpose, 6-well plates of HEK293A cells covered with 1.5% plaque GP agarose were prepared and transduced with virus at 10, 100 and 1000 pfu/well (calculated via physical virus concentration) and analyzed. Adult rat ventricular cardiomyocytes were isolated as described in 2. 2. 19 and transduced with the E1-camps/E1-PLM virus (MOI 300). Imaging experiments were performed 48 h after transduction.

2. 2. 10 Calculating the multiplicity of infection and adenoviral transduction of ARVM

ARVMs were isolated as described (see section 2. 2. 19), counted in a Naubauer Chamber (Celeromics), seeded on 6-well plates and maintained in culture for 1-2 h. Approximately 1-1.5 million ARVMs in total were used for transduction. In order to calculate the volume of virus to achieve the desired multiplicity of infection (MOI) for a specific amount of cells, we used the following equation:

$$\text{Adenovirus volume added } (\mu\text{l}) = (\text{Required MOI} \times \text{number of cells}) / (\text{PFU}/\mu\text{l})$$

The calculated amount was added to a volume of fresh culture medium necessary to cover the cells to be transduced (2 mL/well). The culture medium (Medium 199 supplemented with 5 mmol/L taurine, 5 mmol/L carnitine, 5 mmol/L creatine, penicillin/streptomycin and L-glutamine supplement) of ARVMs was replaced with the viral culture medium, and the ARVMs were further incubated with the adenovirus for 48h at 37°C and 5% CO₂. In case of relatively high amount of dead ARVMs, the culture medium was replaced after 24 h.

2. 2. 11 Cell culture and transfection of the HEK293A cell line

In order to test newly developed FRET biosensors, HEK293A cells were cultured at 37°C and 5% CO₂ using Dulbecco's Modified Eagle's Medium (DMEM medium) supplemented with 4.5 g/L glucose, 10% FCS, 2 mM L-glutamine, 100 U/mL penicillin and 100 µg/ml streptomycin. For passaging, cells were washed with sterile phosphate buffered saline (PBS), detached from the surface of the wells/flask using 2 mL 0.05% Trypsin (Invitrogen), resuspended and split in a ratio of 1:10 in fresh cell medium.

Plated on coverslips in six well plates the HEK293A cells were ready for transfection in 24 h, when they reached 60-70 % confluency. In general, two different transfection methods were used, depending on the purpose of transfection: 1.) The CaCl₂ method for having a reasonable expression rate to analyze the quality of the plasmid and 2.) the Lipofectamine

method to accomplish enhanced transfection efficiency for protein overexpression and quantification analysis.

2. 2. 11. 1 Transfection with CaCl₂ under sterile conditions:

10 µl of Plasmid DNA (1 µg/µl) were added to 440 µl of sterile H₂O. The DNA dilution was mixed with 50 µl of 2.5 M CaCl₂ and 500 µl 2x BBS. After 10 min incubation at RT, 166 µl of the mixture were added dropwise to each well.

2. 2. 11. 2 Transfection with Lipofectamine 2000® under sterile conditions:

Following the manufacturer's instructions for optimal transfection, 36 µl of the Lipofectamine 2000® reagent were diluted with 846 µl Opti-Mem® Medium, and 1.2 µl of the DNA Plasmid (1 µg/µl) in 150 µl of the same medium. After mixing both dilutions, a DNA-lipid complex was allowed to develop for 20 min. Thereafter, 250 µl of the reaction mix was dropwise pipetted onto each well with HEK293 cells in culture medium and the experiments were conducted after a 24 h incubation at 37°C and 5 % CO₂.

To transfect cells with newly generated viral vectors (see section 2. 2. 9), the transfection mix contained 300 µL Opti-MEM, 5 µg linearized DNA in the pAd_CMV_V5DEST vector and 7 µL Lipofectamine 2000® reagent for a 10 cm plate of HEK293A cells.

2. 2. 12 SDS-PAGE and Western Blot analysis

Using SDS-PAGE, proteins were separated according to their size by sodium dodecyl sulfate polyacrylamide gel electrophoresis, whereas in Western Blotting, separated proteins were transferred from the gel onto a polyvinylidene fluoride or nitrocellulose membrane and analyzed for protein expression by using specific antibodies.

Experimental methods for the project phase in London:

For expression analysis of the _{human}PLM-E1 sensor to be examined, transduced HEK293 cells were lysed in 500 µL 2 x SDS sample buffer (100 mMol Tris, 4% SDS, 20% glycerol, 0.2% bromphenol blue, 5% β-mercaptoethanol in H₂O, pH 6.8) per well (if not indicated otherwise), scraped and harvested into 1.5 mL tubes. Gels were prepared beforehand according to following instructions, starting with a 10% acrylamide (Protogel, National Diagnostics) resolving gel, suitable for a 75 kD large protein.

Table 4. Ingredients of the used gels for Western Blot analysis at King's College London

Ingredient	Resolving gel (10 %)	Stacking gel (4.5 %)
Tris HCl (1M) pH 8.8	3.75 mL	-
Tris HCl (1M) pH 6.8	-	0.625 mL
Acrylamide (30%)	3.33 mL	0.75 mL
SDS (10%)	0.1 mL	50 μ L
TEMED	5 μ L	10 μ L
APS (10%)	50 μ L	80 μ L
H ₂ O	2.76 mL	3.465 mL

Protein samples and protein ladder (Precision Plus Protein TM Dual-Colour Standards [Bio-Rad]) were run at constant 100 V for about 1.5 hours in SDS running buffer (0.025 M TRIS, 0.19 M glycine, 1% SDS). The protein migration continued until the blue dye front reached the bottom of the resolving gel. The SDS-PAGE was performed using the Mini protean III Tetra Cell system (Bio-Rad). Upon separating the proteins according to size in the resolving gel, they were transferred onto polyvinylidene fluoride (PVDF) membranes (GE Healthcare) pre-rinsed with methanol and transfer buffer (0.025 M TRIS, 0.19 M glycine, 20 % methanol, 0.1 % SDS). The gels on membranes were sandwiched between six layers of filter paper presoaked in transfer buffer. Next, the transfer in a Hoeffer TE77 semi-dry transfer unit was carried out at 10 V for 35 min with a current restricted to 250 mA per gel.

The proteins were blocked against non-specific binding with PBST (PBS + 0.1 % Tween) + 5% milk powder (Marvel) over night at 4°C, the membrane was then treated with relevant primary antibodies (diluted in blocking buffer) for 2 h at room temperature (RT). The specific dilutions for primary antibodies are detailed in Table 1. The membranes were washed for one hour (each washing step: 10-15 min). To visualize the resulting primary antibody binding, the probes were incubated with horseradish peroxidase (HRP)-conjugated secondary antibody (diluted in blocking buffer) for 2 h at RT. The specific dilutions for secondary antibodies incubations are detailed in Table 2. After another washing procedure for one hour, the membranes were ready for enhanced chemiluminescence (ECL) analysis. Here, the HRP conjugated antibodies formed a complex with the ECL reagent mixture, detected via Hyperfilm ECL high performance X-ray film (GE Healthcare) for different acquisition times and developed using a Fuji RGII automatic processor (Fuji). Upon scanning the protein bands, they were subjected to densitometric analysis.

Experimental methods for the project phase in Göttingen:

Having produced the canine PLM-E1 FRET biosensor construct, SDS-PAGE/Western Blot analysis for characterization of expression and localization of the optimized sensor was performed. Apart from the following small modification, it was accomplished as at King's College London.

Cells (HEK293A or ARVMs) to be analyzed were lysed by 500 µL/well 3x SDS-sample buffer (200 mM Tris, 6 % SDS, 15 % glycerol, 0.3 % bromphenol blue, 10 % 2-mercaptoethanol in H₂O, pH 6.7) and harvested. Next, 2 gels for SDS-PAGE analysis were prepared as follows.

Table 5. Ingredients of the used gels for Western Blot analysis in UMG, Göttingen

Ingredient	Resolving gel (10 %)	Resolving gel (12 %)	Stacking gel (4.5 %)
4x Tris/SDS pH 8.8 (500 mmol/L Tris, 0.4 % SDS)	3.0 mL	3.0 mL	-
4x Tris/SDS pH 6.8 (500 mmol/L Tris, 0.4 % SDS)	-	-	940 µL
Acrylamide (30%)	4 mL	4.8 mL	18.8 µL
TEMED	18 µL	18 µL	7.5 µL
APS (10%)	48 µL	48 µL	80 µL
H ₂ O	5 mL	4.2 mL	2.31 mL

After running the proteins on a gel, they were transferred onto nitrocellulose membranes (Protran, Whatman) inside the Mini Trans-Blot Transfer Cell (Bio-Rad), filled up with ice cold transfer buffer (32 mM Tris, 192 mM glycine, 4 % methanol) and blotted for 2 h at 100 V. To precisely cut the membrane in order to detect multiple proteins for one probe, it was stained with Ponceau S solution (0.5% in 10% acetic acid) for 5 min, washed with water until bands appeared. As described above, the membrane had to be blocked against unspecific binding with 5% milk in TBST (TBS + 1 % Tween), this time at RT for 1h. The incubation with primary antibodies (for dilutions see section 2. 1. 9) was done at 4°C overnight. After membrane incubation with a HRP-coupled secondary antibody (see section 2.1.9) for an hour at RT and treatment with ECL (Thermo Scientific). Films (Fuji Medical X-Ray Films, Fujifilm) were developed using a film processor (SRX 101A Konica, USA) with varying exposure times (1 s-10 min), scanned and analyzed.

2. 2. 13 Co-immunoprecipitation

With this co-immunoprecipitation (co-IP) protocol we were able to prove physical association of proteins expressed either in HEK293A cells or ARVMs. All samples are handled at 4°C during the entire procedure. The lysed protein amount used for one co-IP experiment was equal to cells from 1-3 wells of one six well plate (1 well for transfected HEK293A cells and 3 wells for transduced ARVMs). 20-30 µL of the GFP-Trap® reagent (Chromotek) was washed 5 x 1mL in lysis buffer containing 2 mg/mL octaethylene glycol monododecyl ester (C12E10) in co-IP buffer (1mM EDTA in PBS plus protease and phosphates inhibitors) and equilibrated overnight at 4°C. Upon lysing the cells in 500 µL co-IP lysis buffer, the cells were carefully scraped from the bottom of the well, agitated at 4°C and centrifuged (17000 g) for 5 min at 4°C. The supernatant of the lysed centrifuged cells was incubated with the GFP-Trap® beads over night at 4°C. Thereafter, the beads were washed 5 times (1mL each) with 4°C co-IP buffer (0.5 mg/mL C12E10). The beads were then resuspended in 100 µL 2x SDS PAGE sample buffer supplemented with 5% β-mercaptoethanol.

The same protocol was applied for co-IP analysis by means of primary antibody immobilized on Protein G Sepharose 4 Fast Flow® (GE Healthcare). 20 µL sepharose beads were washed with co-IP lysis buffer (5 x 1mL) and equilibrated overnight at 4°C (or for 1-2 h at RT). 1 µg of primary antibody was pre-immobilized on the beads, again over night at 4°C. The beads were incubated with solubilized and centrifuged supernatants of cells (HEK293A or ARVM) from 1-3 wells of a six-well plate overnight at 4°C.

Collecting samples at each step throughout the entire procedure, including the multiple washing steps, was important to trail protein loss and to facilitate the comparative analysis of starting, unbound and IP - fractions.

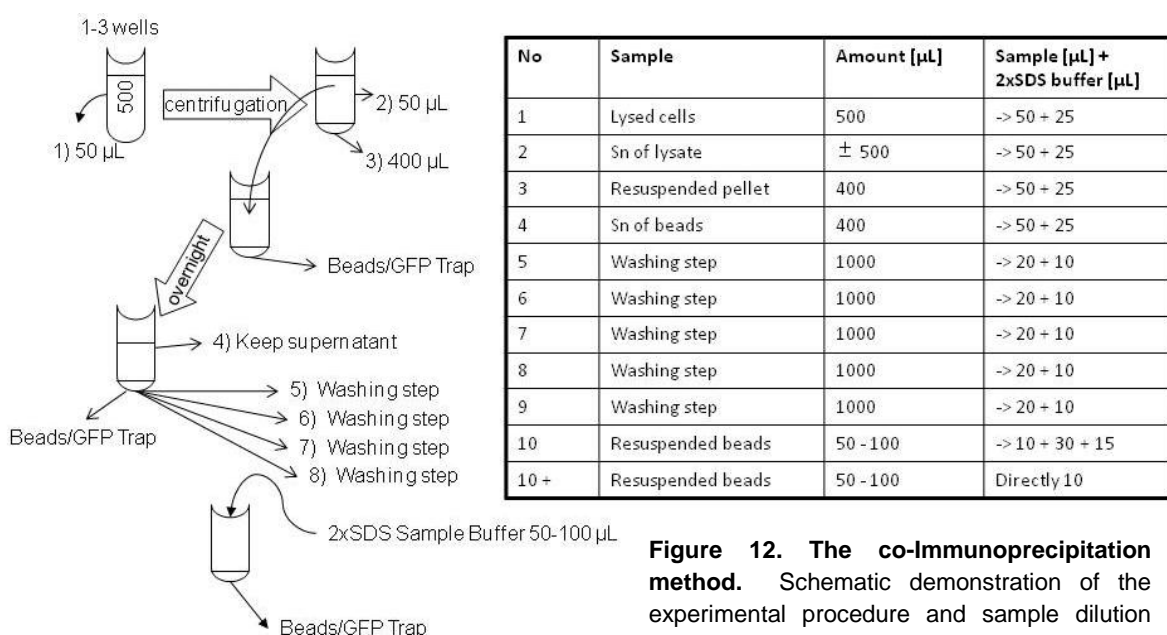


Figure 12. The co-Immunoprecipitation method. Schematic demonstration of the experimental procedure and sample dilution steps.

2. 2. 14 Cell surface biotinylation

Testing the cell surface expression of the PLM-E1 DNA construct was essential to prove correct localization and expression of the developed tagged FRET biosensor. A significant amount of biosensor protein was expected to reach the cell surface. To verify this, HEK293 cells were seeded and cultivated as mentioned in section and transfected with the PLM-E1 plasmid at a confluency of 65 %. One well of a six well plate was washed three times very slowly and carefully with 37°C PBS. Biotinylation solution (1mg/mL sulfo-SS-NHS-biotin in PBS) was added to the cells and incubated for 10 min at 37°C in incubator. After rinsing the cells to remove the excess biotinylation reagent, cells were lysed in 0.5 mL per well of 1% triton X-100 in PBS supplemented with protease inhibitors (lysis buffer) and lysed for 30 min at 4°C. Samples were transferred to tubes (scraped and harvested from plate surface) and spun down at 17500 G for 5 min at 4°C. The supernatant was kept for further analysis, additionally one sample (50 µL) was retained from it and mixed 1:1 with 2x SDS PAGE sample buffer without β-mercaptoethanol (refer to as starting material). The retained supernatant was added to Streptavidin-Sepharose beads. Beforehand ~30 µL beads per sample were washed multiple times, preequilibrated in lysis buffer at 4°C and recovered by centrifuging 1 min at 17500G 4°C. The beads were incubated with the supernatant of the lysed cell pellet for 1-4 hours at 4°C or overnight. The beads were spun down at 17500 G for 2 min at 4°C. A small sample (100 µL) was taken and mixed 1:1 with 2x SDS-PAGE sample buffer with 5% β- mercaptoethanol (refer to as unbound fraction). The beads were washed with lysis buffer. Following final washing step, 100 µL 2x SDS-PAGE sample buffer with 5% β-mercaptoethanol was added. Before SDS-PAGE/Western Blot analysis, samples were heated at 60°C for 15 min to elute proteins in the bound fraction (refer to as beads fraction).

2. 2. 15 Generation of a HEK293A cell line stably expressing PLM-E1

Using the principle of selection via antibiotic resistance, HEK293A cells exclusively expressing the PLM-E1 construct were selected, propagated and stocked at -80°C. HEK293A cells were seeded on a 10 cm dish to achieve around 75 % confluency overnight. On the next day, they were transfected with a mix of 300 µg DMEM Medium without supplements, 3 µg PLM-E1 DNA plasmid and 7 µL Lipofectamine 2000®. One day after transfection, the medium was changed to DMEM medium containing 4 µL/mL Genitacin antibiotic (50mg/mL, Thermo Fischer). Non-transfected cells usually started to detach during after one week of incubation at 37°C, while transfected cells started to form small colonies, which were detectable macroscopically and could be picked. Using a flexible tube and a pasteur pipette, the colonies were picked by sucking and blowing each of the colonies back into wells of a 12-well plate containing DMEM Medium without supplements (1 mL/well). After

overnight incubation at 37°C, cells were treated again with Genticin, which permitted PLM-E1 expressing HEK293A cells to proliferate and to reach maximum confluency. Next, cells were transferred to a 6-well plate, and subsequently to a 10 cm dish to propagate the line. After sufficient amount of cells has been cultured, they were washed with PBS, trypsinized and resuspended in the 10 cm dish with 6 mL of DMEM culture medium without supplements, 1.7 mL FCS and 0.7 mL DMSO. The cell suspension was divided into Kryocups (1mL), labelled and frozen at -80°C.

2. 2. 16 Ouabain sensitive ⁸⁶Rb uptake measurements

We measured the ouabain sensitive ⁸⁶Rb uptake as a surrogate for potassium to determine the NKA activity of transfected HEK293A cells or untransfected cells as described by Howie et al.²⁵². Cells were cultured on 12-well plates until they reached 70% confluency. The measurements were performed in presence of the sodium ionophore monensin (Sigma) to ensure consistent intracellular Na⁺ and the Na/K/2Cl cotransporter inhibitor bumetanide (Sigma) to depress background uptake of ⁸⁶Rb. Cells were rinsed with the extracellular solution and equilibrated with exactly 1 mL/well of same solution for 20 min at 37°C. During change of the medium, we added 100 µM ouabain to half of the wells and PBS (vehicle) to the other half and incubated at 37°C for 5 min before initiating ⁸⁶Rb uptake by the addition of 1 µCi/mL ⁸⁶Rb per well. The cells were incubated at 37°C for exactly 15 min previous to stopping the uptake by rapidly washing steps in three baths of ice cold PBS. The complete wash protocol should take ~30 sec. Hereupon, cells were lysed in 0.2 mL lysis buffer per well (1% Triton-100 in PBS). The specific activity of the ⁸⁶Rb solution is determined through 3x measurements of 1 µL ⁸⁶Rb solution in 3 scintillation vials ('total counts vials'). Next to this, 3x 50 µL of each cell lysate per well was transferred to 3 separate scintillation vials for. Likewise 3x 5 µL cell lysate volume to 3x cuvettes containing protein assay reagent. The number of ⁸⁶Rb molecules of the lysates were measured in a liquid scintillation counter, and the protein content of lysates was measured in a spectrophotometer using a Bradford assay with bovine serum albumin as a standard.

Extracellular solution (pH7.4)

20mm NaCl	10mM HEPES
120mM NMDG-Cl	10 µg/mL monensin
1mM MgCl ₂	10mM glucose
1mM CaCl ₂	100 µM bumetanide
5mM KCl	

2. 2. 17 Immunofluorescence

Immunofluorescence antibody staining was performed on transduced and nontransduced cardiac myocytes to visualize expression, localization and co-localization of single and multiple stained proteins. Even though crosslinking agents, like paraformaldehyde, are better in preserving cell structure, they reduced the antigenicity of some cell components, which was the case in most of our test experiments. For this reason, cells were fixed for 20 min with ice-cold 99.9 % ethanol at -20°C to immobilize antigens. Fixed cells were either stored in PBS at 4°C or directly blocked with blocking buffer (20% FCS and 0.15% Triton X in PBS) for 2 h. The cells were washed with PBS and co-stained with rabbit polyclonal anti- FXYD1 (abcam) and either mouse monoclonal anti- α_1 antibody (Millipore) or goat polyclonal anti-PDE3A (Santa Cruz) antibodies in in blocking buffer over night at 4°C, washed once with PBS, followed by the incubation with secondary antibodies diluted as mentioned in section 2. 1. 9 for 2h at RT. Confocal imaging was performed using Zeiss LSM 710 laser scanning confocal microscope (Carl Zeiss MicroImaging) equipped with a Plan-Apochromat x63/1.40 oil-immersion objective.

2. 2. 18 Heart failure rat model: Myocardial Infarction

For the animal model used in this project, adult male Sprague Dawley rats (250-300 g) were subjected to proximal coronary ligation to induce chronic myocardial infarction as described before¹⁴⁵. All surgeries and experiments with failing cells were performed at Imperial College London (lab of Prof. Julia Gorelik). Briefly, the rats were anesthetized after treatment with antibiotics and buprenorphine (0.03 mg/kg). After an incision into the pleural space of the chest, the left anterior descending coronary artery was ligated by a suture with 6-0 silk. Sixteen weeks post surgery the MI-rats were subjected to echocardiography analysis via Vevo, 770 micro-imaging system, Visualsonics. Upon extraction at 16 weeks post MI, hearts and aged matched control (AMC) hearts were weighed. The measured heart weight to tibia length ratio (HW/TL) served as an indicator of progressive hypertrophy next to ejection fraction volume, which was determined from M-mode of the used imaging system.

2. 2. 19 ARVM Isolation by Langendorff perfusion

The adult rat ventricular myocytes were isolated by Langendorff perfusion by Tobias Goldak, (AG Nikolaev, Gö).

Before the isolation process started, the heart perfusion system was turned on in order to warm up the waterbath and its plastic tubing system. At 37°C reached in the water bath optimal tissue digestion could be performed. To do this, adult rats were anaesthetized and

sacrificed by cervical dislocation. The thorax was cut open, leaving the atrias easy to access. 1 mL of Heparin (25000 I.E./5ml, Rotexmedica) was injected to one of the atrias. After reducing the bleeding with some paper tissue, the heart was rapidly excised. After washing the heart gently but quickly in 5 mL ice cold 1 x perfusion buffer, it was transferred to a petri dish filled with ice cold 1 x perfusion buffer. The aorta was mounted onto a grooved cannula with the help of two tweezers under a stereomicroscope as quickly as possible (not more than 2 min), secured with a clip and tied with suture. The heart was perfused with 1 x perfusion buffer through the tubing systems (8 mL/min). As soon as the blood was washed (as judged by checking the color of the collected perfusion buffer, which went through the coronary arteries (1-2 min perfusion)), the solution was switched to the digestion buffer. We digested for 11 minutes, whilst collecting the collagenase buffer and recirculating by topping up the reservoir until the required time of the digestion is attained. Before the digestion time ended, 5 mL of digestion buffer was collected and transferred to a beaker. After 11 minutes of digestion the perfusion system was shut down and the ventricles of the heart were removed from the cannula into the prepared beaker. The ventricles were cut into small pieces to increase the surface area for digestion. The smaller pieces were homogenised via a 10 mL pipette mechanically. This procedure was repeated after adding 10 mL of stopping buffer into the cell suspension. The suspension was topped up to 25 mL with stopping buffer and filtered using a nylon mesh and left to settle for 8 min and washed twice with 25 mL stopping buffer having 8 min settlement time in between each step.

The sedimented cardiomyocytes were further subjected to re-calcification protocol. Intracellular calcium was increased in 3 steps to have a final concentration of 1 mM, letting the cells settle for 8 minutes after each step:

25 mL stopping buffer	2.5 μ L CaCl ₂ 1 M	final concentration	100 μ M
25 mL of stopping buffer	10 μ L CaCl ₂ 1 M	final concentration	400 μ M
25 mL of stopping buffer	22.5 μ L CaCl ₂ 1M	final concentration	900 μ M

Upon recalcification the cardiomyocytes were resuspended in 10 mL M199 medium with supplements. Before plating the freshly isolated ARVMs on laminin (Sigma) coated glass coverslips, the cells were counted in a counting chamber (Naubauer Chamber) in order to calculate the desired amount of cells per well for adenoviral transfection. Cells were maintained in culture at 37°C / 5% CO₂ for at least 2h prior to use in biochemical/ adenoviral infection experiments.

10 x Perfusion buffer (substances in mmol/L): 120.4 NaCl, 14.7 KCl, 0.6 KH₂PO₄, 0.6 Na₂HPO₄·2H₂O, 1.2 MgSO₄·7H₂O, 10 Na-HEPES, pH 7.4 in H₂O.

1 x Perfusion buffer (substances in mmol/L): 4.6 NaHCO₃, 30 taurine, 10 2,3-butanedione-monoxime, 5.5 glucose, 50 mL 1 x perfusion buffer ad 500 mL H₂O.

digestion buffer: straight before use, 50 mL of the perfusion buffer were supplemented with 40 µM CaCl₂ and 0.1 g Collagenase Typ II.

stopping buffer: 130 mL supplemented with 10 % FCS and 12.5 µM CaCl₂.

culture medium: 500 mL M199 medium (Sigma) was supplemented with 312.5 mg taurine, 500 mg D,L-Carnitine and 327.5 mg D,L-Creatine, 5 mL antibiotics (100 U/mL penicillin, 100 µg/mL streptomycin).

Hearts from adult male rats with the induced myocardial infarction model and aged matched control rats were isolated as previously described²⁵³ by Peter O'Gara at the Imperial College London.

2. 2. 20 FRET measurements of ARVMs transduced with PLM-E1 and E1-camps

Cardiomyocytes on laminin coated coverslips underwent a 48 hours incubation upon adenovirus transduction and were washed off excessive viral particles once with fresh culture medium before starting the FRET experiments. The coverslips with transduced cells on them were mounted in the cell chamber, which was used during imaging experiments. Cells were washed once and 400 µL fresh FRET buffer was added (300 µL if one was using 3 or more substances during experiments). All substances used during FRET experiments were diluted in FRET buffer. Using a drop of immersion oil, the chamber was placed onto the objective (x63) of the microscope.

Measurements were performed on an inverted fluorescent microscope and analyzed using ImageJ software. The components of a FRET microscope system included a light source to excite donor protein at its excitation wavelength, a beam splitter to divide the emission light of the donor and acceptor protein into two independent channels, and a camera to detect donor and acceptor channel intensities simultaneously (Figure 13). As described before²³⁹ a CoolLED single-wavelength light emitting diode was used as the light source for all FRET experiments. ARVMs with a good sensor expression were quickly selected using live fluorescent light mode manually to avoid photobleaching effects. The cyan fluorescent protein (CFP), integrated in our FRET biosensors as the donor protein, was excited at 440 nm. The general emitted light from the cell was split into CFP and YFP emission channels using a DualView beam splitter and detected via a CCD camera in two separate channels.

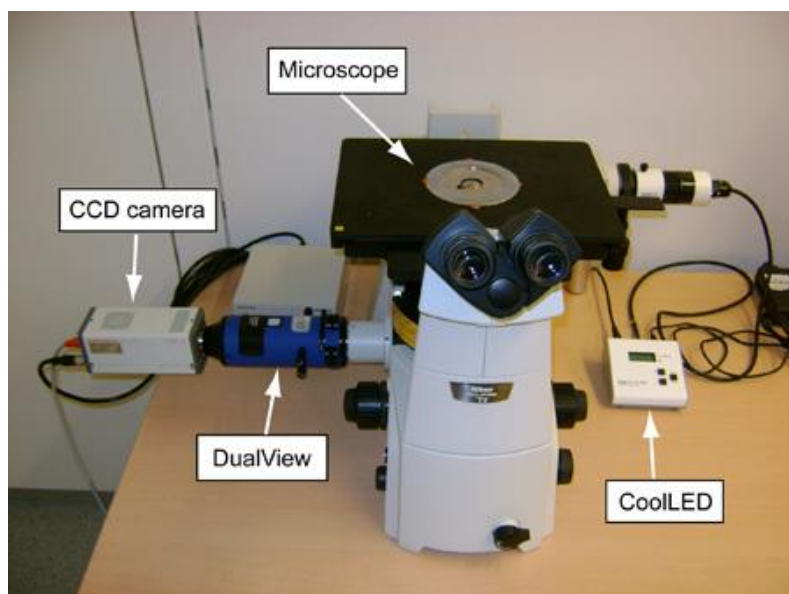


Figure 13. Layout of the FRET imaging setup comprised of a CoolLED, inverted Nikon microscope, DV2 DualView, and ORCA-03G CCD camera. taken from Sprenger et al.²³⁹

Since viral expression of the biosensor protein inside the single cardiomyocyte vary from very strong to very low, sporadically showing perinuclear overexpression, cells with homologous fluorescence intensities are chosen for experiments. Perinuclear overexpression aggregates were excluded from the region of interest in all measurements. Upon adjusting the exposure time between 20-40 ms to have a relatively good signal-to-noise ratio, especially at the baseline, the images of the CFP and YFP emission channels were recorded every 5 seconds. As soon as a stable baseline had been reached, the compound dilutions at a volume of 400 μL (or 300 μL) were gently added and changes of the YFP/CFP FRET ratio were monitored. The obtained raw data for CFP and YFP channel intensities were analyzed offline using Microsoft Excel and Origin 8.5 software. For precise quantification of the changes in intensities during a single measurement, the YFP/CFP intensity ratio was corrected for the bleedthrough (0.9 coefficient) of the donor fluorescence into the acceptor channel:

$$\text{FRET}_{\text{ratio}} = (\text{YFP}_{\text{intensity}} - 0.9 \times \text{CFP}_{\text{intensity}}) / \text{CFP}_{\text{intensity}}$$

All data shown in section 3 are corrected FRET ratios calculated from the raw intensity data.

2. 2. 21 Statistics

All data were analyzed using Origin Pro 8.5 software and shown in means \pm SE and differences between experimental groups were analyzed using the one-way ANOVA test. Differences were considered significant at $p < 0.05$.

3. Results

3. 1 Generation of the first version of the PLM-E1 FRET Biosensor

In order to measure spatio-temporal regulation of cAMP dynamics in the vicinity of Phospholemman (PLM), we developed a FRET based biosensor derived from the cytosolic cAMP sensor E1-camps or simply E1-camps²⁴⁹ fused to the carboxyl terminus of the human PLM cDNA provided by Prof. Michael Shattock. The cytosolic E1-camps sensor is based on a single cAMP binding domain and was used as control in all FRET experiments. The reason to use Epac1-camps is its capability previously identified in other studies to show a larger FRET change upon cAMP binding in cells, although having a slightly lower affinity than some other cAMP sensor such as Epac2-camps ($\sim 2 \mu\text{M}$ vs. $\sim 1 \mu\text{M}$)²³⁹.

The human PLM sequence was fused to the YFP-Epac1-CFP sequence of E1-camps cDNA via NheI restriction endonuclease site to create the plasmid PLM-E1 in the pcDNA3.0 vector. Additionally, the sequence between PLM and YFP contained a special linker consisting of 18 bp (encoding GSGSAS), which should ensure a proper folding of the sensor during the translation of the protein (Figure 14).

Hereupon, one had to test the functionality of the targeted cAMP sensor in living cells.

The pcDNA3.0 vector with its cytomegalovirus enhancer-promoter drives sensor expression in mammalian cells and simplifies its expression in HEK 293A cells after transfection with the PLM-E1 biosensor plasmid.

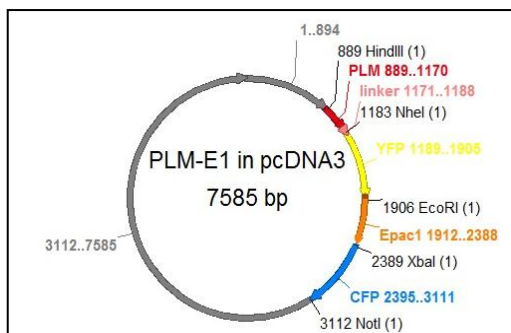


Figure 14. PLM-E1 construct in pcDNA3.0 vector.

The vector containing the PLM-E1 coding sequence contain a short linker (18 bp) GGA TCC GGA TCT GCT AGC between human PLM and YFP sequences.

3. 1. 1 Expression and functional analysis

First tests of transiently transfected HEK 293A cells were performed under a fluorescent microscope to analyze subcellular localization and to do first experiments of the FRET functionality of the targeted sensor. Epifluorescence images of PLM-E1 containing HEK293A cells showed a regional sensor expression pattern (Figure 15A), as expected. PLM-E1 localized at the plasma membrane and exhibited robust FRET. Upon β -adrenergic agonist isoproterenol (Iso) mediated cAMP stimulation, the PLM-E1 transfected HEK293A cells responded with a change in FRET ratio, proving its functionality in the sensor (Figure 15C). SDS Page/Western blotting was carried out to check the size of the expressed protein. Based on the generated sequence, the PLM-E1 protein should have a theoretical size of approximately 75 kD. Immunoblot analysis of PLM-E1 transfected HEK293 cells under non-stimulated conditions were performed and investigated regarding relative expression level and molecular weight. Using anti-GFP antibodies, we observed bands corresponding to this theoretical weight for products expressed from the pcDNA construct including one additional band at about 20 kD corresponding to the size of a monomeric GFP (CFP/YFP), indicating a possible partial degradation of the sensor protein (Figure 15B). Thus, our results indicate that the functional sensor construct is well expressed after transfection into HEK293 cells.

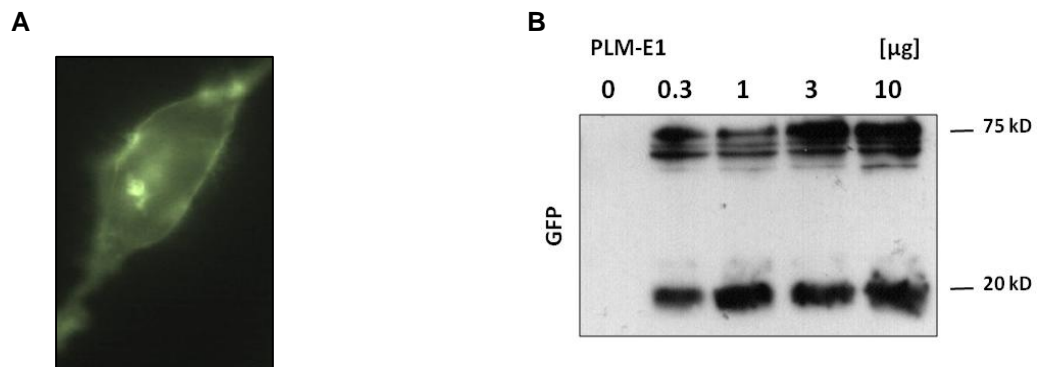
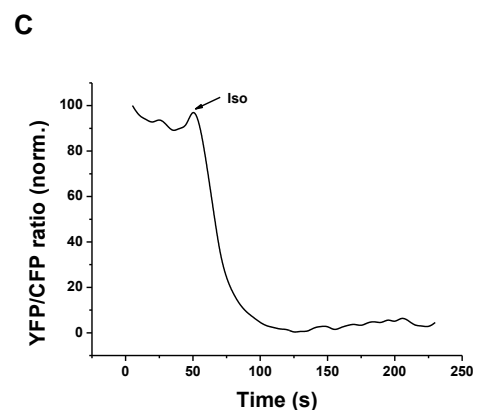


Figure 15. Expression, function and localization of PLM-E1 in HEK 293 cells.

(A) An epifluorescence image of a PLM-E1 transduced HEK 293A shows a predominant location on the plasma membrane, as expected. (B) Immunoblot analysis of PLM-E1 protein (~75 kD) expression after 24 hour transfection of increasing plasmid amounts into HEK293 cells probed with anti-GFP antibody. Blot is representative of at least three individual experiments. (C) FRET ratio trace recorded in HEK293A cells expressing PLM-E1. Isoprenaline (Iso) 100 nM induced an increase in cAMP visualized by a decrease in YFP/CFP FRET ratio, proving good sensor protein functionality.



3. 1. 2 Localization analysis

Since we plan to use the PLM-E1 as a tool to detect cAMP dynamics in the microdomain formed by PLM and the Sodium Potassium Pump in adult rat ventricular myocytes (ARVMs), it is obligatory to prove the physical association of the newly developed tagged PLM-E1 FRET biosensor with the α_1 -subunit (α_1 -SU) of the NKA, comparable to endogenously expressed PLM in ARVMs. Using anti-NKA α_1 -SU antibodies immobilized on protein G-Sepharose beads, α_1 -SU was immunoprecipitated from PLM-E1 transfected HEK 293A cells, and all samples taken during the experiment were probed with anti-GFP antibodies. Interestingly, we could not detect any signal in the IP fraction (Figure 16A), likely due to the fact that although the biosensor is highly membrane localized, the expressed PLM-E1 protein is not associated with the α_1 -subunit. Troubleshooting for this problem led to optimization of the PLM-E1 construct with the already published *canine* PLM-YFP sequence, for which positive co-IP with the NKA has been published²⁵⁴. Of note, it is well known that HEK293 cells do not natively express any PLM. Considering this, it is not possible to detect any endogenous PLM in the following co-immunoprecipitation experiments.

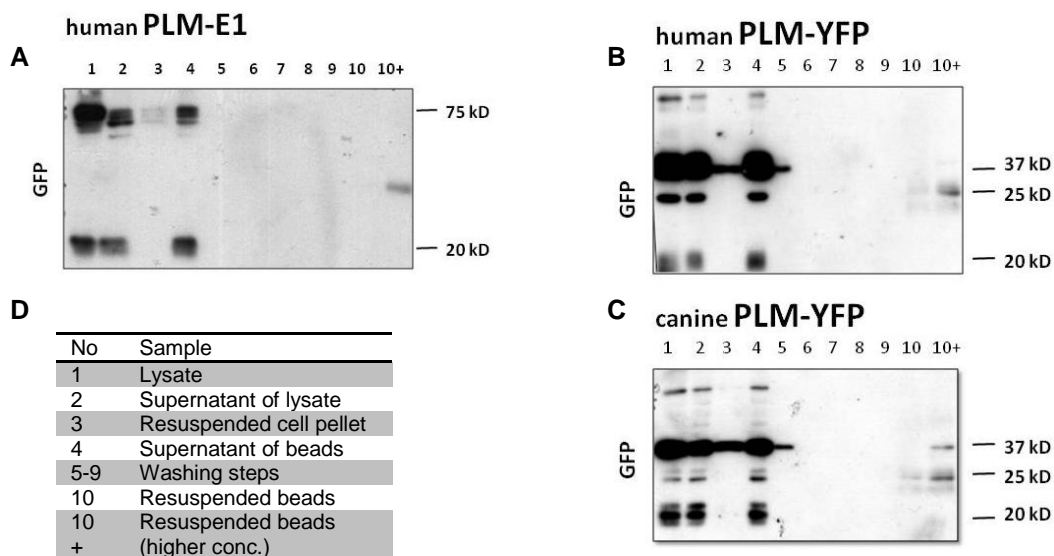


Figure 16. Co-immunoprecipitation by 1 μ g α_1 -SU antibodies immobilized on Sepharose beads with the previously established protocol (see Methods) is shown. (A) PLM-E1 could not be immunoprecipitated from HEK 293A cells transfected with the PLM-E1 plasmid. (B) 24 h transfection of HEK 293A cells with *human* PLM-YFP and (C) *canine* PLM-YFP varying in their linker length were used as controls for the co-IP experiments. (D) Immunoprecipitation starting material (No 1-3), material not immunoprecipitated (No 4: not IP-ed fraction) and immunoprecipitated material (No 5-10+: IP fraction) were separated on SDS-PAGE (10% gel), gels were transferred to membranes immunoblotted as shown. The protein folding does influence the association of PLM-E1 with the sodium pump α_1 -subunit. *canine* PLM-YFP with a long linker shows a high capacity in binding to the α_1 -SU of the NKA.

3. 2 Generation of the optimized PLM-E1 FRET Biosensor and the adenoviral construct

Despite of testing the functionality of the PLM-E1 and the clear change in cAMP induced FRET signal responses (Figure 15C) as well as the obvious membrane localization and translation of the developed PLM-E1 sensor protein (Figure 15A) , it did not show any positive results regarding co-immunoprecipitation with the α_1 -SU of the NKA (Figure 16A). We considered a special *canine*PLM-YFP cDNA (kindly provided by Dr. William Fuller) as a possible alternative for FRET sensor backbone.

As mentioned in the last section, we also demonstrated that the *canine*PLM-YFP fusion protein construct is clearly associated with the α_1 -SU of the sodium-potassium pump in HEK 293A cells (Figure 16C). It is inserted in a pEYFP N1 vector (Clontech, Paulo Alto, CA) and has a long linker sequence (60 bp) KRSRAQASNSAVDGTPVATG between the coding sequence for PLM and YFP.

Upon comparing both PLM-YFP sequences with different linker lengths (18 vs. 60 bp) in co-IP experiments the *canine*PLM-YFP was found to built a physical interaction with the α_1 -SU of the NKA (Figure 16B,C). Therefore, this fusion protein was used in all further experiments to generate the adenovirus for transfection and FRET analysis of adult rat ventricular myocytes (ARVM).

To produce the recombinant PLM-E1 protein, the yellow fluorescent protein sequence was excised from the provided *canine*PLM-YFP containing pEYFP N1 vector via KpnI (5'end) and NotI (3'end) restriction endonuclease sites and ligated via triple-ligation at its C-Terminus with the complete YFP sequence amplified from the pEYFP N1 vector through PCR with designed primers flanking KpnI and EcoRI sites and the Epac1-CFP sequence digested from the Epac1-camps cDNA by EcoRI and NotI to create the plasmid PLM-E1 in the given pEYFP N1 vector (Figure 17A).

As the objective of this project is to characterize β -adrenoreceptor (β -AR) mediated cAMP dynamics in the PLM/NKA microdomain in ARVM, we created an adenovirus encoding E1-PLM using the *Invitrogen Gateway® Cloning System*. The sensor sequence was amplified with specially designed primers containing flanking DNA recombination sequences called BP sites. After PCR amplification of an approximately 2255 bp product and gel purification the construct was cloned into an entry vector. The PLM-E1 construct was than subcloned into an expression vector using the LR Reaction based on DNA recombination. Here, the entry vector is combined with the destination vector called pAd_CMV_V5DEST (Figure 17B) and further used for amplification in HEK 293A cells. The expression vector contains human recombinant deficient (deletion in E3 gene) adenovirus type 5 with a cytomegalovirus promotor to drive protein expression of PLM-E1 in mammalian cells.

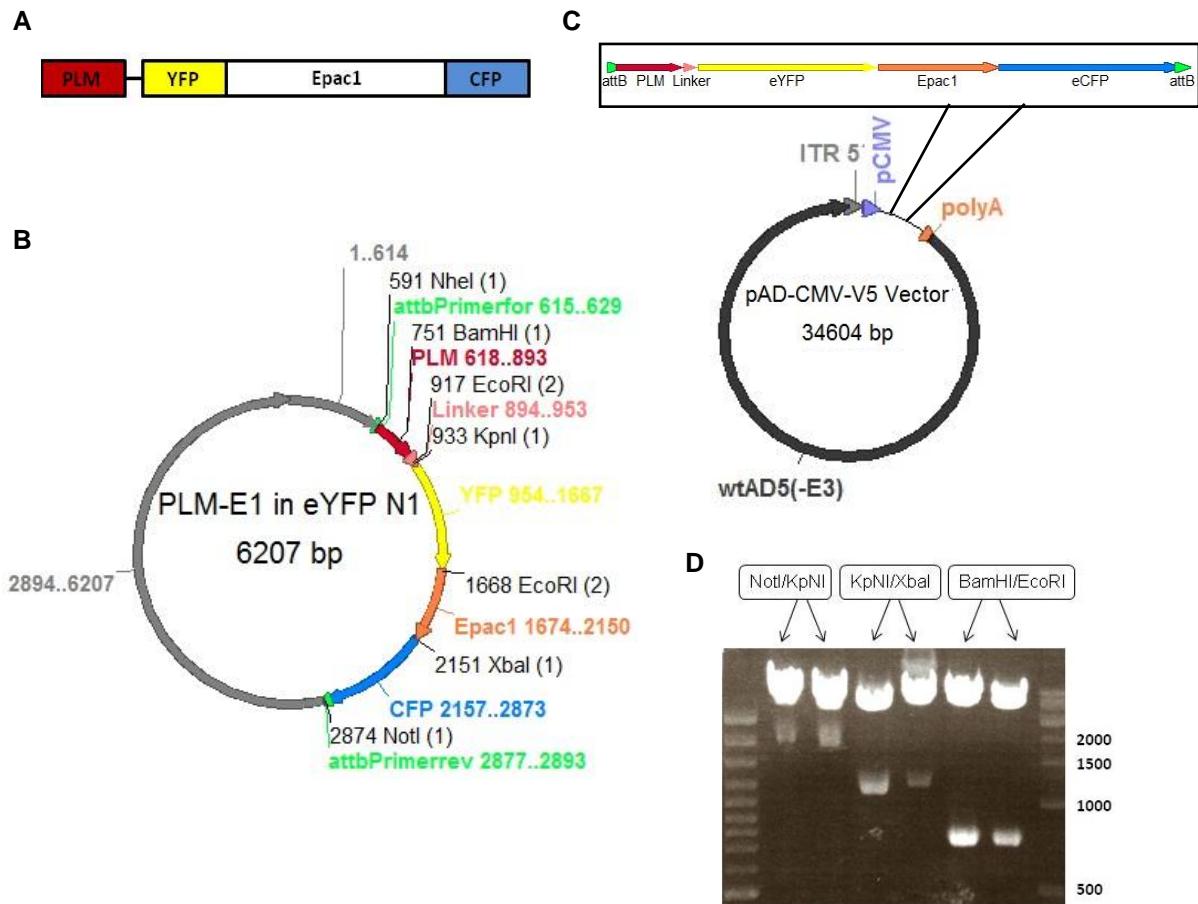


Figure 17. Design of the optimized PLM-E1 biosensor construct.

(A) Schematic representation of the PLM-E1 sensor construct that includes two fluorophores, yellow (YFP) and cyan fluorescent proteins (CFP), sandwiching the cAMP-binding domain Epac1 and fused to phospholemman (PLM). (B) pEYFP-N1 vector containing the coding sequence for PLM-E1 and showing attb forw. and rev. primer binding sequences used for further cloning steps into the final adenoviral vector. (C) Map of the recombinant adenoviral vector with the PLM-E1 sequence. It has a truncated version of human adenovirus type 5 and a CMV promoter for expression in ARVMs. (D) 1% agarose gel demonstrates DNA segments control digestion of the PLM-E1 construct in the pEYFP-N1 vector at ~1900 bp (NotI/KpNI), at ~1250 bp (KpNI/XbaI) and ~750 bp (BamHI/EcoRI).

3. 2. 1 Sensor characterization - expression

To investigate molecular weight and the expression pattern of the developed PLM-E1 sensor, we transfected ARVMs with the PLM-E1 adenoviral construct at a range of MOI between 0 and 1000. The lysates were subjected to Western Blot analysis using anti-total PLM antibody and anti-GFP antibody. Based on the sequence of the sensor, its theoretical molecular weight is expected at 75 kD (Figure 18B). Using the total PLM and the GFP antibody we detected a cluster of additional bands at 37 kD and transfection rate dependent bands at 50 kD and 22 kD, suggesting gene products originating from unexpected protein modification and trafficking in the Golgi apparatus. With regards to sensor expression, we examined confocal pictures of ARVMs transfected with the cytosolic E1-camps sensor, used for comparative real time measurements for cytosolic cAMP dynamics, versus the PLM

tagged version PLM-E1, which should be spatially localized in the PLM/NKA microdomain. The genetically modified PLM-E1 sensor expresses the two fluorophores YFP and CFP like its predecessor E1-camps, which are recorded in separate detection channels with excitation wavelengths at 514 nm and 442 nm (Figure 18A).

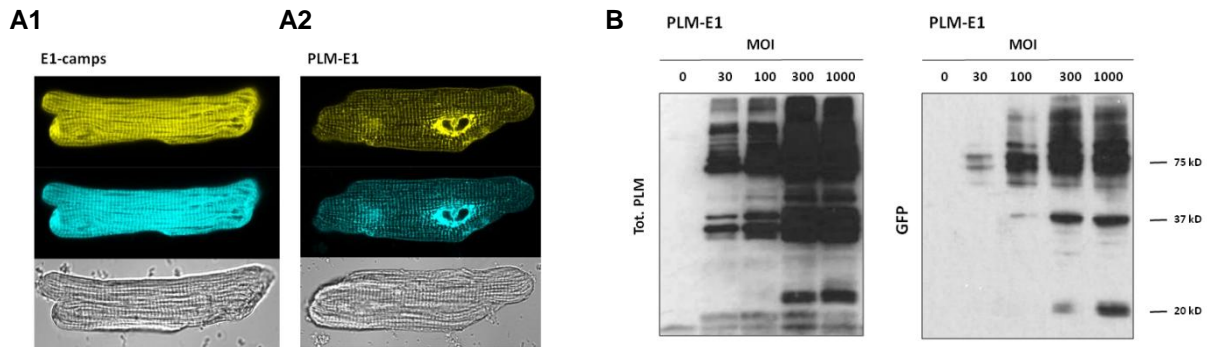


Figure 18. Expression of the PLM-E1 sensor. (A) Confocal images of AVRMs transfected with adenoviral constructs (A1) E1-camps and (A2) PLM-E1. YFP and CFP channels are recorded separately reveal a confined Z line dominant pattern for the expression and localization of the targeted PLM-E1 compared to Epac1-camps, which is more evenly distributed in the cytosol and membrane parts. (B) Immunoblot expression analysis for PLM-E1 transfected ARVM. Cultured ARVMs were transfected for 48 h with the adenoviral vectors at 10, 30, 100, 300 or 1000 MOI. Cell lysates were subjected to SDS-PAGE (10% gel) and Western blot analysis using an anti-total PLM (1:10000) and anti-GFP (1:160000) antibody. Blots are representative of at least three individual experiments.

In the confocal pictures, the PLM-E1 sensor revealed a predominant membrane localization, although there were always some aggregates observed in the perinuclear regions which could be excluded from analysis of live cell imaging data.

3. 2. 2 Sensor characterization - localization

To insure accurate FRET measurements in the proper compartment of ARVMs, we carried out a biotin labelling and purifying procedure of cell surface proteins of PLM-E1 transfected ARVMs and saw a clear localization of the biosensor in the surface membrane fraction (Figure 19). The sensor was detected with an anti-GFP antibody against the fluorophores and appeared at 75 kD in the surface membrane fraction alongside the α_1 -SU.

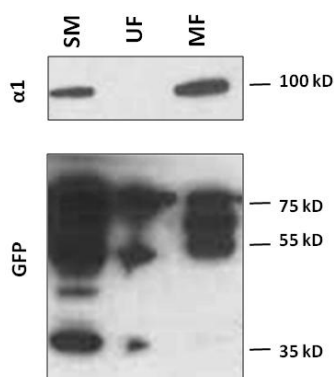


Figure 19. Cell surface biotinylation of PLM-E1 transduced ARVM. PLM-E1 transfected ARVMs were briefly incubated with sulfo-NHS-SS-biotin and then incubated for 10 min. Thereafter, cells were lysed in 1% triton X-100 in PBS supplemented with protease inhibitors (lysis buffer) for 30 min at 4°C. Biotinylated proteins that had not been degraded (Starting Material, SM) were purified (4 h to overnight at 4 °C) using Streptavidin-Sepharose beads (GE Healthcare). Upon washes in lysis buffer and collecting the unbound fractions (UF), cell surface proteins in the membrane fraction (MF) were eluted in SDS-PAGE sample buffer supplemented with 5% (v/v) -mercaptoethanol by heating at 60 °C for 10 min. All samples were immunoblotted for PLM-E1 using anti-GFP antibody and sodium pump α_1 -subunit.

To prove the correct localization of the sensor in the PLM/NKA microdomain, confocal images of PLM-E1 transfected adult rat ventricular myocytes with a transfection efficiency about 80 % (data not shown) were analyzed and revealed a T-tubular pattern and sporadically occurring perinuclear regions with enhanced fluorescence intensity (Figure 18A2). Compared to E1-camps, which is expressed throughout the entire cytosol with intense striations at the membrane (Figure 18A1), the PLM-E1 sensor is predominantly membrane bound as desired. To visualize the physical interaction of the α_1 -SU with its genetically modified regulatory sensor protein PLM-E1, we immunostained the α_1 -SU in PLM-E1 transfected cardiomyocytes. The colocalization analysis demonstrates that there is a nearly perfect overlay of the sensor signal (Figure 20B) as well as of the stained endogenous PLM (Figure 20A) signal with the α_1 -SU, indicating that the sensor localization corresponds to the endogenous PLM and NKA location.

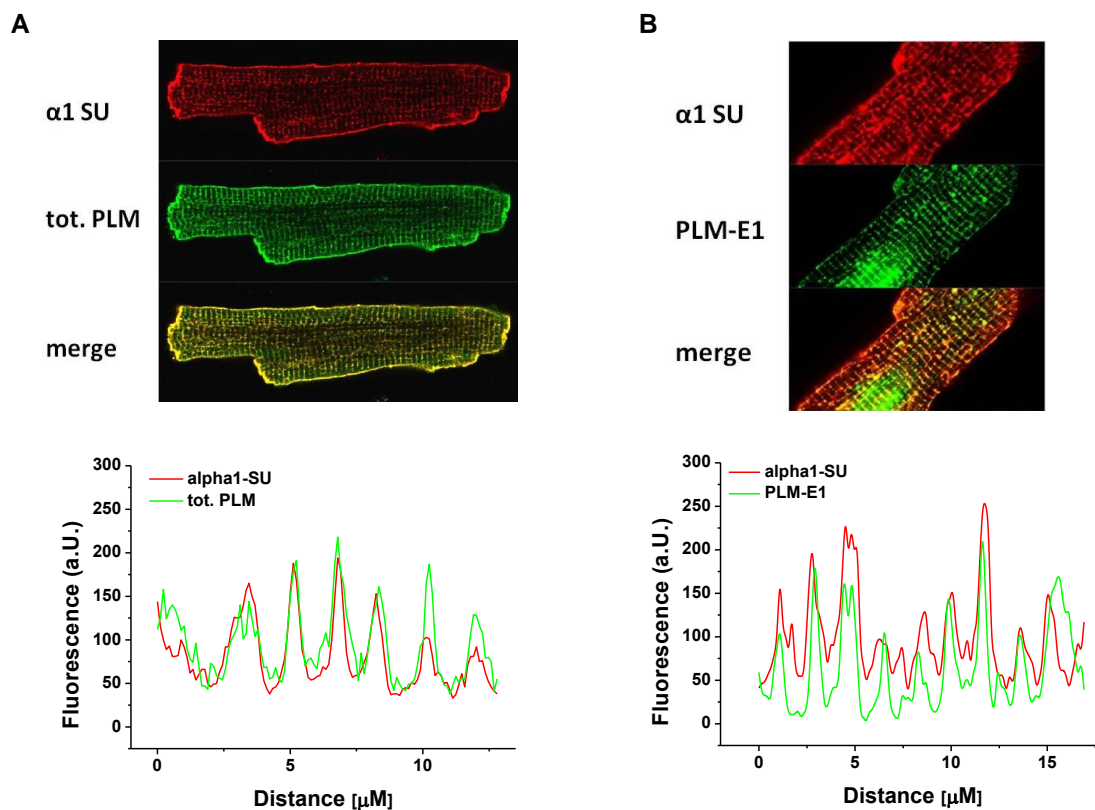


Figure 20. Co-localization of PLM-E1 with the sodium pump. Representative confocal images ($n > 5$ for each) of immunostained (A) Wildtype and (C) PLM-E1 transfected (300 MOI) ARVMs. Co-localization of PLM with α_1 -SU of the NKA is confirmed for endogenously expressed PLM and the overexpressed PLM-E1 by the intensity overlay of both fluorescent signals - see A, bottom and B, bottom.

With regards to biochemical evidence, co-immunoprecipitation experiments revealed the association of PLM-E1 with the α_1 -subunit in transduced ARVM and thus the correct localization of the sensor (Figure 21).

For this purpose, we first conducted co-immunoprecipitation experiments with immobilised α_1 -SU antibodies on protein G-Sepharose beads to detect total phospholemman of PLM-E1 transduced ARVM. As expected, the beads caught endogenous phospholemman at 17 kD and the expressed the biosensor at 75 kD amongst other PLM including bands, characteristic for the sensor protein PLM-E1 (Figure 21A). Equally, we analysed E1-camps transfected ARVMs as a negative control, in which case only the endogenous PLM at 17 kD could be pulled down from the lysed cells (Figure 21A).

To insure the association of PLM-E1 with the endogenous NKA- α_1 -SU, we have additionally used the GFP-Trap reagent (Chromotek), which has an excellent binding to fluorescent proteins, with no background or non-specific capture. Because the antibody is raised in lamas, one gets no interference of heavy and light IgG chains with sodium pump antibodies when immunoblotting. Compared to the E1-camps transduced ARVMs as a negative control, the α_1 -SU could be successfully pulled down almost entirely from the unbound fraction (No. 4) into the IP-fraction (No. 10; 10+) (Figure 21B). We looked further into the co-immunoprecipitated GFP fractions of the sensor protein and detected a strong GFP band in the IP fraction at the expected size of 75 kD. Additional bands at 37 and 22 kD were detected, which are characteristic for PLM-E1 expression in cardiomyocytes, as indicated in the section 3. 2. 1.

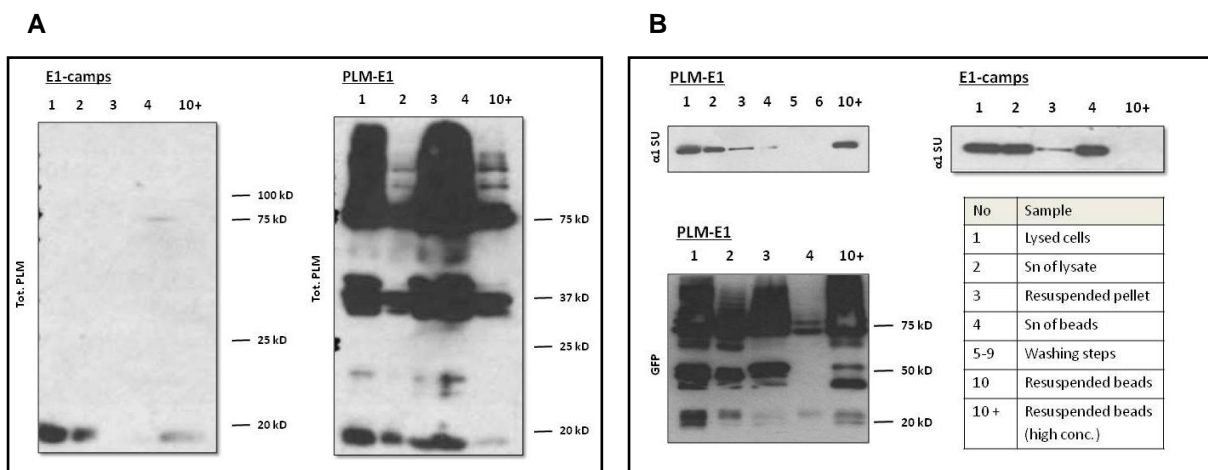


Figure 21. Association of PLM-E1 with the sodium-potassium pump α_1 subunit.

(A) Representative immunoblots containing α_1 -NKA+PLM coIP analysis in PLM-E1 and E1-camps transfected ARVM. For co-IP of PLM-E1 and the α_1 -NKA, three wells (~ 90.000 cells) of PLM-E1 and E1-camps (neg. control) transfected ARVM were used. Myocytes were lysed in 2 mg/ml C12E10 (Sigma) in PBS supplemented with protease inhibitor cocktail (Roche) and PhosStop (Roche) phosphatase inhibitor mixtures, insoluble material was removed by centrifugation at $17,500 \times g$ for 5 min at 4 °C. Supernatants were agitated overnight at 4°C with anti-NKA- α_1 -subunit monoclonal C464.6 (Santa Cruz Biotechnology) preimmobilized on protein G-Sepharose beads (GE Healthcare). After multiple washes in 0.5 mg/ml C12E10 in PBS, all samples taken during the immunoprecipitation procedure were eluted in SDS-PAGE sample buffer, separated by SDS-PAGE (12 % gel), transferred to membranes, and immunoblotted for total PLM.

(B) Representative Western Blots with immunoprecipitation experiments of fluorophores of PLM-E1 and E1-camps transfected ARVM (~ 90.000) precipitated using GFP-Trap (Chromotek) under identical conditions, and samples were immunoblotted as shown. All blots are representatives for at least three individual experiments.

3. 2. 3 Sensor characterization - function

For functional analysis of the inhibitory effect of the PLM-E1 sensor on NKA, we measured the ouabain-sensitive influx of radioactive $^{86}\text{Rb}^+$, thereby monitoring the NKA activity in HEK 293 cells stably expressing PLM-E1. Stable transfection of HEK293 with the sensor resulted in approximately 37 % loss of NKA activity showing a significant decrease in $^{86}\text{Rb}^+$ uptake compared to a non-PLM-expressing HEK 293 line (Figure 22), indicating that the expression of PLM-E1 inhibits the sodium pump. Hence, sensor protein PLM-E1 is properly inhibiting the NKA, as the endogenous PLM does.

To test the FRET capability of the PLM-E1 sensor, we stimulated transduced ARVMs with the β -AR agonist isoproterenol (Iso) and monitored a clear decrease in YFP/CFP ratio as a consequence of the local microdomain cAMP increase, thus proving sensor functionality (Figure 23). Therefore, this new sensor could be used in all further FRET experiments.

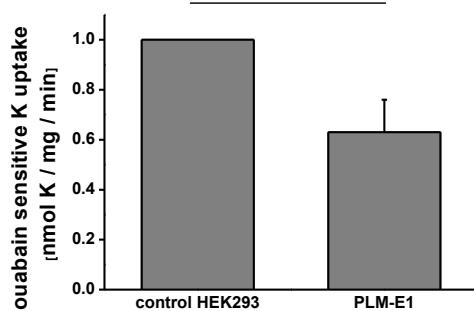


Figure 22. Inhibition of NKA activity by PLM-E1. Na pump activity was measured as ouabain-sensitive ^{86}Rb uptake by cells stably expressing PLM-E1. In this assay pump activity is expressed as a percentage of the activity in the same cell line which do not express PLM. PLM-E1 expressing HEK293 cells inhibit the sodium pump, HEK293 do not ($n = 3$; $*P < 0.05$)

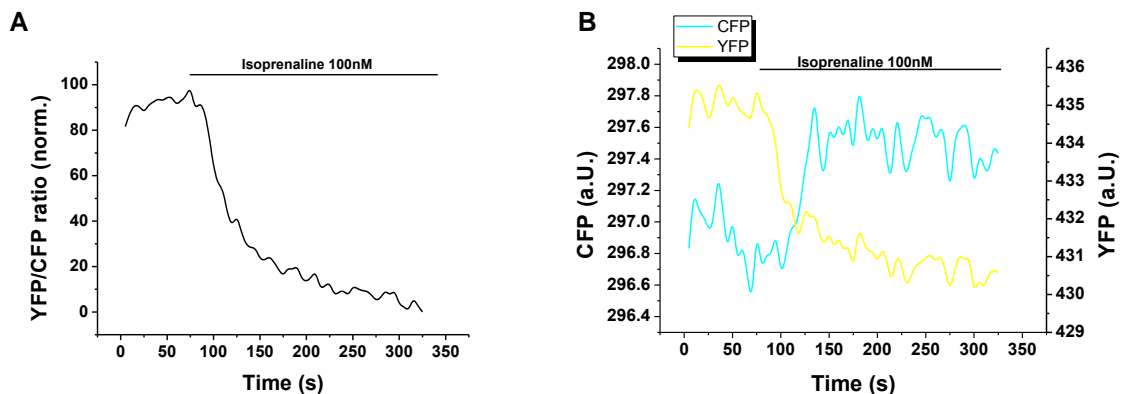


Figure 23. Sensor function in PLM-E1 transduced ARVMs. (A) Representative FRET signal trace recorded in a PLM-E1 transfected myocyte. Treatment with isoprenaline 100 nM induces an increase in cAMP and a significant decrease in YFP/CFP ratio. (B) Recorded single YFP (acceptor) and CFP (donor) intensities for the same experiment. (C) Representative region of interest for a single FRET experiment in PLM-E1 transfected ARVM excluding strongly fluorescent perinuclear regions of the cell.

The next step was to exclude PLM-E1 sensor affinity for cAMP and Isoprenaline sensitivity. Transduced cardiomyocytes were treated with the adenylyl cyclase inhibitor MDL12,330A to minimize basal intracellular cAMP before performing the concentration-response FRET experiments with the cAMP analogue 8-Br-2'-O-Me-cAMP-AM. In addition, the biosensor sensitivities were compared between the localized PLM-tagged and the cytosolic sensor in terms of FRET response to increasing concentrations of Iso.

We demonstrated that the membrane localized PLM-E1 sensor has a slightly lower affinity to cAMP than the cytosolic E1-camps ($EC_{50}= 4.1 \pm 1.1$ vs. $0.9 \pm 0.2 \mu\text{M}$, respectively) (Figure 24A). The concentration response dependency for Iso revealed a comparable sensitivity of PLM-E1 with the cytosolic E1-camps (Figure 24B). Hence, the non-tagged biosensor does not show a more intense perception of FRET changes in the cytosol than the localized sensor meaning that we could expect commensurate results for microdomain and cytosol in the following experiment.

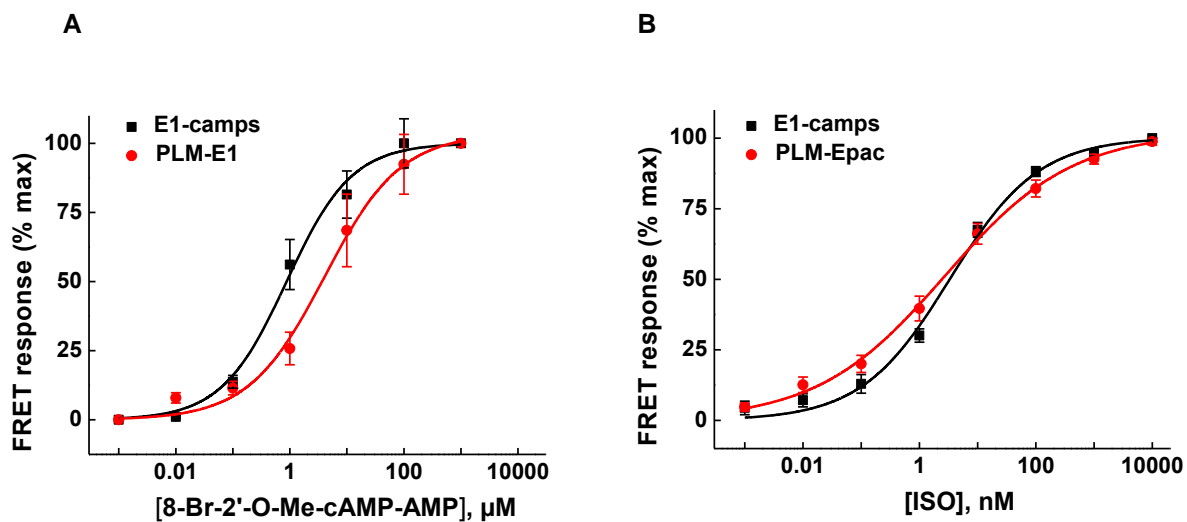


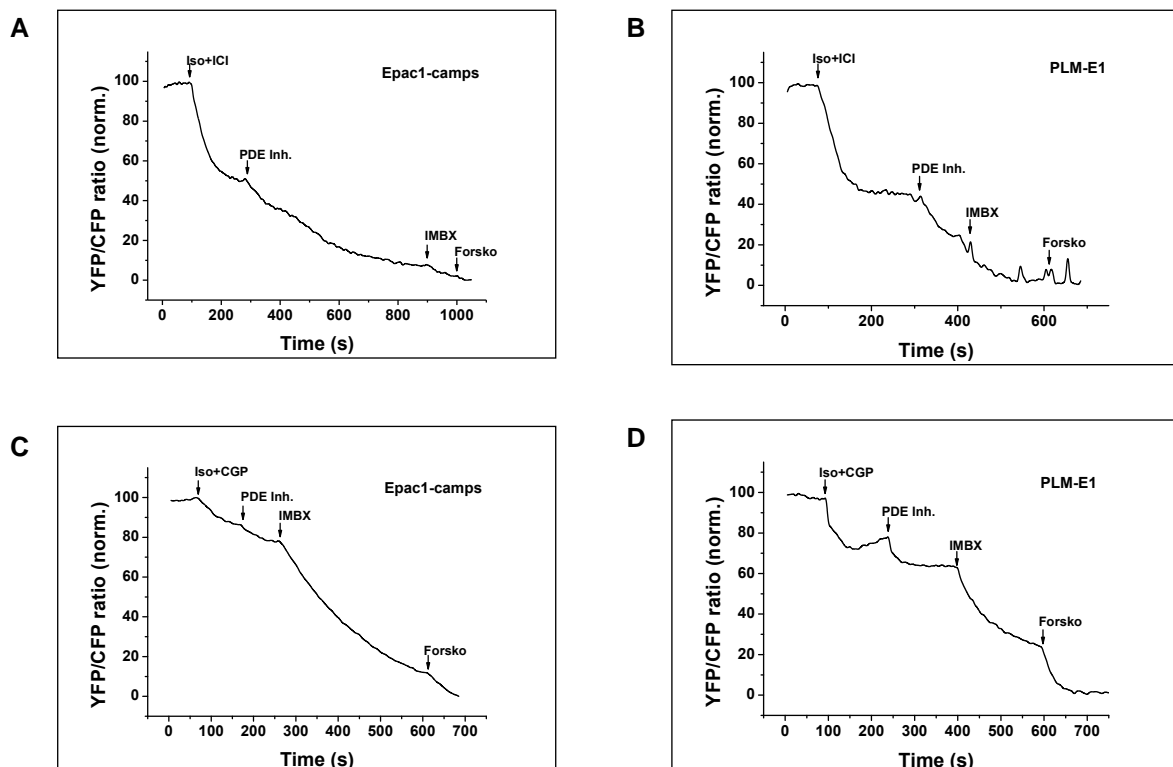
Figure 24. Sensitivity of E1-camps and PLM-E1 to cAMP and increasing isoprenaline (ISO) concentrations. (A) Concentration response dependencies measured in PLM-E1 and E1-camps transduced ARVMs pretreated with the adenylyl cyclase inhibitor MDL12,330A (100 μM) for 10 minutes and treated with increasing concentrations of the cell-permeable cAMP analogue cAMP 8-Br-2'-O-Me-cAMP-AM. PLM-E1 shows a ~4-times lower affinity for than the cytosolic E1-camps biosensor ($EC_{50}= 4.1 \pm 1.1$ vs $EC_{50}=0.9 \pm 0.2 \mu\text{M}$). Means \pm SE, $n=7-12$ cells from 4-5 rat hearts each. (B) Isoprenaline induced FRET response for the Epac1-camps and the PLM-E1 sensor. Accordingly transfected ARVM treated with Iso concentrations ranging between 0.001 nM and 1 μM displayed no significant differences regarding the sensor Iso sensitivity for the targeted PLM-E1 and cytosolic E1-camps sensors EC_{50} values were 4.4 ± 1.2 and 4.3 ± 0.7 nM, respectively. Means $\pm n=15$ and 10 cells from 4 rat hearts each.

3. 3 Comparative FRET analysis of E1-camps and PLM-E1 transduced ARVMs

Phospholemman exerts its inhibitory effect on the Na⁺/K⁺-ATPase only when it is not phosphorylated by kinases, for example at its Ser-68 residue by the PKA, which is downstream of the adrenergic β_1 - or β_2 -adrenergic receptor subtypes.

3. 3. 1 Effects of individual β -AR subtypes

To investigate which subtype is involved in the receptor-cAMP signaling pathway in the PLM/NKA microdomain, we performed the following FRET-based experiments. Individual β -AR subtypes were selectively stimulated in E1-camps and PLM-E1 transduced ARVMs of 8-10 weeks old rats. To do so, we inhibited the β_1 -AR with CGP-20712A (100 nM) and the β_2 -AR with ICI 118551 (50 nM) and stimulated the cAMP production with Isoprenaline (100 nM). As a result, in the cytosol, we could detect proportionally the same signal strength in β_1 -AR FRET response as in the PLM microdomain. In contrast, we measured a significantly higher amount (~ 65 %) of β_2 -AR-cAMP induced FRET ratio change in the PLM/NKA microdomain compared to the cytosol (Figure 25E). β_2 -AR signals have been previously demonstrated to be localized at T-tubular membranes and to be highly locally confined²⁹. This data correlates with the displayed expression pattern of PLM-E1 sensor (Figure 18A2) and its ability to particularly well distinguish between the previously shown global β_1 -AR and localized β_2 -AR cAMP pools²⁸.



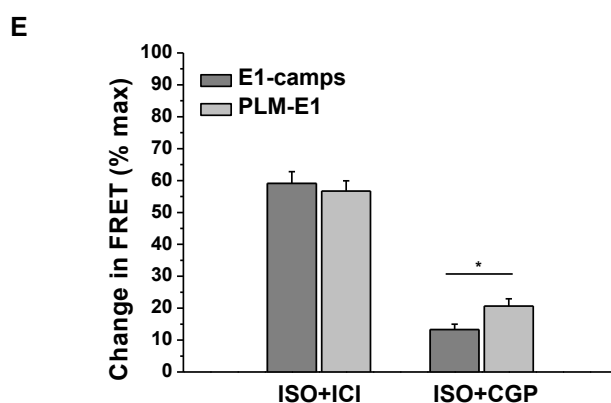


Figure 25. Predominant control of β_2 -AR over the PLM/NKA microdomain.

(A,B) Representative FRET traces for E1-camps and PLM-E1 expressing rat cardiomyocytes upon β_1 -AR-selective stimulation (100 nM ISO + 50 nM of the β_2 -AR blocker ICI 118551). (C,D) Representative FRET traces from Epac1-camps and PLM-E1 rat cardiomyocytes after β_2 -AR-selective stimulation (100 nM ISO + 100 nM of the β_1 -AR blocker CGP-20712A). β_1 -AR stimulation showed no significant difference in FRET response between bulk cytosol and the PLM/NKA compartment. Maximal stimulation of adenylyl cyclase was achieved by selective PDE inhibitors used in different concentrations described in the next section, the unselective PDE inhibitor IBMX (100 μ M) and the direct adenylyl cyclase activator forskolin (10 μ M). (E) Quantification of the FRET experiments. Selective β_2 -AR stimulations strongly rise cAMP the PLM/NKA microdomain and resulted a significant difference to the cytosolic FRET response. β_1 -AR stimulation did not show a different percentage in max. FRET responses in the PLM/NKA microdomain compared to bulk cytosol. Means \pm SE, n=30-40 cells from 3-4 rat hearts per condition.

3. 3. 2 PDE Profiles in PLM-E1 and E1-camps transduced ARVMs

It is well known, that through local activities of specific phosphodiesterases (PDEs), cAMP in the heart is organized in distinct microdomains. To investigate the organization of cAMP signal transduction in the PLM/NKA microdomain, we performed a series of experiments to analyze the regulation of cAMP dynamics via PDE families in the vicinity of Phospholemman versus the cytosol. Since the low availability of the inhibitors for PDE1, 8 and 9 prohibited further investigation in terms of their role in modulation of cyclic nucleotide signaling in the PLM/NKA microdomain and as the predominant cAMP degrading PDE subtypes in the heart are PDE2, 3 and 4, we focused on the latter ones. Looking at basal actions of the Phosphodiesterases and their control of local cAMP microdomains, we measured FRET responses without β -AR stimulation of ARVM transduced with PLM-E1 and E1-camps. We used specific inhibitors for PDE2, 3 and 4 without prestimulating with Iso and continued with a general PDE blocker IBMX and further increase the cAMP production, adding Iso and Forskolin (Forsko) as the last steps until we fully saturated the FRET sensor. For calculations, we related the data to the maximal stimulation signal of the sensor. Interestingly, we detected no significant difference between any PDE family in E1-camps cells, but an important contribution of PDE2 in the PLM microdomain (Figure 26C), which

seems to be strongly regulating basal cAMP levels in close proximity of PLM, as compared to the general cytosolic level of FRET response. In rat cardiac myocytes, splice variants of the PDE2 isoform, especially PDE2A2 and PDE2A3 have been found as preferentially associated with functional membrane structures, such as plasma membrane¹¹⁴, which could be responsible for the regulation of local cAMP pools in the vicinity of PLM.

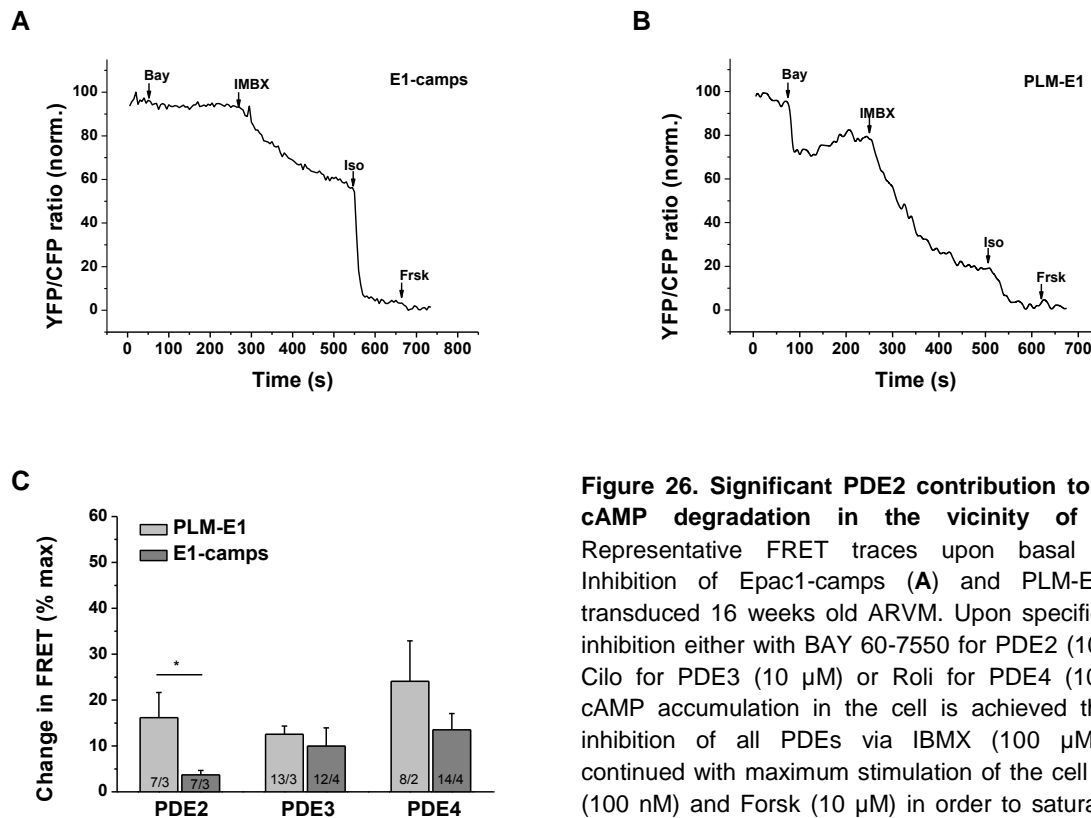


Figure 26. Significant PDE2 contribution to basal cAMP degradation in the vicinity of PLM. Representative FRET traces upon basal PDE2 inhibition of Epac1-camps (A) and PLM-E1 (B) transduced 16 weeks old ARVM. Upon specific PDE inhibition either with BAY 60-7550 for PDE2 (100nM), Cilo for PDE3 (10 μM) or Roli for PDE4 (10 μM), cAMP accumulation in the cell is achieved through inhibition of all PDEs via IBMX (100 μM) and continued with maximum stimulation of the cell by Iso (100 nM) and Forsk (10 μM) in order to saturate the sensor. (C) Quantification of FRET experiments as related to the maximum stimulation uncovered PDE2 as the PDE family crucial for confining the PLM/NKA compartment from the bulk cytosol. Means ± SE, n cells from N rat hearts per condition is written on the bars. * - significant differences at p<0.05.

In the next set of experiments, we focused on the effects of PDE inhibition in the presence of isoproterenol. Under selective stimulation of β_1 - and β_2 -ARs, we analyzed the PDE profiles of PDE2, 3 and 4 after subtype specific β -adrenergic stimulation in the microdomain versus the cytosol and could not find any differences amongst the groups regarding the β_1 -subtype stimulation (Figure 27C). Looking at the FRET responses to individual PDE inhibitors after β_2 -AR stimulation, we discovered that cAMP dynamics in the vicinity of the membrane protein Phospholemman are predominantly regulated via PDE3 in the PLM/NKA microdomain (Figure 27D). The localized PLM-E1 sensor detected an up to two-fold higher FRET signal change in the microdomain, in comparison to cells which were treated with PDE2 or PDE4

inhibitors after selective β_2 -AR stimulation. The obtained results were precisely calculated as the ratio of the PDE Inhibitor effect over the general PDE Inhibition by IBMX.

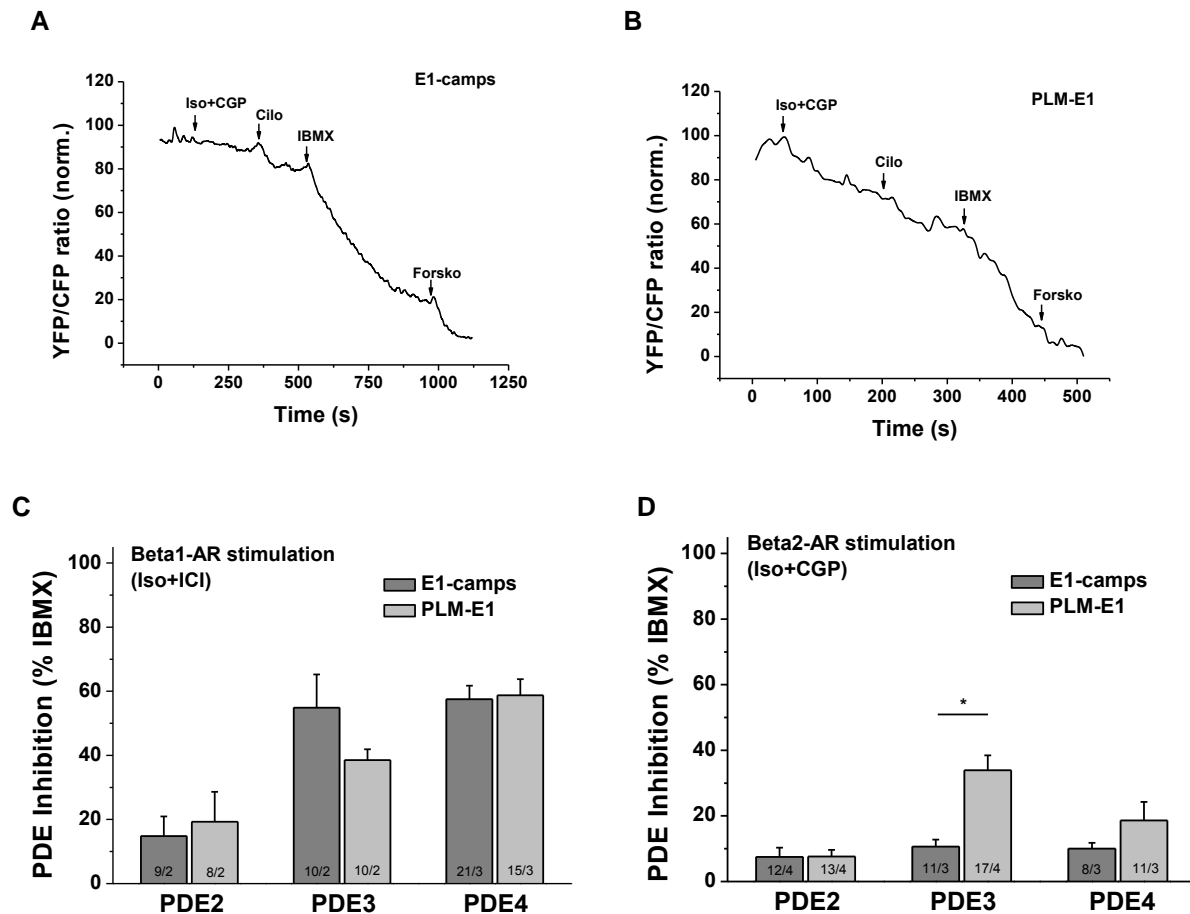


Figure 27. PDE3 pool in the vicinity of PLM confines β_2 -AR mediated cAMP signals to the PLM/NKA microdomain. Representative FRET ratio traces demonstrating PDE3 effects in E1-camps (A) and PLM-E1 (B) transduced ARVMs after β_2 -AR stimulation with Iso+CGP. (C, D) Quantifications of the PDE Inhibitor signals as a % of the general PDE inhibitor IBMX effect. There is a markedly increased response to PDE3 Inhibition after selective β_2 -AR stimulation in the PLM/NKA compartment in contrast to the bulk cytosol. * - significant differences at $p < 0.05$. Shown are means \pm SE, n =cells from N =rat hearts per condition written on the bars. Substance concentrations: ISO 100 nM, IBMX 100 μ M, BAY 60-7550 100 nM (PDE2 inhibitor), cilostamide 10 μ M (PDE3 inhibitor), rolipram 10 μ M (PDE4 inhibitor).

3. 3. 3 ANP/cGMP mediated PDE3 response in the PLM/NKA microdomain

Since there is an indication, that there is a β_2 -AR mediated cAMP pool controlled by local PDE3 activity in the PLM/NKA microdomain, we tested whether the stimulation of the cGMP-producing ANP receptors in PLM-E1 transduced ARVMs have any effect on cAMP levels. cGMP can activate PDE2 through by an allosteric mechanism. It can also inhibit PDE3, since cGMP acts as a competitive inhibitor of the cAMP hydrolysis by this PDE (for cAMP/cGMP crosstalk see Introduction, section 1. 1. 3). Indeed, quantification of all experiments (Figure 29C) as well as the representative traces for β_2 -AR (Iso+CGP) prestimulated PLM-E1 cells

(Figure 29A,B), demonstrate that β_2 -AR-triggered FRET signals could be further decreased by the addition of ANP and abolished via Cilo-pretreatment (Figure 29B). PLM and PDE3 colocalization was analyzed by confocal imaging experiments with cells from 8-10 weeks old animals. Thus, freshly isolated ARVM were immunostained with PDE3 and total PLM specific antibodies (Figure 28A) to study the degree of the overlay (Figure 28B). Good colocalization of PDE3 with the endogenous Phospholemman could be confirmed, which supports the FRET results in this section.

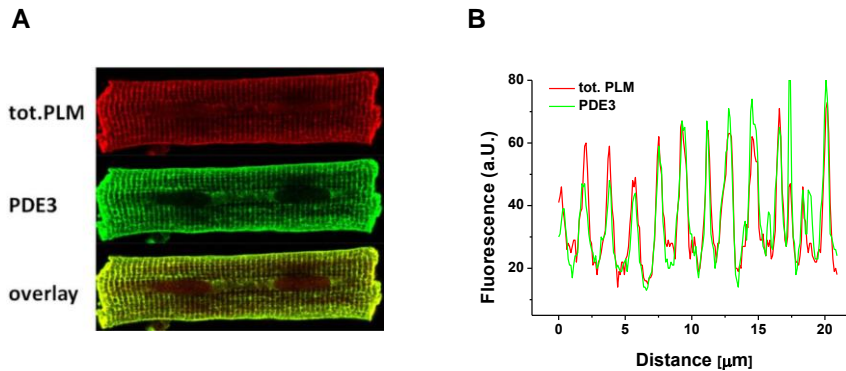


Figure 28. Co-localization of the PDE3A isoform with the PLM microdomain. (A) Representative ARVM immunostained with specific anti-PLM and anti-PDE3 antibodies (B) showing a high degree of colocalization (n>10).

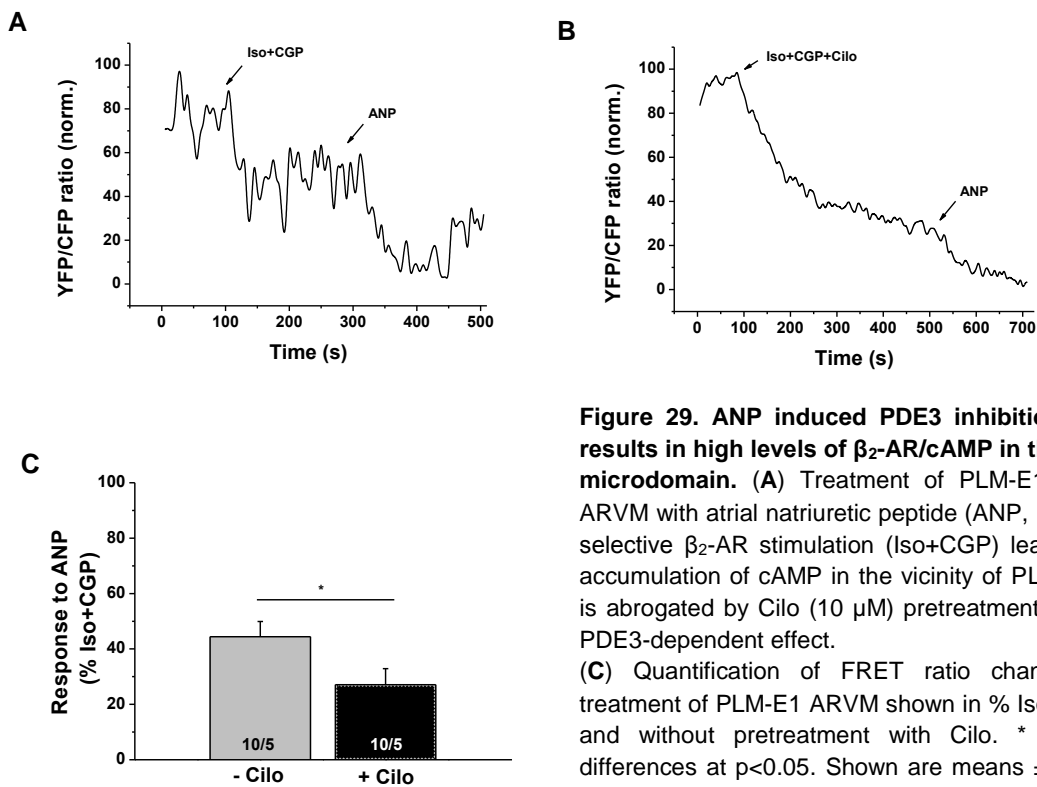


Figure 29. ANP induced PDE3 inhibition in ARVM results in high levels of β_2 -AR/cAMP in the PLM/NKA microdomain. (A) Treatment of PLM-E1 transfected ARVM with atrial natriuretic peptide (ANP, 100 nM) after selective β_2 -AR stimulation (Iso+CGP) leads to further accumulation of cAMP in the vicinity of PLM, (B) which is abrogated by Cilo (10 μ M) pretreatment, indicating a PDE3-dependent effect. (C) Quantification of FRET ratio change to ANP treatment of PLM-E1 ARVM shown in % Iso + CGP with and without pretreatment with Cilo. * - significant differences at p<0.05. Shown are means \pm SE, n=cells from N=rat hearts per condition written on the bars.

3. 3. 4 FRET measurements in PLM-E1 and E1-camps transfected ARVMs

Considering the important pathological changes in β -AR - cAMP - PKA signaling at the subcellular level, we investigated possible alterations of spatiotemporal cAMP regulation in the vicinity of Phospholemman in ARVMs isolated from animals after myocardial infarction (MI). Sprague-Dawley rats were used to generate the progressive chronic heart failure model by ligation of the left anterior descending coronary artery via a suture. 16 weeks after MI surgery, heart function was significantly decreased in MI vs. aged matched control (AMC) group as measured by echocardiography (Table 6).

Table 6. Phenotyping of aged matched control and 16 weeks post MI hearts. The results were calculated from M-mode echocardiography recordings (Vevo 770 micro-imaging system, Visualsonics) as a marker of alterations in wall contractile functionality. Additionally, the heart weight to tibia length (HW/TL) ratio was measured after isolation of the respective hearts as an indicator of progressive hypertrophy.

Parameter	24 weeks old aged matched control (AMC)			16 weeks post myocardial infarction (MI)		
	Value	p	N	Value	p	N
Ejection fraction [%]	84.3 \pm 1.5	--	3	57.0 \pm 5.6	p < 0.05	4
Heart hypertrophy [mg/mm]	29.5 \pm 0.5	--	3	36.8 \pm 2.3	p < 0.05	4

3. 3. 5 Alterations in local PDE dependent cAMP regulation in the PLM/NKA microdomain

We found out that the communication between the β_2 - AR and the PLM/NKA microdomain is predominantly driven by PDE3 in wildtype (WT) 8-12 weeks old Wistar rat hearts (Figure 27D). For that reason, we tested if this communication is deteriorated during the pathological state of myocardial infarction. We isolated cardiac cells from 16 weeks post-MI Sprague Dawley rats as control animals and transduced them with the PLM-E1 and E1-camps biosensor adenoviruses. After preblocking of the β_1 -AR with CGP-20712A, we stimulated PLM-E1 transfected MI myocytes with Iso and looked at the different PDE inhibitor contributions by relating them to the proportion of IBMX induced FRET signal decrease. We demonstrated, that upon β_2 -AR stimulation, PDE3 hydrolyzing activity is downregulated in the PLM/NKA microdomain. Concomitantly, PDE2 activity at the sarcolemmal PLM/NKA domain is upregulated (Figure 30F). There was no significant change in PDE contribution in response to β_2 mediated cAMP detected using the cytosolic E1-camps sensor (Figure 30E).

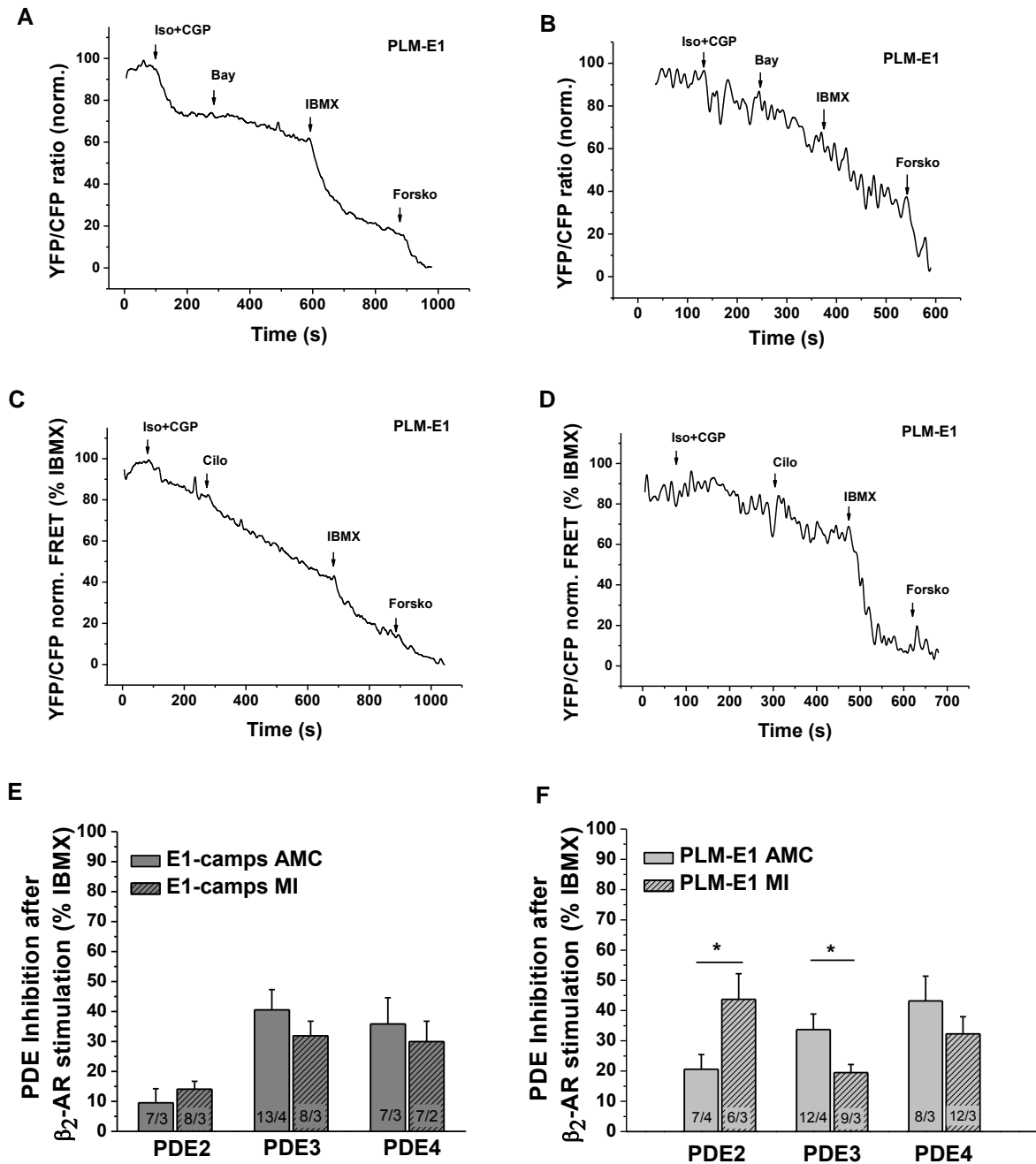


Figure 30. Contributions of individual PDEs to cAMP hydrolysis after β_2 -AR stimulation in AMC and MI cardiomyocytes. (A,C) Representative FRET traces from AMC and (B,D) MI cardiomyocytes expressing PLM-E1, treated with 100 nM Iso+CGP for β_2 -AR stimulation and subsequently with PDE2 inhibitor BAY 60-7550 (Bay, 100 nM) or PDE3 inhibitor cilosamide (Cilo, 10 μ M), respectively. (E) Quantification of cytosolic (E1-camps) FRET experiments revealed no significant changes of any PDE contribution after MI. (F) Quantification of PLM-E1 specific (PLM-E1) FRET experiments showed a significant increase of PDE2 contribution in the microdomain of MI cells, while PDE3 response was strongly decreased. Means \pm SE, n=cells from N=rat hearts per condition. * - significant differences at $p < 0.05$.

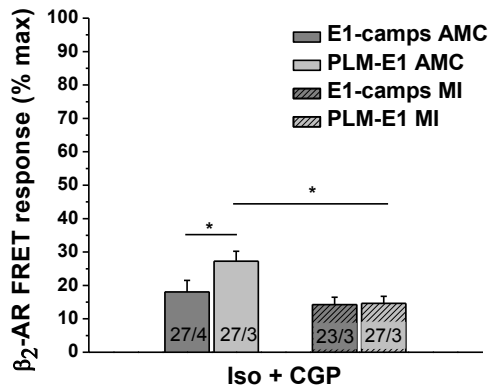


Figure 31. β_2 -AR effects in AMC vs. MI cells. Comparison of the magnitudes of Iso (100 nM) responses measured with the targeted PLM-E1 and cytosolic E1-camps in an experiment performed as described in Figure 14. These data suggests a serious loss of receptor signal to the microdomain after MI regarding β_2 adrenoreceptor signals. Means \pm SE, n=cells from N=rat hearts per condition. * - significant differences at $p < 0.05$.

We checked for possible alterations in β_2 -AR signal responses (Figure 31). Interestingly, the MI cells did no longer show a difference between cytosolic and PLM-E1 microdomain characteristic responses to Iso. The experiments revealed alterations regarding β_2 -subtype specific cAMP responses, suggesting that the β_2 -receptor-microdomain communication is seriously impaired in myocardial infarcted hearts.

3. 3. 6 cAMP degrading PDE3 pools in the PLM/NKA microdomain are delocalized in the hypertrophied heart

Since we showed that β_2 -AR/cAMP signals are confined in the PLM/NKA microdomain through PDE3 activity, we focused on defining the alterations of this confined signaling in the chronic heart failure disease model. PDE3 dependent subtype specific β_2 -AR responses were dramatically diminished in hypertrophied heart cells compared to FRET responses in 24 weeks old aged matched control (AMC) rat heart cells (Figure 30F). We demonstrated the loss of PDE3 localization in the microdomain by immunostaining cardiomyocytes isolated from hearts after myocardial infarction with total PLM and PDE3A subfamily specific antibodies (Figure 32). Quantification of confocal images using the Pearson's coefficient, which is an indicator for the degree of co-localization, uncovered a disturbed localization of PDE3 in the microdomain in hypertrophied cells compared to aged matched control myocytes (0.85 vs. 0.92) (Figure 32). It was no more locally confined and in comparison to healthy aged matched control cells visibly altered.

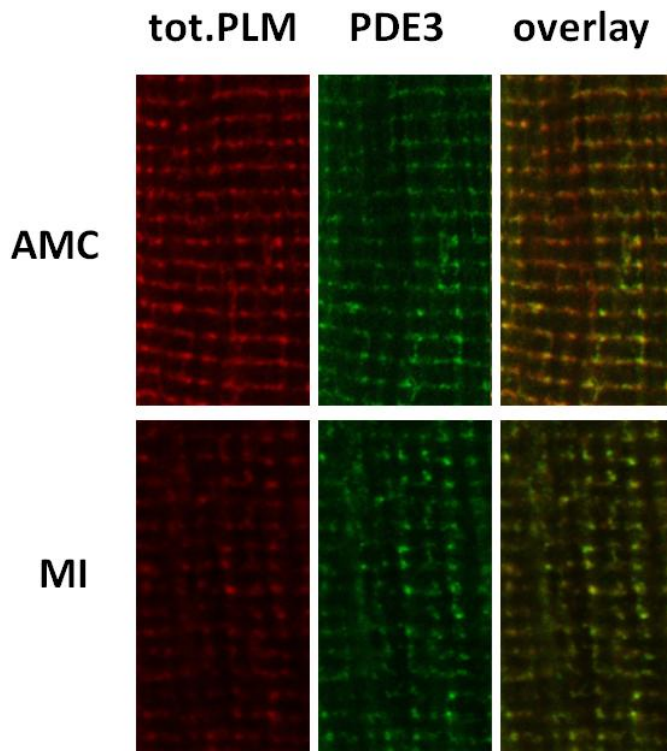
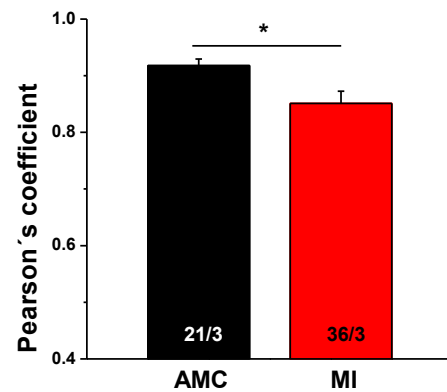


Figure 32. Confocal microscopy analysis of PDE3 localization. Aged matched control and MI cells were immunostained with the PDE3 family specific antibody. Significant delocalization of locally confined PDE3 in hypertrophied cardiomyocytes were detected. Means \pm SE, n=cells from N=rat hearts per condition. * - significant differences at $p < 0.05$.



However, when the same protocol for the ANP FRET experiments (3. 3. 3) were applied during our analysis for MI-ARVM, we could not detect any clear FRET signals, so that it was not possible to conclude if there are better or worse ANP responses compared to aged matched control cardiomyocytes (data not shown).

4. Discussion

4. 1 Challenges in generating novel PLM-E1 FRET biosensors with correct structural and functional properties

The orchestrated action of specific subsets of PDEs, AKAPs, PKA subtypes and other scaffolding proteins involved in creating a local cAMP signalosome in subcellular microdomains has been proposed by numerous studies from different labs (see section 1. 1. 3). The well-accepted model of cAMP compartmentation can explain the observed different physiological events operated by the same second messenger. Alterations in NKA activity and PLM expression^{230,255} are known to be associated with cardiac disease and are probably connected with a modification of cAMP/PKA dependent NKA regulation. In order to directly monitor cAMP dynamics at the PLM/NKA compartment and their changes in heart failure, the PLM-E1 FRET-based biosensor was generated. PLM-E1 is a targeted version of the cytosolic Epac1-camps²⁴⁹ (E1-camps) biosensor which carries the full-length PLM sequence on its N-terminus. Initially, it was attempted to generate the recombinant DNA encoding for the PLM-E1 biosensor by tagging the cAMP sensitive single chain biosensor E1-camps to the human PLM via a 18 bp long linker region located between PLM and the YFP moiety (Figure 14).

Before generating the recombinant adenovirus with the PLM-E1 insert, non-viral HEK293 cell transfection served as a more 'easy-to-handle' gene delivery method to test functionality and localization of the sensor. Consistent with previous observations for the predominantly membrane expressed YFP-PLM^{205,254}, the inclusion of the PLM sequence in the E1-camps construct showed an expected distribution of the targeted sensor exclusively at the plasma membrane (Figure 15A). Furthermore, the PLM-E1 sensor showed a correct expression pattern (Figure 15B) upon titration using Western blot with anti-GFP antibodies; the bands observed corresponded to the respective molecular weight (74 kD). The additional protein structure at 20 kD might have been cleaved off during intracellular trafficking. However, we demonstrated that this had no effect on the functionality of the sensor (Figure 15C). The PLM-E1 transfected HEK293 cells showed a clear decrease in the FRET response triggered by Iso mediated intracellular cAMP elevation. Although the optical and functional results were as expected, the localized sensor did not co-immunoprecipitate with the endogenously expressed NKA- α -SU (Figure 16A) from HEK293 cells in contrast to positive controls (Figure 16 B,C). This behavior of the sensor construct did not comply with the requirement for the PLM/NKA microdomain specific cAMP measurements. This discrepancy could potentially be caused by inaccurate folding of the protein of this size as we used a relatively short linker to connect the sequences of PLM and YFP. The optimized version with a 60 bp linker based on *canine*PLM-YFP (Figure 17B), which was successfully used in FRET studies before²⁰⁵,

showed equal expression properties like *human* PLM-E1 in HEK293 cells (data not shown). According to the cDNA sequence, dog and rat PLM are highly homologous²⁵⁶, so there was no concern about the compatibility of canine PLM-E1 FRET sensor in ARVMs. While working with titer controlled adenoviral gene delivery systems promises 100% transduction efficiency, such *in vitro* studies require a high quality cardiomyocyte population and successful cell isolation and culture²⁵⁷. Using an adenoviral vector to transfer the genetically modified biosensor sequence into cardiomyocytes is an efficient method which does not require damaging treatments for cells such as electroporation, somewhat similar to transgenic animal models^{154,251,258}. This adenovirus mediated gene transfer approach has been used in many studies to demonstrate discrete spatial and temporal compartmentalization of cAMP in adult cardiac myocytes^{65,111,155,259-261}. A clear advantage of *in vitro* adenoviral system studies is that there is no possibility for adverse effects on cardiac morphology and function, as compared to transgenic animals. Additionally, in our experiments the adenoviral transduction had no effect on cell viability or morphology of the cultured cells compared to non transfected cells. Upon generating the adenoviral vector with PLM-E1 as insert (Figure 17C), it was possible to characterize the sensor in ARVMs. It is confirmed in several studies that cardiac PLM resides at the surface membrane and its phosphorylation status plays an important role in the regulatory effect on the NKA^{166,262}. Similarly, confocal imaging experiments of PLM-E1 transduced ARVMs (Figure 18A2 and Figure 20B) revealed thin parallel striations in correspondence of the sarcomeric Z lines where endogenous PLM (end. PLM) is also expressed next to the NKA- α_1 -SU (Figure 20A). Despite of the observations of strongly fluorescent perinuclear clustering of the sensor in ARVMs, it could be demonstrated that there is enough protein expressed at the cell surface which co-immunoprecipitates with the NKA- α_1 -SU (Figure 21). Detailed sensor expression analysis with the tot. PLM antibody revealed bands corresponding to the respective molecular weights of the PLM-E1 sensor and end. PLM, indicating that not all of end. PLM was replaced by the sensor (Figure 18B). The assessed inhibitory effect of the sensor PLM on the NKA was in agreement with the end. PLM action⁷⁶ (Figure 22). Here, we have used a HEK293 cell line engineered to stably express PLM-E1, as experiments with transiently transfected cells may be confounded by transfection efficiency.

After adenoviral gene transfer of the PLM-E1 FRET biosensor into ARVMs, excitation of CFP at 436 nm and YFP at 514 nm led to robust fluorescent signals in both channels, proving the successful integration of donor and acceptor fluorescent proteins into the adenoviral FRET construct (Figure 18A2). Excluding areas of sporadically occurring strongly fluorescent perinuclear regions, presumably emerging from adenoviral overexpression and incorrect intracellular trafficking of the sensor, PLM-E1 was capable of generating a strong FRET signal in response to an elevation in intracellular cAMP concentration (Figure 10). This was

similar to the unimolecular cytosolic E1-camps sensor which has been known to have a relatively large FRET ratio change and a high signal-to-noise ratio²⁴⁸. The kinetic properties of PLM-E1 are comparable to those of the E1-camps sensor (Figure 24), allowing FRET measurements with a high dynamic range at saturation (i.e. 100 nM) and subsaturating concentrations of Iso, which was particularly suitable for comparative measurements of PDE effects in the vicinity of PLM and bulk cytosol.

4. 2 Comparative FRET analysis of healthy ARVMs expressing adenoviral PLM-E1 and E1-camps biosensors reveal differentially regulated local β -adrenergic signaling

Molecular mechanisms involving cAMP/PKA actions in the vicinity of PLM are known to be highly important in regulating cardiac function¹⁷⁰. Especially during β -adrenergic stimulation PLM is an indispensable regulator of sodium and indirect calcium efflux¹⁹⁰, whose absence and changes in regulatory properties may lead to alterations in cardiac function^{230,255}. In this part of the study, the successful implementation of the localized FRET-based cAMP sensor PLM-E1 for direct monitoring of cAMP dynamics exclusively in sarcolemmal PLM/NKA microdomain could be demonstrated. Using this approach, it became possible to characterize the highly compartmentalized signals in the vicinity of PLM.

4. 2. 1 Restricted cAMP diffusion to the NKA/PLM complex via basal activity of phosphodiesterases

It was observed that in PLM-E1 transduced ARVMs without concomitant cAMP stimulation, inhibition of PDE2 significantly raises cAMP as detected by the cAMP sensitive locally expressed biosensor (Figure 26C). Although the overall PDE2 action in cardiac myocytes is small compared to PDE3 and PDE4 activities⁶⁵, its contribution in cAMP degradation in the vicinity of PLM might be of great importance. This almost three-fold higher local PDE2 responses compared to FRET changes monitored by the cytosolic E1-camps sensor is the first direct evidence of PDE2 confining the PLM microdomain from the bulk cytosol. The basal PDE2 action in the PLM microdomain may serve to protect PLM in the subcellular compartment from excessive phosphorylation. All three PDE2 splice variants have been characterized to be located either at the cytosolic or at membrane fractions of cardiac myocytes. At the plasma membrane, there is a predominant control of PDE2A2 and PDE2A3 isoenzyme activities where it can hydrolyze both cAMP and cGMP and regulate the second messengers in a compartment-specific manner⁹¹. Indeed, it was shown that PDE2 is involved in cGMP dependent cAMP regulation of LTCCs of frog ventricular myocytes and human atrial cardiac myocytes^{91,263,264}. PDE2 controlled cAMP might play a role in PLM phosphorylation and therefore in NKA regulation.

It is noteworthy that PDE2 enzyme activity is stimulated by cGMP (as mentioned in chapter 1. 1. 3). Whether cGMP-mediated, PDE2-dependent decrease of basal cAMP blunts PLM phosphorylation and NKA activity remains to be defined. There is still a debate if cGMP is involved in PLM phosphorylation^{219,265}. Madhani et al. have reported that the PLM-Ser69 phosphorylation could contribute to sildenafil (PDE5 inhibitor) induced cardioprotection against reperfusion injury via a NO/cGMP dependent pathway. Interestingly, experiments in field stimulated cardiomyocytes with an increase in endogenous NO levels revealed PLM phosphorylation and increasing NKA activity to be independent of the cGMP/sGC/PKG pathway.

PLM is described to be functionally quiescent in terms of regulating intracellular Ca²⁺ and Na⁺ levels¹⁷⁰, and hence cardiac contractility at basal state. Rather it is recognized as a cardiac stress protein under conditions of fight-or-flight response, when it enhances NKA activity to minimize the risk of arrhythmogenesis but inhibits NCX to preserve inotropy during stress¹⁷³. Nevertheless, our experiments regarding the control of PDEs over basal cAMP in the vicinity of PLM uncovered a possible role of PDE2 cAMP hydrolysis under normal physiological conditions. Indeed, further experiments are required to quantify PDE2 regulated NKA activity and PDE2 dependent basal phosphorylation rate of PLM for a complete awareness of the physiological regulation of NKA with potentially PDE2 modulated PKA targeting of PLM.

Several studies reported the prominent role of PDE4 in cAMP compartmentation in proximity to Ca²⁺ handling proteins important for cardiac contraction. PDE4 isoforms PDE4B and PDE4D regulate cardiac contractility and Ca²⁺ cycling¹⁰⁶, furthermore, PDE4D3 was reported to act on PKA-mediated RyR2 phosphorylation¹⁰⁸. Our findings suggest a trend towards an elevated basal PDE4 inhibition effect on the PLM associated cAMP levels but this was found to be not statistically different.

4. 2. 2 Locally confined β_2 -AR mediates cAMP signaling pathway proximal to the PLM/NKA complex

It is well known that β_1 -AR induce far-reaching cAMP signals, whereas β_2 -AR signals remain locally confined²⁸. Indeed, we found that β_1 -AR responses in PLM-E1 transduced ARVMs to Iso induced stimulation were similar to signals detected in the bulk cytosol (Figure 16C). Likewise, PDE-dependent regulation of these signals in the microdomain was not significantly different from cytosolic β_1 -AR cAMP signals which is in line with the far-reaching control of β_1 -ARs. In contrast, highly compartment specific β_2 -AR signals led to greater cAMP dependent signal change in the PLM/NKA complex. There is an experimental evidence that Cav3 selectively modulates the localization of β_2 -AR and spatially compartmentalizes its signaling to the T-tubular membrane compartments¹⁴⁶. In conjunction with this, NKA is

compartmentalized by its β -SU in Cav3 rich domains²⁶⁶, also suggested by previous observations in co-immunostainings of the NKA- α -SU organized within cardiac caveolin-rich microdomains²⁶⁷. Based on our findings, it can be reasoned that β_2 -ARs phosphorylate PLM and build a local signalosome, which might also contain NKA and NCX in close proximity (see chapter 1. 2. 1). The signal transduction to the PLM/NKA complex is tightly coupled to the regulation of intracellular Ca^{2+} and cardiac contractility²⁶⁸. Furthermore, Mohler et al. report that NKA, NCX1, and InsP_3R are complexed with ankyrin-B, an adapter protein within a microdomain of cardiomyocyte T-tubules⁷⁵. This subcellular complex is demonstrated as an essential requirement for Ca^{2+} homeostasis and proper cardiac function. This is consistent with our assumption that β_2 -AR signals, which originate in T-tubules, reach the PLM compartment having an impact on Na^+ and Ca^{2+} cycling in cardiomyocytes.

As many previous publications²⁶⁹, this study used cultivated cardiomyocytes expressing cytosolic and targeted FRET biosensors introduced by adenoviruses, which might cause some structural remodeling on t-tubular level²⁷⁰. Despite application of the adenoviral system onto control cells transduced with cytosolic E1-camps, there was still the risk in losing the proper structure of important cAMP compartments in the complex intracellular architecture of cardiomyocytes during cultivation. However, recent studies using morphological analysis of cell membrane morphology in rat myocytes after 48 h of adenoviral transduction in culture under similar conditions could demonstrate the well-preserved integrity of sarcolemmal T-tubules²⁹. These morphological findings are supported by our experiments. Obtaining clearly distinct results for locally confined β_2 -AR signals in the microdomain formed by PLM, we could confirm different organization of cytosolic and local signaling complex at the subcellular level.

4. 2. 3 Critical PDE3-dependent regulation of β_2 -AR mediated cAMP in the vicinity of PLM

Next to their differential coupling to G_s and G_i proteins, the β -ARs differ in subtype specific cAMP signaling pathways and phosphorylation of substrates by local pools of PKA. This phenomenon is justified mainly through compartmentation of signaling events, such as the formation of signalosomes by AKAPs and PDEs (see chapter 1. 1. 2). Nikolaev et al. demonstrated that β_1 -AR-mediated cytoplasmic cAMP is mainly controlled by PDE4, whereas cAMP produced after β_2 -AR stimulation is under the control of multiple PDE isoforms²⁸. β_2 -ARs have a number of interacting proteins including different isoforms of PDE4D, whereas PDE4D8 has been shown to be associated with β_1 -ARs²⁷¹. Recently, it was demonstrated that membrane localized β_2 -AR associated microdomains in caveolin-rich membrane compartments are primarily modulated by PDE3²⁵¹. Similarly, in our FRET experiments we obtained increased β_2 -cAMP sensing under Iso+CGP stimulated PLM-E1 transduced

cardiomyocytes by inhibiting PDE3 (Figure 30F). PDE3 and PDE4 show equal contributions to the control of β_2 -AR mediated cAMP signals in the cytosol (Figure 14D). Since the PLM-E1 biosensor can relatively well resolve β_2 -signals in the microdomain (Figure 12), it revealed the strong cAMP augmenting effect of PDE3 selective inhibitor cilostamide. This clearly suggested a strong PDE3 contribution in the signaling effect of β_2 -cAMP directly at the site of the PLM/NKA complex. Preventing cAMP diffusion from β_2 -AR into the cytosol, PDE3 might act as a scaffolding enzyme to localize generated cAMP to the PLM compartment with its downstream targets, such as PKA. Even though some groups characterized β_2 -ARs signals to be in tight control of PDE4D isoenzymes possibly organized by arrestins^{110,272}, we and others²⁵¹ have proven that PDE3 might also play a significant role in β_2 -AR associated microdomains, such as the PLM/NKA complex. Experiments demonstrate that cGMP inhibited PDE3 provides a sustained increase in cAMP under ANP stimulation, which can be abolished by pretreatment with the PDE3 selective inhibitor cilostamide (Figure 29). Physical proof of microdomain specific PDE3 activity was provided by co-localization analysis with co-immunostained freshly isolated WT-ARVMs. Here PDE3 showed a high co-localization with end. PLM (Figure 28). It is intriguing to argue that PDE3 is primarily responsible for the local modulation of PKA phosphorylation of PLM via β_2 -ARs. Indeed, through previous work it was shown that PDE3 isoenzymes work as scaffolding proteins in spatially confined microdomains. For example, PDE3A localizes at the SERCA2 and SR-membrane whereby it tightly controls basal cardiac contractility by regulating cAMP mediated phosphorylation of PLB and sarcoplasmic Ca^{2+} uptake through the SERCA2²⁷³. As PDE3 is recognized to have a largely interacting role in cardiac Ca^{2+} cycling and serves as a clinical cardiotoxic target to regulate β -AR inotropic responses in the heart^{274,275}, it is likely that its compartmentalized regulation of PLM under neurohormonal stimulation of β_2 -ARs is coupled to Ca^{2+} -regulatory proteins residing in the same cardiac microdomain, i.e. the NCX.

The important finding in this work is the predominant activity of the PDE3 enzyme in the β_2 -AR-cAMP pool in the vicinity of PLM, where cGMP can act here as a competitive inhibitor of PDE3 (Figure 16C). For that reason functional NO-GC activity and effective cGMP synthesis might be essential within this microdomain, which in turn appears to be myocyte and species specific in previous findings²⁷⁶. In case of the L-Type Ca^{2+} current, it was shown that its regulation via cGMP dependent PDE2/3 vary in different species and source of myocytes^{263,277}. Similar conditions prevailed in FRET experiments with aged matched control (AMC) animals used in this Ph.D. thesis, which in contrast did not reveal dominant PDE3 control over β_2 -AR, rather generally comparable PDE profiles with the PLM microdomain were detected. The discrepancy between our findings in 8-12 weeks old Wistar rats and 24 weeks old Sprague Dawley aged matched control (AMC) animals regarding PDE responses to β_2 -AR could be caused by age dependent alterations of the cardiac physiology, the race

difference or this could be another example of local cGMP dependent PDE2/PDE3 crosstalk. Despite being not significantly different ($p=0.13$), there is indeed a clear trend of local PDE2 to respond to selective inhibition upon β_2 -AR stimulation in Sprague Dawley AMC animals. So there is an appreciated level of potentially cGMP activated PDE2 pool in the β_2 -AR controlled PLM microdomain in 24 weeks old rats. In this regard, further experiments in these animals are necessary, which could better explain the moderate FRET change in local PDE3 response compared to Wistar rats (i.e. different NO-GC-cGMP levels, age related and race dependent differences in cardiac physiology, differences of genetic background).

In conclusion, one could postulate that there is a locally confined cAMP effect on PLM regulated by potentially cGMP dependent PDE3, which specifically hydrolyzes the local pool of β_2 -AR-cAMP thereby forming a microdomain and disabling diffusion of the second messenger into the cytosol. In addition to its effects on the NKA and NCX (see chapter 1. 2. 1) there is a possibility that in cardiomyocytes, PLM might potentially be involved in the kinetics of LTCCs²⁰⁷. Under these conditions our findings about the role PDE3 in the PLM-NKA microdomain might have a higher complexity in terms of cardiac contractility. As stated above, PDE3 inhibiting cardiotonic compounds are used in the clinic and could also induce a local increase in β_2 -cAMP and subsequent PKA phosphorylation of PLM resulting in higher sodium and calcium efflux. The enhanced lusitropic effects would protect from Na^+ and Ca^{2+} overload in hypertrophied hearts and limit risks associated with NKA inhibition by cardiac glycosides, such as triggered arrhythmias.

4. 3. Alterations of β_2 -AR control over subsarcolemmal PLM microdomain through localized PDE2/PDE3 subsets in ARVM with chronic heart failure

FRET measurements in ARVMs from animals 16 weeks after myocardial infarction showed that the significant differences in β_2 -AR stimulation between the bulk cytosol and the PLM/NKA microdomain were abolished (Figure 31 and Figure 32). This loss of communication between β_2 -AR and the PLM microdomain is in line with pathophysiological changes occurring during transitioning from early cardiac disease to the functionally decompensated state of the heart, which comes along with structural deformation of subcellular systems and global as well as local alterations in signaling complexes important for proper cardiac function (Figure 5C). Especially, alterations in PDE effects are recognized in hypertrophied cells. Increasing body of evidence demonstrate a clear increase in whole cell PDE2 activity at end stage of heart failure^{155,278} protecting the diseased heart from stress, which is caused by excessive catecholamine dumping at this state. Also in early stage of HF, it was shown that locally detected PDE2 effects at the β_2 -AR were changed, while whole cell PDE2 amounts and activities remained stable²⁵¹. This microdomain specific replacement of cGMP inhibited PDE3 with cGMP activated PDE2 was postulated to be a positive adaptive

mechanism to increased ANP/cGMP effects in hypertrophy. Similarly, our FRET experiments in PLM-E1 transduced MI cardiomyocytes revealed a significant decrease of PDE3 response after β_2 -AR stimulation whereas PDE2 contributions increased in the PLM/NKA microdomain. Likewise, PDE3 and PLM co-immunostained MI cells showed a significantly decreased co-localization pattern compared to AMC cells (Figure 32). Interestingly, after β_2 -AR stimulation no differences between AMC and MI cells in PDE contributions to cAMP hydrolysis in the bulk cytosol were detected. This might indicate that there is no change in global PDE activity after congestive heart failure in ARVMs, but rather subcellular alterations in PDE catalytic activity. Previously, it was shown that in rat hearts post-MI, the NKA expression and activity were depressed, although the determined overexpression of PLM in MI cells may also account for reduced NKA activity¹⁷³ and altered cardiac contractility²⁷⁹. In addition to previous findings, we detected a change in local β_2 -AR signals in MI myocytes and a decrease in PDE3 controlled β_2 -cAMP in the PLM microdomain being substituted by an increasing PDE2 effect. Our findings suggest impaired local signaling in the β_2 -PLM-NKA network which may contribute to contractile and electrical dysfunction in arrhythmia upon ischemic disease. Since the implemented disease model for this Ph.D. thesis is an example of decompensated hypertrophy and chronic heart failure, further investigations about sarcolemmal architecture, altered β -AR densities and PLM localized changes of PDE effects on β_1 -AR-cAMP would serve for a more detailed characterization of adrenergic signaling cascade between the receptor and PLM microdomain in cardiac disease.

5. Conclusion and Outlook

The PLM/NKA complex provides the only significant cardiac Na⁺ efflux pathway and is therefore vital for normal physiological function and an important target for therapy during congestive heart failure. The aim of this thesis was to extensively study real time dynamics of cAMP in the PLM-associated microdomain controlled by β -adrenergic signaling and its alterations in chronic heart disease. In order to determine differential regulation of the PLM microdomain via subtype specific β -AR signaling and changes of PDE effects over local pools of cAMP, a new localized FRET based cAMP sensitive biosensor named PLM-E1 was successfully generated and characterized. For the FRET based experiments an adenoviral system was used, which enabled titer controlled measurements in transduced cardiomyocytes after 48 h cultivation. The present study confirmed the existence of a differentially regulated PLM/NKA compartment confined from the cytosolic domain through individual PDE subtype contributions to the cAMP degradation under selective stimulation of β -AR subtypes. It identified a PDE2 dependent local cAMP regulation in the vicinity of PLM (Figure 33), which could be further explored in subsequent biochemical or electrophysiological studies, giving insights about PDE2 controlled PLM phosphorylation and NKA function or both. The second essential finding is that there is a tight coupling of β_2 -AR signals to the PLM/NKA complex regulated by a specific PDE pattern, which is changed dramatically in post-infarcted failing cardiomyocytes (Figure 34). We provided some interesting insights but in terms of PDE regulated cAMP/PKA signaling to PLM it would be exciting to investigate sodium and calcium induced local changes in cAMP at the plasma membrane. Considering its importance in cardiac ECC and the complex role of PLM controlling NKA, NCX or LTCCs²⁰⁷ by having three different substrate residues for PKA and PKC, it would be intriguing to investigate kinase activities and cGMP dynamics via PKC and cGMP sensitive FRET based localized biosensors.

In the longer term, our observations of PDE-dependent cAMP dynamics at the PLM/NKA complex and their changes in heart failure may serve not only as a basis for further studies but may also be interesting for clinical treatment of impaired NKA activity leading to sodium and calcium overload. Particularly, selective targeting of PDE2 could be a therapeutic approach during cardiac arrhythmia or increased catecholaminergic stress which may lead to low intracellular sodium levels by elevating the sodium pump activity.

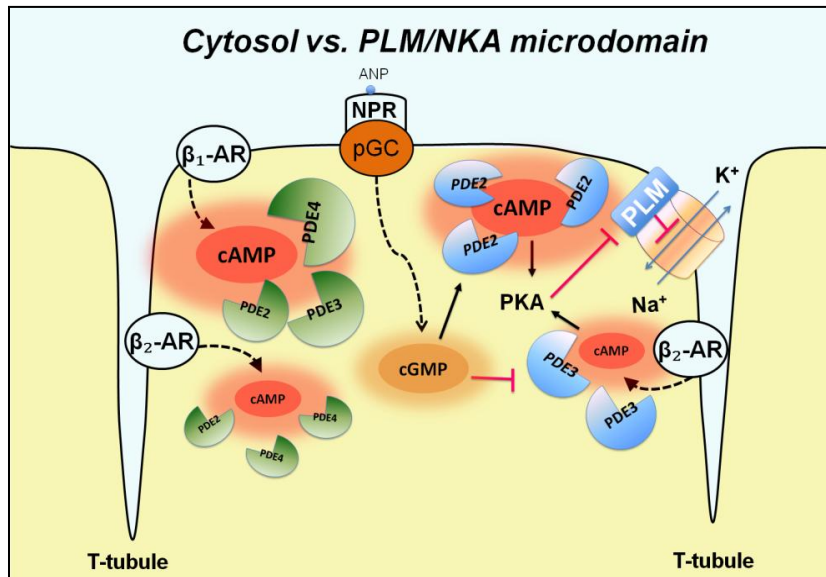


Figure 33. Cartoon showing highly confined basal cAMP dynamics and a distinct β_2 -cAMP effect in the PLM microdomain of ARVMs. There is a predominant PDE2 control of the basal cAMP pool in the vicinity of PLM, whilst the microdomain specific PDE activities under β_1 -AR stimulation are comparable to those in the cytosol (PDE4>PDE3>>PDE2). Far reaching β_1 -AR signals equally effect the PLM/NKA complex. The β_2 -AR mediated cAMP effects on PLM are mainly controlled via cGMP dependent PDE3, while the low cytosolic cAMP amounts are hydrolyzed uniformly by PDE2-4. The cAMP/PKA regulation of the β_2 -AR associated PLM/NKA complex strongly rely on PDE enzymes activated (PDE2) and inhibited (PDE3) by cGMP.

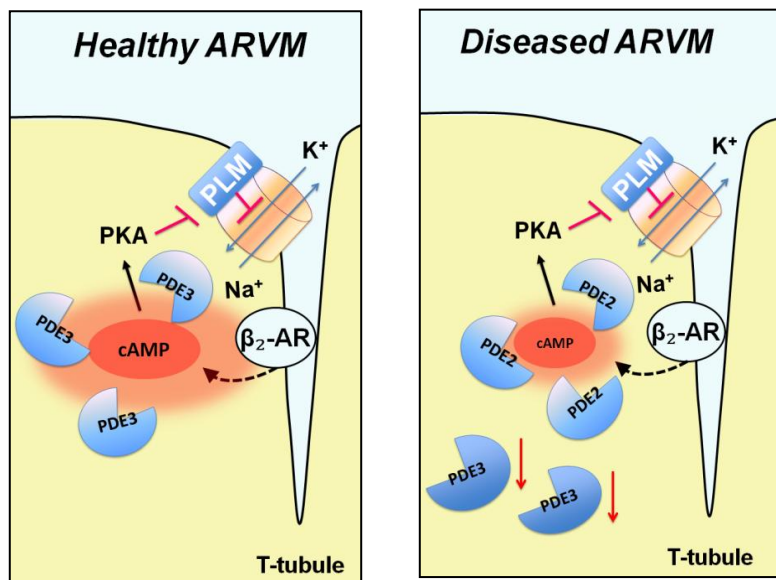


Figure 34. Cartoon demonstrating the change in local cAMP dynamics at the cardiac PLM microdomain. In healthy ARVMs there is a privileged communication between β_2 -AR and PLM/NKA microdomain, which is altered in chronic heart failure. This includes the general decrease in the β_2 -AR mediated cAMP effect and the substitution of its former PDE3 regulation with PDE2 at the β_2 -AR linked PLM/NKA complex.

6. Bibliography

- 1 Lafontan, M. *et al.* Adrenergic regulation of adipocyte metabolism. *Human reproduction* **12 Suppl 1**, 6-20 (1997).
- 2 Brudvik, K. W. & Tasken, K. Modulation of T cell immune functions by the prostaglandin E(2) - cAMP pathway in chronic inflammatory states. *British journal of pharmacology* **166**, 411-419, doi:10.1111/j.1476-5381.2011.01800.x (2012).
- 3 Nishimura, K., Tamaoki, J., Isono, K., Aoshiba, K. & Nagai, A. Beta-adrenergic receptor-mediated growth of human airway epithelial cell lines. *The European respiratory journal* **20**, 353-358 (2002).
- 4 Morgado, M., Cairrao, E., Santos-Silva, A. J. & Verde, I. Cyclic nucleotide-dependent relaxation pathways in vascular smooth muscle. *Cellular and molecular life sciences : CMLS* **69**, 247-266, doi:10.1007/s00018-011-0815-2 (2012).
- 5 Iwai-Kanai, E. *et al.* alpha- and beta-adrenergic pathways differentially regulate cell type-specific apoptosis in rat cardiac myocytes. *Circulation* **100**, 305-311 (1999).
- 6 Gordan, R., Gwathmey, J. K. & Xie, L. H. Autonomic and endocrine control of cardiovascular function. *World journal of cardiology* **7**, 204-214, doi:10.4330/wjc.v7.i4.204 (2015).
- 7 Madamanchi, A. Beta-adrenergic receptor signaling in cardiac function and heart failure. *McGill journal of medicine : MJM : an international forum for the advancement of medical sciences by students* **10**, 99-104 (2007).
- 8 Taylor, S. S., Buechler, J. A. & Yonemoto, W. cAMP-dependent protein kinase: framework for a diverse family of regulatory enzymes. *Annual review of biochemistry* **59**, 971-1005, doi:10.1146/annurev.bi.59.070190.004543 (1990).
- 9 Biel, M. & Michalakakis, S. Cyclic nucleotide-gated channels. *Handbook of experimental pharmacology*, 111-136, doi:10.1007/978-3-540-68964-5_7 (2009).
- 10 Wright, P. T., Schobesberger, S. & Gorelik, J. Studying GPCR/cAMP pharmacology from the perspective of cellular structure. *Frontiers in pharmacology* **6**, 148, doi:10.3389/fphar.2015.00148 (2015).
- 11 de Rooij, J. *et al.* Epac is a Rap1 guanine-nucleotide-exchange factor directly activated by cyclic AMP. *Nature* **396**, 474-477, doi:10.1038/24884 (1998).
- 12 Metrich, M. *et al.* Epac mediates beta-adrenergic receptor-induced cardiomyocyte hypertrophy. *Circulation research* **102**, 959-965, doi:10.1161/CIRCRESAHA.107.164947 (2008).
- 13 Krebs, E. G. & Beavo, J. A. Phosphorylation-dephosphorylation of enzymes. *Annual review of biochemistry* **48**, 923-959, doi:10.1146/annurev.bi.48.070179.004423 (1979).
- 14 Lohse, M. J., Engelhardt, S. & Eschenhagen, T. What is the role of beta-adrenergic signaling in heart failure? *Circulation research* **93**, 896-906, doi:10.1161/01.RES.0000102042.83024.CA (2003).
- 15 Despa, S. *et al.* Phospholemman-phosphorylation mediates the beta-adrenergic effects on Na/K pump function in cardiac myocytes. *Circulation research* **97**, 252-259, doi:10.1161/01.RES.0000176532.97731.e5 (2005).
- 16 Bers, D. M. Cardiac excitation-contraction coupling. *Nature* **415**, 198-205, doi:10.1038/415198a (2002).
- 17 Bers, D. M. & Despa, S. Na/K-ATPase--an integral player in the adrenergic fight-or-flight response. *Trends in cardiovascular medicine* **19**, 111-118, doi:10.1016/j.tcm.2009.07.001 (2009).
- 18 Grimm, M. & Brown, J. H. Beta-adrenergic receptor signaling in the heart: role of CaMKII. *Journal of molecular and cellular cardiology* **48**, 322-330, doi:10.1016/j.yjmcc.2009.10.016 (2010).
- 19 Abraham, G., Kneuer, C., Ehrhardt, C., Honscha, W. & Ungemach, F. R. Expression of functional beta2-adrenergic receptors in the lung epithelial cell lines 16HBE14o(-), Calu-3 and

- A549. *Biochimica et biophysica acta* **1691**, 169-179, doi:10.1016/j.bbamcr.2004.02.002 (2004).
- 20 Healy, D. P., Munzel, P. A. & Insel, P. A. Localization of beta 1- and beta 2-adrenergic
receptors in rat kidney by autoradiography. *Circulation research* **57**, 278-284 (1985).
- 21 Zhou, Y. Y. *et al.* Localized cAMP-dependent signaling mediates beta 2-adrenergic modulation
of cardiac excitation-contraction coupling. *The American journal of physiology* **273**, H1611-
1618 (1997).
- 22 Xiao, R. P., Ji, X. & Lakatta, E. G. Functional coupling of the beta 2-adrenoceptor to a pertussis
toxin-sensitive G protein in cardiac myocytes. *Molecular pharmacology* **47**, 322-329 (1995).
- 23 Kuschel, M. *et al.* beta2-adrenergic cAMP signaling is uncoupled from phosphorylation of
cytoplasmic proteins in canine heart. *Circulation* **99**, 2458-2465 (1999).
- 24 Altschuld, R. A. *et al.* Response of failing canine and human heart cells to beta 2-adrenergic
stimulation. *Circulation* **92**, 1612-1618 (1995).
- 25 Levy, F. O., Zhu, X., Kaumann, A. J. & Birnbaumer, L. Efficacy of beta 1-adrenergic receptors is
lower than that of beta 2-adrenergic receptors. *Proceedings of the National Academy of
Sciences of the United States of America* **90**, 10798-10802 (1993).
- 26 Bristow, M. R., Hershberger, R. E., Port, J. D., Minobe, W. & Rasmussen, R. Beta 1- and beta
2-adrenergic receptor-mediated adenylate cyclase stimulation in nonfailing and failing
human ventricular myocardium. *Molecular pharmacology* **35**, 295-303 (1989).
- 27 Green, S. A., Holt, B. D. & Liggett, S. B. Beta 1- and beta 2-adrenergic receptors display
subtype-selective coupling to Gs. *Molecular pharmacology* **41**, 889-893 (1992).
- 28 Nikolaev, V. O., Bunemann, M., Schmitteckert, E., Lohse, M. J. & Engelhardt, S. Cyclic AMP
imaging in adult cardiac myocytes reveals far-reaching beta1-adrenergic but locally confined
beta2-adrenergic receptor-mediated signaling. *Circulation research* **99**, 1084-1091,
doi:10.1161/01.RES.0000250046.69918.d5 (2006).
- 29 Nikolaev, V. O. *et al.* Beta2-adrenergic receptor redistribution in heart failure changes cAMP
compartmentation. *Science* **327**, 1653-1657, doi:10.1126/science.1185988 (2010).
- 30 Chen-Izu, Y. *et al.* G(i)-dependent localization of beta(2)-adrenergic receptor signaling to L-
type Ca(2+) channels. *Biophysical journal* **79**, 2547-2556, doi:10.1016/S0006-3495(00)76495-
2 (2000).
- 31 Zheng, M., Han, Q. D. & Xiao, R. P. Distinct beta-adrenergic receptor subtype signaling in the
heart and their pathophysiological relevance. *Sheng li xue bao : [Acta physiologica Sinica]* **56**,
1-15 (2004).
- 32 Zhu, W. Z. *et al.* Dual modulation of cell survival and cell death by beta(2)-adrenergic
signaling in adult mouse cardiac myocytes. *Proceedings of the National Academy of Sciences
of the United States of America* **98**, 1607-1612, doi:10.1073/pnas.98.4.1607 (2001).
- 33 Cannavo, A., Liccardo, D. & Koch, W. J. Targeting cardiac beta-adrenergic signaling via GRK2
inhibition for heart failure therapy. *Frontiers in physiology* **4**, 264,
doi:10.3389/fphys.2013.00264 (2013).
- 34 Lohse, M. J., Benovic, J. L., Codina, J., Caron, M. G. & Lefkowitz, R. J. beta-Arrestin: a protein
that regulates beta-adrenergic receptor function. *Science* **248**, 1547-1550 (1990).
- 35 Bristow, M. R. *et al.* Beta 1- and beta 2-adrenergic-receptor subpopulations in nonfailing and
failing human ventricular myocardium: coupling of both receptor subtypes to muscle
contraction and selective beta 1-receptor down-regulation in heart failure. *Circulation
research* **59**, 297-309 (1986).
- 36 Brodde, O. E. Beta-adrenoceptors in cardiac disease. *Pharmacology & therapeutics* **60**, 405-
430 (1993).
- 37 Bristow, M. R. *et al.* Decreased catecholamine sensitivity and beta-adrenergic-receptor
density in failing human hearts. *The New England journal of medicine* **307**, 205-211,
doi:10.1056/NEJM198207223070401 (1982).

- 38 Communal, C., Singh, K., Sawyer, D. B. & Colucci, W. S. Opposing effects of beta(1)- and beta(2)-adrenergic receptors on cardiac myocyte apoptosis : role of a pertussis toxin-sensitive G protein. *Circulation* **100**, 2210-2212 (1999).
- 39 Brodde, O. E. The functional importance of beta 1 and beta 2 adrenoceptors in the human heart. *The American journal of cardiology* **62**, 24C-29C (1988).
- 40 Krief, S. *et al.* Tissue distribution of beta 3-adrenergic receptor mRNA in man. *The Journal of clinical investigation* **91**, 344-349, doi:10.1172/JCI116191 (1993).
- 41 Devic, E., Xiang, Y., Gould, D. & Kobilka, B. Beta-adrenergic receptor subtype-specific signaling in cardiac myocytes from beta(1) and beta(2) adrenoceptor knockout mice. *Molecular pharmacology* **60**, 577-583 (2001).
- 42 Kohout, T. A. *et al.* Augmentation of cardiac contractility mediated by the human beta(3)-adrenergic receptor overexpressed in the hearts of transgenic mice. *Circulation* **104**, 2485-2491 (2001).
- 43 Gerhardt, C. C., Gros, J., Strosberg, A. D. & Issad, T. Stimulation of the extracellular signal-regulated kinase 1/2 pathway by human beta-3 adrenergic receptor: new pharmacological profile and mechanism of activation. *Molecular pharmacology* **55**, 255-262 (1999).
- 44 Soeder, K. J. *et al.* The beta3-adrenergic receptor activates mitogen-activated protein kinase in adipocytes through a Gi-dependent mechanism. *The Journal of biological chemistry* **274**, 12017-12022 (1999).
- 45 Belge, C. *et al.* Enhanced expression of beta3-adrenoceptors in cardiac myocytes attenuates neurohormone-induced hypertrophic remodeling through nitric oxide synthase. *Circulation* **129**, 451-462, doi:10.1161/CIRCULATIONAHA.113.004940 (2014).
- 46 Hammond, J. & Balligand, J. L. Nitric oxide synthase and cyclic GMP signaling in cardiac myocytes: from contractility to remodeling. *Journal of molecular and cellular cardiology* **52**, 330-340, doi:10.1016/j.yjmcc.2011.07.029 (2012).
- 47 Berthet, J., Rall, T. W. & Sutherland, E. W. The relationship of epinephrine and glucagon to liver phosphorylase. IV. Effect of epinephrine and glucagon on the reactivation of phosphorylase in liver homogenates. *The Journal of biological chemistry* **224**, 463-475 (1957).
- 48 Kandel, E. R. The molecular biology of memory: cAMP, PKA, CRE, CREB-1, CREB-2, and CPEB. *Molecular brain* **5**, 14, doi:10.1186/1756-6606-5-14 (2012).
- 49 Shi, W. X. & Bunney, B. S. Roles of intracellular cAMP and protein kinase A in the actions of dopamine and neurotensin on midbrain dopamine neurons. *The Journal of neuroscience : the official journal of the Society for Neuroscience* **12**, 2433-2438 (1992).
- 50 Yajima, H. *et al.* cAMP enhances insulin secretion by an action on the ATP-sensitive K⁺ channel-independent pathway of glucose signaling in rat pancreatic islets. *Diabetes* **48**, 1006-1012 (1999).
- 51 Tengholm, A. & Gylfe, E. Oscillatory control of insulin secretion. *Molecular and cellular endocrinology* **297**, 58-72, doi:10.1016/j.mce.2008.07.009 (2009).
- 52 Mayr, B. M., Canettieri, G. & Montminy, M. R. Distinct effects of cAMP and mitogenic signals on CREB-binding protein recruitment impart specificity to target gene activation via CREB. *Proceedings of the National Academy of Sciences of the United States of America* **98**, 10936-10941, doi:10.1073/pnas.191152098 (2001).
- 53 Altarejos, J. Y. & Montminy, M. CREB and the CRTC co-activators: sensors for hormonal and metabolic signals. *Nature reviews. Molecular cell biology* **12**, 141-151, doi:10.1038/nrm3072 (2011).
- 54 Bodor, J. *et al.* Cyclic AMP underpins suppression by regulatory T cells. *European journal of immunology* **42**, 1375-1384, doi:10.1002/eji.201141578 (2012).
- 55 Zagotta, W. N. *et al.* Structural basis for modulation and agonist specificity of HCN pacemaker channels. *Nature* **425**, 200-205, doi:10.1038/nature01922 (2003).
- 56 Bai, Y. & Sanderson, M. J. Airway smooth muscle relaxation results from a reduction in the frequency of Ca²⁺ oscillations induced by a cAMP-mediated inhibition of the IP₃ receptor. *Respiratory research* **7**, 34, doi:10.1186/1465-9921-7-34 (2006).

- 57 Hayes, J. S., Brunton, L. L., Brown, J. H., Reese, J. B. & Mayer, S. E. Hormonally specific expression of cardiac protein kinase activity. *Proceedings of the National Academy of Sciences of the United States of America* **76**, 1570-1574 (1979).
- 58 Vila Petroff, M. G., Egan, J. M., Wang, X. & Sollott, S. J. Glucagon-like peptide-1 increases cAMP but fails to augment contraction in adult rat cardiac myocytes. *Circulation research* **89**, 445-452 (2001).
- 59 Hohl, C. M. & Li, Q. A. Compartmentation of cAMP in adult canine ventricular myocytes. Relation to single-cell free Ca²⁺ transients. *Circulation research* **69**, 1369-1379 (1991).
- 60 Xiao, R. P. *et al.* Beta 2-adrenergic receptor-stimulated increase in cAMP in rat heart cells is not coupled to changes in Ca²⁺ dynamics, contractility, or phospholamban phosphorylation. *The Journal of biological chemistry* **269**, 19151-19156 (1994).
- 61 Di Benedetto, G. *et al.* Protein kinase A type I and type II define distinct intracellular signaling compartments. *Circulation research* **103**, 836-844, doi:10.1161/CIRCRESAHA.108.174813 (2008).
- 62 Zaccolo, M. cAMP signal transduction in the heart: understanding spatial control for the development of novel therapeutic strategies. *British journal of pharmacology* **158**, 50-60, doi:10.1111/j.1476-5381.2009.00185.x (2009).
- 63 Lefkimmatis, K., Lerondi, D. & Hofer, A. M. The inner and outer compartments of mitochondria are sites of distinct cAMP/PKA signaling dynamics. *The Journal of cell biology* **202**, 453-462, doi:10.1083/jcb.201303159 (2013).
- 64 Sample, V. *et al.* Regulation of nuclear PKA revealed by spatiotemporal manipulation of cyclic AMP. *Nature chemical biology* **8**, 375-382, doi:10.1038/nchembio.799 (2012).
- 65 Mongillo, M. *et al.* Fluorescence resonance energy transfer-based analysis of cAMP dynamics in live neonatal rat cardiac myocytes reveals distinct functions of compartmentalized phosphodiesterases. *Circulation research* **95**, 67-75, doi:10.1161/01.RES.0000134629.84732.11 (2004).
- 66 DiPilato, L. M. & Zhang, J. The role of membrane microdomains in shaping beta2-adrenergic receptor-mediated cAMP dynamics. *Molecular bioSystems* **5**, 832-837, doi:10.1039/b823243a (2009).
- 67 Rich, T. C. *et al.* Cellular mechanisms underlying prostaglandin-induced transient cAMP signals near the plasma membrane of HEK-293 cells. *American journal of physiology. Cell physiology* **292**, C319-331, doi:10.1152/ajpcell.00121.2006 (2007).
- 68 Agarwal, S. R. *et al.* Role of membrane microdomains in compartmentation of cAMP signaling. *PLoS one* **9**, e95835, doi:10.1371/journal.pone.0095835 (2014).
- 69 Pani, B. & Singh, B. B. Lipid rafts/caveolae as microdomains of calcium signaling. *Cell calcium* **45**, 625-633, doi:10.1016/j.ceca.2009.02.009 (2009).
- 70 Jurevicius, J. & Fischmeister, R. cAMP compartmentation is responsible for a local activation of cardiac Ca²⁺ channels by beta-adrenergic agonists. *Proceedings of the National Academy of Sciences of the United States of America* **93**, 295-299 (1996).
- 71 Davare, M. A. *et al.* A beta2 adrenergic receptor signaling complex assembled with the Ca²⁺ channel Cav1.2. *Science* **293**, 98-101, doi:10.1126/science.293.5527.98 (2001).
- 72 Zaccolo, M. & Pozzan, T. Discrete microdomains with high concentration of cAMP in stimulated rat neonatal cardiac myocytes. *Science* **295**, 1711-1715, doi:10.1126/science.1069982 (2002).
- 73 Hulme, J. T., Lin, T. W., Westenbroek, R. E., Scheuer, T. & Catterall, W. A. Beta-adrenergic regulation requires direct anchoring of PKA to cardiac CaV1.2 channels via a leucine zipper interaction with A kinase-anchoring protein 15. *Proceedings of the National Academy of Sciences of the United States of America* **100**, 13093-13098, doi:10.1073/pnas.2135335100 (2003).
- 74 Hofmann, F., Flockerzi, V., Kahl, S. & Wegener, J. W. L-type CaV1.2 calcium channels: from in vitro findings to in vivo function. *Physiological reviews* **94**, 303-326, doi:10.1152/physrev.00016.2013 (2014).

- 75 Mohler, P. J., Davis, J. Q. & Bennett, V. Ankyrin-B coordinates the Na/K ATPase, Na/Ca exchanger, and InsP3 receptor in a cardiac T-tubule/SR microdomain. *PLoS biology* **3**, e423, doi:10.1371/journal.pbio.0030423 (2005).
- 76 Crambert, G., Fuzesi, M., Garty, H., Karlsh, S. & Geering, K. Phospholemman (FXD1) associates with Na,K-ATPase and regulates its transport properties. *Proceedings of the National Academy of Sciences of the United States of America* **99**, 11476-11481, doi:10.1073/pnas.182267299 (2002).
- 77 Brette, F., Salle, L. & Orchard, C. H. Quantification of calcium entry at the T-tubules and surface membrane in rat ventricular myocytes. *Biophysical journal* **90**, 381-389, doi:10.1529/biophysj.105.069013 (2006).
- 78 Brette, F. & Orchard, C. T-tubule function in mammalian cardiac myocytes. *Circulation research* **92**, 1182-1192, doi:10.1161/01.RES.0000074908.17214.FD (2003).
- 79 Perera, R. K. & Nikolaev, V. O. Compartmentation of cAMP signalling in cardiomyocytes in health and disease. *Acta physiologica* **207**, 650-662, doi:10.1111/apha.12077 (2013).
- 80 Conti, M. & Beavo, J. Biochemistry and physiology of cyclic nucleotide phosphodiesterases: essential components in cyclic nucleotide signaling. *Annual review of biochemistry* **76**, 481-511, doi:10.1146/annurev.biochem.76.060305.150444 (2007).
- 81 Francis, S. H., Blount, M. A. & Corbin, J. D. Mammalian cyclic nucleotide phosphodiesterases: molecular mechanisms and physiological functions. *Physiological reviews* **91**, 651-690, doi:10.1152/physrev.00030.2010 (2011).
- 82 Lugnier, C. Cyclic nucleotide phosphodiesterase (PDE) superfamily: a new target for the development of specific therapeutic agents. *Pharmacology & therapeutics* **109**, 366-398, doi:10.1016/j.pharmthera.2005.07.003 (2006).
- 83 Zhang, M. & Kass, D. A. Phosphodiesterases and cardiac cGMP: evolving roles and controversies. *Trends in pharmacological sciences* **32**, 360-365, doi:10.1016/j.tips.2011.02.019 (2011).
- 84 Takimoto, E. Cyclic GMP-dependent signaling in cardiac myocytes. *Circulation journal : official journal of the Japanese Circulation Society* **76**, 1819-1825 (2012).
- 85 Nikolaev, V. O. & Lohse, M. J. Monitoring of cAMP synthesis and degradation in living cells. *Physiology* **21**, 86-92, doi:10.1152/physiol.00057.2005 (2006).
- 86 Sonnenburg, W. K., Seger, D. & Beavo, J. A. Molecular cloning of a cDNA encoding the "61-kDa" calmodulin-stimulated cyclic nucleotide phosphodiesterase. Tissue-specific expression of structurally related isoforms. *The Journal of biological chemistry* **268**, 645-652 (1993).
- 87 Miller, C. L. & Yan, C. Targeting cyclic nucleotide phosphodiesterase in the heart: therapeutic implications. *Journal of cardiovascular translational research* **3**, 507-515, doi:10.1007/s12265-010-9203-9 (2010).
- 88 Vandeput, F. *et al.* Cyclic nucleotide phosphodiesterase PDE1C1 in human cardiac myocytes. *The Journal of biological chemistry* **282**, 32749-32757, doi:10.1074/jbc.M703173200 (2007).
- 89 Miller, C. L. *et al.* Role of Ca²⁺/calmodulin-stimulated cyclic nucleotide phosphodiesterase 1 in mediating cardiomyocyte hypertrophy. *Circulation research* **105**, 956-964, doi:10.1161/CIRCRESAHA.109.198515 (2009).
- 90 Martinez, S. E. *et al.* The two GAF domains in phosphodiesterase 2A have distinct roles in dimerization and in cGMP binding. *Proceedings of the National Academy of Sciences of the United States of America* **99**, 13260-13265, doi:10.1073/pnas.192374899 (2002).
- 91 Mongillo, M. *et al.* Compartmentalized phosphodiesterase-2 activity blunts beta-adrenergic cardiac inotropy via an NO/cGMP-dependent pathway. *Circulation research* **98**, 226-234, doi:10.1161/01.RES.0000200178.34179.93 (2006).
- 92 Muller, B., Stoclet, J. C. & Lugnier, C. Cytosolic and membrane-bound cyclic nucleotide phosphodiesterases from guinea pig cardiac ventricles. *European journal of pharmacology* **225**, 263-272 (1992).

- 93 Castro, L. R., Verde, I., Cooper, D. M. & Fischmeister, R. Cyclic guanosine monophosphate compartmentation in rat cardiac myocytes. *Circulation* **113**, 2221-2228, doi:10.1161/CIRCULATIONAHA.105.599241 (2006).
- 94 Stangherlin, A. *et al.* cGMP signals modulate cAMP levels in a compartment-specific manner to regulate catecholamine-dependent signaling in cardiac myocytes. *Circulation research* **108**, 929-939, doi:10.1161/CIRCRESAHA.110.230698 (2011).
- 95 Wechsler, J. *et al.* Isoforms of cyclic nucleotide phosphodiesterase PDE3A in cardiac myocytes. *The Journal of biological chemistry* **277**, 38072-38078, doi:10.1074/jbc.M203647200 (2002).
- 96 Shakur, Y. *et al.* Regulation and function of the cyclic nucleotide phosphodiesterase (PDE3) gene family. *Progress in nucleic acid research and molecular biology* **66**, 241-277 (2001).
- 97 Sun, B. *et al.* Role of phosphodiesterase type 3A and 3B in regulating platelet and cardiac function using subtype-selective knockout mice. *Cellular signalling* **19**, 1765-1771, doi:10.1016/j.cellsig.2007.03.012 (2007).
- 98 Hambleton, R. *et al.* Isoforms of cyclic nucleotide phosphodiesterase PDE3 and their contribution to cAMP hydrolytic activity in subcellular fractions of human myocardium. *The Journal of biological chemistry* **280**, 39168-39174, doi:10.1074/jbc.M506760200 (2005).
- 99 Murashima, S., Tanaka, T., Hockman, S. & Manganiello, V. Characterization of particulate cyclic nucleotide phosphodiesterases from bovine brain: purification of a distinct cGMP-stimulated isoenzyme. *Biochemistry* **29**, 5285-5292 (1990).
- 100 Shakur, Y. *et al.* Membrane localization of cyclic nucleotide phosphodiesterase 3 (PDE3). Two N-terminal domains are required for the efficient targeting to, and association of, PDE3 with endoplasmic reticulum. *The Journal of biological chemistry* **275**, 38749-38761, doi:10.1074/jbc.M001734200 (2000).
- 101 Degerman, E., Belfrage, P. & Manganiello, V. C. Structure, localization, and regulation of cGMP-inhibited phosphodiesterase (PDE3). *The Journal of biological chemistry* **272**, 6823-6826 (1997).
- 102 Abi-Gerges, A. *et al.* Decreased expression and activity of cAMP phosphodiesterases in cardiac hypertrophy and its impact on beta-adrenergic cAMP signals. *Circulation research* **105**, 784-792, doi:10.1161/CIRCRESAHA.109.197947 (2009).
- 103 Fischmeister, R. *et al.* Compartmentation of cyclic nucleotide signaling in the heart: the role of cyclic nucleotide phosphodiesterases. *Circulation research* **99**, 816-828, doi:10.1161/01.RES.0000246118.98832.04 (2006).
- 104 Richter, W., Jin, S. L. & Conti, M. Splice variants of the cyclic nucleotide phosphodiesterase PDE4D are differentially expressed and regulated in rat tissue. *The Biochemical journal* **388**, 803-811, doi:10.1042/BJ20050030 (2005).
- 105 Baillie, G. S. & Houslay, M. D. Arrestin times for compartmentalised cAMP signalling and phosphodiesterase-4 enzymes. *Current opinion in cell biology* **17**, 129-134, doi:10.1016/j.ceb.2005.01.003 (2005).
- 106 Leroy, J. *et al.* Phosphodiesterase 4B in the cardiac L-type Ca(2)(+) channel complex regulates Ca(2)(+) current and protects against ventricular arrhythmias in mice. *The Journal of clinical investigation* **121**, 2651-2661, doi:10.1172/JCI44747 (2011).
- 107 Dodge, K. L. *et al.* mAkap assembles a protein kinase A/PDE4 phosphodiesterase cAMP signaling module. *The EMBO journal* **20**, 1921-1930, doi:10.1093/emboj/20.8.1921 (2001).
- 108 Lehnart, S. E. *et al.* Phosphodiesterase 4D deficiency in the ryanodine-receptor complex promotes heart failure and arrhythmias. *Cell* **123**, 25-35, doi:10.1016/j.cell.2005.07.030 (2005).
- 109 Perry, S. J. *et al.* Targeting of cyclic AMP degradation to beta 2-adrenergic receptors by beta-arrestins. *Science* **298**, 834-836, doi:10.1126/science.1074683 (2002).
- 110 Richter, W. *et al.* Signaling from beta1- and beta2-adrenergic receptors is defined by differential interactions with PDE4. *The EMBO journal* **27**, 384-393, doi:10.1038/sj.emboj.7601968 (2008).

- 111 Ghigo, A. *et al.* Phosphoinositide 3-kinase gamma protects against catecholamine-induced ventricular arrhythmia through protein kinase A-mediated regulation of distinct phosphodiesterases. *Circulation* **126**, 2073-2083, doi:10.1161/CIRCULATIONAHA.112.114074 (2012).
- 112 Lindman, B. R. *et al.* Effects of phosphodiesterase type 5 inhibition on systemic and pulmonary hemodynamics and ventricular function in patients with severe symptomatic aortic stenosis. *Circulation* **125**, 2353-2362, doi:10.1161/CIRCULATIONAHA.111.081125 (2012).
- 113 Shan, X. *et al.* Differential expression of PDE5 in failing and nonfailing human myocardium. *Circulation. Heart failure* **5**, 79-86, doi:10.1161/CIRCHEARTFAILURE.111.961706 (2012).
- 114 Lee, D. I. & Kass, D. A. Phosphodiesterases and cyclic GMP regulation in heart muscle. *Physiology* **27**, 248-258, doi:10.1152/physiol.00011.2012 (2012).
- 115 Guazzi, M., Vicenzi, M., Arena, R. & Guazzi, M. D. PDE5 inhibition with sildenafil improves left ventricular diastolic function, cardiac geometry, and clinical status in patients with stable systolic heart failure: results of a 1-year, prospective, randomized, placebo-controlled study. *Circulation. Heart failure* **4**, 8-17, doi:10.1161/CIRCHEARTFAILURE.110.944694 (2011).
- 116 Soderling, S. H., Bayuga, S. J. & Beavo, J. A. Cloning and characterization of a cAMP-specific cyclic nucleotide phosphodiesterase. *Proceedings of the National Academy of Sciences of the United States of America* **95**, 8991-8996 (1998).
- 117 Fisher, D. A., Smith, J. F., Pillar, J. S., St Denis, S. H. & Cheng, J. B. Isolation and characterization of PDE8A, a novel human cAMP-specific phosphodiesterase. *Biochemical and biophysical research communications* **246**, 570-577, doi:10.1006/bbrc.1998.8684 (1998).
- 118 Hayashi, M. *et al.* Molecular cloning and characterization of human PDE8B, a novel thyroid-specific isozyme of 3',5'-cyclic nucleotide phosphodiesterase. *Biochemical and biophysical research communications* **250**, 751-756, doi:10.1006/bbrc.1998.9379 (1998).
- 119 Brown, K. M., Lee, L. C., Findlay, J. E., Day, J. P. & Baillie, G. S. Cyclic AMP-specific phosphodiesterase, PDE8A1, is activated by protein kinase A-mediated phosphorylation. *FEBS letters* **586**, 1631-1637, doi:10.1016/j.febslet.2012.04.033 (2012).
- 120 Patrucco, E., Albergine, M. S., Santana, L. F. & Beavo, J. A. Phosphodiesterase 8A (PDE8A) regulates excitation-contraction coupling in ventricular myocytes. *Journal of molecular and cellular cardiology* **49**, 330-333, doi:10.1016/j.yjmcc.2010.03.016 (2010).
- 121 Fisher, D. A., Smith, J. F., Pillar, J. S., St Denis, S. H. & Cheng, J. B. Isolation and characterization of PDE9A, a novel human cGMP-specific phosphodiesterase. *The Journal of biological chemistry* **273**, 15559-15564 (1998).
- 122 Lee, D. I. *et al.* Phosphodiesterase 9A controls nitric-oxide-independent cGMP and hypertrophic heart disease. *Nature* **519**, 472-476, doi:10.1038/nature14332 (2015).
- 123 Diviani, D., Dodge-Kafka, K. L., Li, J. & Kapiloff, M. S. A-kinase anchoring proteins: scaffolding proteins in the heart. *American journal of physiology. Heart and circulatory physiology* **301**, H1742-1753, doi:10.1152/ajpheart.00569.2011 (2011).
- 124 Perino, A., Ghigo, A., Scott, J. D. & Hirsch, E. Anchoring proteins as regulators of signaling pathways. *Circulation research* **111**, 482-492, doi:10.1161/CIRCRESAHA.111.262899 (2012).
- 125 Scott, J. D. & Santana, L. F. A-kinase anchoring proteins: getting to the heart of the matter. *Circulation* **121**, 1264-1271, doi:10.1161/CIRCULATIONAHA.109.896357 (2010).
- 126 Troger, J., Moutty, M. C., Skroblin, P. & Klussmann, E. A-kinase anchoring proteins as potential drug targets. *British journal of pharmacology* **166**, 420-433, doi:10.1111/j.1476-5381.2011.01796.x (2012).
- 127 Scott, J. D., Dessauer, C. W. & Tasken, K. Creating order from chaos: cellular regulation by kinase anchoring. *Annual review of pharmacology and toxicology* **53**, 187-210, doi:10.1146/annurev-pharmtox-011112-140204 (2013).
- 128 Gao, T. *et al.* cAMP-dependent regulation of cardiac L-type Ca²⁺ channels requires membrane targeting of PKA and phosphorylation of channel subunits. *Neuron* **19**, 185-196 (1997).

- 129 Nichols, C. B. *et al.* Sympathetic stimulation of adult cardiomyocytes requires association of AKAP5 with a subpopulation of L-type calcium channels. *Circulation research* **107**, 747-756, doi:10.1161/CIRCRESAHA.109.216127 (2010).
- 130 Henn, V. *et al.* Identification of a novel A-kinase anchoring protein 18 isoform and evidence for its role in the vasopressin-induced aquaporin-2 shuttle in renal principal cells. *The Journal of biological chemistry* **279**, 26654-26665, doi:10.1074/jbc.M312835200 (2004).
- 131 Lygren, B. *et al.* AKAP complex regulates Ca²⁺ re-uptake into heart sarcoplasmic reticulum. *EMBO reports* **8**, 1061-1067, doi:10.1038/sj.embor.7401081 (2007).
- 132 Marx, S. O. *et al.* Requirement of a macromolecular signaling complex for beta adrenergic receptor modulation of the KCNQ1-KCNE1 potassium channel. *Science* **295**, 496-499, doi:10.1126/science.1066843 (2002).
- 133 Terrenoire, C., Houslay, M. D., Baillie, G. S. & Kass, R. S. The cardiac IKs potassium channel macromolecular complex includes the phosphodiesterase PDE4D3. *The Journal of biological chemistry* **284**, 9140-9146, doi:10.1074/jbc.M805366200 (2009).
- 134 Kapiloff, M. S. *et al.* An adenylyl cyclase-mAKAPbeta signaling complex regulates cAMP levels in cardiac myocytes. *The Journal of biological chemistry* **284**, 23540-23546, doi:10.1074/jbc.M109.030072 (2009).
- 135 Dodge-Kafka, K. L. *et al.* The protein kinase A anchoring protein mAKAP coordinates two integrated cAMP effector pathways. *Nature* **437**, 574-578, doi:10.1038/nature03966 (2005).
- 136 Tucci, P. J. Pathophysiological characteristics of the post-myocardial infarction heart failure model in rats. *Arquivos brasileiros de cardiologia* **96**, 420-424 (2011).
- 137 Kolk, M. V. *et al.* LAD-ligation: a murine model of myocardial infarction. *Journal of visualized experiments : JoVE*, doi:10.3791/1438 (2009).
- 138 Rubin, S. A., Fishbein, M. C. & Swan, H. J. Compensatory hypertrophy in the heart after myocardial infarction in the rat. *Journal of the American College of Cardiology* **1**, 1435-1441 (1983).
- 139 Frangogiannis, N. G. Pathophysiology of Myocardial Infarction. *Comprehensive Physiology* **5**, 1841-1875, doi:10.1002/cphy.c150006 (2015).
- 140 Diwan, A. & Dorn, G. W., 2nd. Decompensation of cardiac hypertrophy: cellular mechanisms and novel therapeutic targets. *Physiology* **22**, 56-64, doi:10.1152/physiol.00033.2006 (2007).
- 141 BenedPrognostic significance of plasma norepinephrine in patients with asymptomatic left ventricular dysfunction. SOLVD Regulation of PKA binding to AKAPs in the heart: alterations in human heart failureict, C. R. *et al.* Prognostic significance of plasma norepinephrine in patients with asymptomatic left ventricular dysfunction. SOLVD Investigators. *Circulation* **94**, 690-697 (1996).
- 142 Movsesian, M. A. & Bristow, M. R. Alterations in cAMP-mediated signaling and their role in the pathophysiology of dilated cardiomyopathy. *Current topics in developmental biology* **68**, 25-48, doi:10.1016/S0070-2153(05)68002-7 (2005).
- 143 Ungerer, M., Bohm, M., Elce, J. S., Erdmann, E. & Lohse, M. J. Altered expression of beta-adrenergic receptor kinase and beta 1-adrenergic receptors in the failing human heart. *Circulation* **87**, 454-463 (1993).
- 144 Wagner, E. *et al.* Stimulated emission depletion live-cell super-resolution imaging shows proliferative remodeling of T-tubule membrane structures after myocardial infarction. *Circulation research* **111**, 402-414, doi:10.1161/CIRCRESAHA.112.274530 (2012).
- 145 Lyon, A. R. *et al.* Loss of T-tubules and other changes to surface topography in ventricular myocytes from failing human and rat heart. *Proceedings of the National Academy of Sciences of the United States of America* **106**, 6854-6859, doi:10.1073/pnas.0809777106 (2009).
- 146 Wright, P. T. *et al.* Caveolin-3 regulates compartmentation of cardiomyocyte beta2-adrenergic receptor-mediated cAMP signaling. *Journal of molecular and cellular cardiology* **67**, 38-48, doi:10.1016/j.yjmcc.2013.12.003 (2014).
- 147 Zakhary, D. R., Moravec, C. S. & Bond, M. Regulation of PKA binding to AKAPs in the heart: alterations in human heart failure. *Circulation* **101**, 1459-1464 (2000).

- 148 McConnell, B. K., Moravec, C. S. & Bond, M. Troponin I phosphorylation and myofilament calcium sensitivity during decompensated cardiac hypertrophy. *The American journal of physiology* **274**, H385-396 (1998).
- 149 Zakhary, D. R., Moravec, C. S., Stewart, R. W. & Bond, M. Protein kinase A (PKA)-dependent troponin-I phosphorylation and PKA regulatory subunits are decreased in human dilated cardiomyopathy. *Circulation* **99**, 505-510 (1999).
- 150 Marx, S. O. *et al.* PKA phosphorylation dissociates FKBP12.6 from the calcium release channel (ryanodine receptor): defective regulation in failing hearts. *Cell* **101**, 365-376 (2000).
- 151 Wehrens, X. H. *et al.* FKBP12.6 deficiency and defective calcium release channel (ryanodine receptor) function linked to exercise-induced sudden cardiac death. *Cell* **113**, 829-840 (2003).
- 152 Shan, J. *et al.* Role of chronic ryanodine receptor phosphorylation in heart failure and beta-adrenergic receptor blockade in mice. *The Journal of clinical investigation* **120**, 4375-4387, doi:10.1172/JCI37649 (2010).
- 153 Pare, G. C. *et al.* The mAKAP complex participates in the induction of cardiac myocyte hypertrophy by adrenergic receptor signaling. *Journal of cell science* **118**, 5637-5646, doi:10.1242/jcs.02675 (2005).
- 154 Sprenger, J. U. *et al.* In vivo model with targeted cAMP biosensor reveals changes in receptor-microdomain communication in cardiac disease. *Nature communications* **6**, 6965, doi:10.1038/ncomms7965 (2015).
- 155 Mehel, H. *et al.* Phosphodiesterase-2 is up-regulated in human failing hearts and blunts beta-adrenergic responses in cardiomyocytes. *Journal of the American College of Cardiology* **62**, 1596-1606, doi:10.1016/j.jacc.2013.05.057 (2013).
- 156 Ding, B. *et al.* Functional role of phosphodiesterase 3 in cardiomyocyte apoptosis: implication in heart failure. *Circulation* **111**, 2469-2476, doi:10.1161/01.CIR.0000165128.39715.87 (2005).
- 157 Smith, C. J. *et al.* Development of decompensated dilated cardiomyopathy is associated with decreased gene expression and activity of the milrinone-sensitive cAMP phosphodiesterase PDE3A. *Circulation* **96**, 3116-3123 (1997).
- 158 Baim, D. S. *et al.* Evaluation of a new bipyridine inotropic agent--milrinone--in patients with severe congestive heart failure. *The New England journal of medicine* **309**, 748-756, doi:10.1056/NEJM198309293091302 (1983).
- 159 Packer, M. *et al.* Effect of oral milrinone on mortality in severe chronic heart failure. The PROMISE Study Research Group. *The New England journal of medicine* **325**, 1468-1475, doi:10.1056/NEJM199111213252103 (1991).
- 160 Froese, A. & Nikolaev, V. O. Imaging alterations of cardiomyocyte cAMP microdomains in disease. *Frontiers in pharmacology* **6**, 172, doi:10.3389/fphar.2015.00172 (2015).
- 161 Skou, J. C. The influence of some cations on an adenosine triphosphatase from peripheral nerves. *Biochimica et biophysica acta* **23**, 394-401 (1957).
- 162 Blaustein, M. P. Sodium ions, calcium ions, blood pressure regulation, and hypertension: a reassessment and a hypothesis. *The American journal of physiology* **232**, C165-173 (1977).
- 163 Molitoris, B. A. & Kinne, R. Ischemia induces surface membrane dysfunction. Mechanism of altered Na⁺-dependent glucose transport. *The Journal of clinical investigation* **80**, 647-654, doi:10.1172/JCI113117 (1987).
- 164 Bers, D. M. & Despa, S. Na⁺ transport in cardiac myocytes; Implications for excitation-contraction coupling. *IUBMB life* **61**, 215-221, doi:10.1002/iub.163 (2009).
- 165 Bers, D. M., Barry, W. H. & Despa, S. Intracellular Na⁺ regulation in cardiac myocytes. *Cardiovascular research* **57**, 897-912 (2003).
- 166 Fuller, W. *et al.* Regulation of the cardiac sodium pump. *Cellular and molecular life sciences : CMLS* **70**, 1357-1380, doi:10.1007/s00018-012-1134-y (2013).
- 167 Clausen, T. Quantification of Na⁺,K⁺ pumps and their transport rate in skeletal muscle: functional significance. *The Journal of general physiology* **142**, 327-345, doi:10.1085/jgp.201310980 (2013).

- 168 Hunt, S. A. *et al.* 2009 focused update incorporated into the ACC/AHA 2005 Guidelines for the Diagnosis and Management of Heart Failure in Adults: a report of the American College of Cardiology Foundation/American Heart Association Task Force on Practice Guidelines: developed in collaboration with the International Society for Heart and Lung Transplantation. *Circulation* **119**, e391-479, doi:10.1161/CIRCULATIONAHA.109.192065 (2009).
- 169 Simmerman, H. K. & Jones, L. R. Phospholamban: protein structure, mechanism of action, and role in cardiac function. *Physiological reviews* **78**, 921-947 (1998).
- 170 Cheung, J. Y. *et al.* Phospholemman: a novel cardiac stress protein. *Clinical and translational science* **3**, 189-196, doi:10.1111/j.1752-8062.2010.00213.x (2010).
- 171 Bossuyt, J., Despa, S., Martin, J. L. & Bers, D. M. Phospholemman phosphorylation alters its fluorescence resonance energy transfer with the Na/K-ATPase pump. *The Journal of biological chemistry* **281**, 32765-32773, doi:10.1074/jbc.M606254200 (2006).
- 172 Bibert, S., Roy, S., Schaer, D., Horisberger, J. D. & Geering, K. Phosphorylation of phospholemman (FXD1) by protein kinases A and C modulates distinct Na,K-ATPase isozymes. *The Journal of biological chemistry* **283**, 476-486, doi:10.1074/jbc.M705830200 (2008).
- 173 Zhang, X. Q. *et al.* Phospholemman inhibition of the cardiac Na⁺/Ca²⁺ exchanger. Role of phosphorylation. *The Journal of biological chemistry* **281**, 7784-7792, doi:10.1074/jbc.M512092200 (2006).
- 174 Fuller, W. *et al.* FXD1 phosphorylation in vitro and in adult rat cardiac myocytes: threonine 69 is a novel substrate for protein kinase C. *American journal of physiology. Cell physiology* **296**, C1346-1355, doi:10.1152/ajpcell.00523.2008 (2009).
- 175 Morth, J. P. *et al.* Crystal structure of the sodium-potassium pump. *Nature* **450**, 1043-1049, doi:10.1038/nature06419 (2007).
- 176 Shinoda, T., Ogawa, H., Cornelius, F. & Toyoshima, C. Crystal structure of the sodium-potassium pump at 2.4 Å resolution. *Nature* **459**, 446-450, doi:10.1038/nature07939 (2009).
- 177 Ogawa, H., Shinoda, T., Cornelius, F. & Toyoshima, C. Crystal structure of the sodium-potassium pump (Na⁺,K⁺-ATPase) with bound potassium and ouabain. *Proceedings of the National Academy of Sciences of the United States of America* **106**, 13742-13747, doi:10.1073/pnas.0907054106 (2009).
- 178 Kaplan, J. H. Biochemistry of Na,K-ATPase. *Annual review of biochemistry* **71**, 511-535, doi:10.1146/annurev.biochem.71.102201.141218 (2002).
- 179 Sweadner, K. J. Isozymes of the Na⁺/K⁺-ATPase. *Biochimica et biophysica acta* **988**, 185-220 (1989).
- 180 Geering, K. The functional role of the beta-subunit in the maturation and intracellular transport of Na,K-ATPase. *FEBS letters* **285**, 189-193 (1991).
- 181 Sweadner, K. J. & Rael, E. The FXD gene family of small ion transport regulators or channels: cDNA sequence, protein signature sequence, and expression. *Genomics* **68**, 41-56, doi:10.1006/geno.2000.6274 (2000).
- 182 Cornelius, F. & Mahmmoud, Y. A. Functional modulation of the sodium pump: the regulatory proteins "Fixit". *News in physiological sciences : an international journal of physiology produced jointly by the International Union of Physiological Sciences and the American Physiological Society* **18**, 119-124 (2003).
- 183 Horisberger, J. D., Jaunin, P., Good, P. J., Rossier, B. C. & Geering, K. Coexpression of alpha 1 with putative beta 3 subunits results in functional Na⁺/K⁺ pumps in *Xenopus* oocytes. *Proceedings of the National Academy of Sciences of the United States of America* **88**, 8397-8400 (1991).
- 184 Berry, R. G., Despa, S., Fuller, W., Bers, D. M. & Shattock, M. J. Differential distribution and regulation of mouse cardiac Na⁺/K⁺-ATPase alpha1 and alpha2 subunits in T-tubule and surface sarcolemmal membranes. *Cardiovascular research* **73**, 92-100, doi:10.1016/j.cardiores.2006.11.006 (2007).

- 185 Swift, F., Tovsrud, N., Enger, U. H., Sjaastad, I. & Sejersted, O. M. The Na⁺/K⁺-ATPase alpha2-isoform regulates cardiac contractility in rat cardiomyocytes. *Cardiovascular research* **75**, 109-117, doi:10.1016/j.cardiores.2007.03.017 (2007).
- 186 Swift, F. *et al.* Altered Na⁺/Ca²⁺-exchanger activity due to downregulation of Na⁺/K⁺-ATPase alpha2-isoform in heart failure. *Cardiovascular research* **78**, 71-78, doi:10.1093/cvr/cvn013 (2008).
- 187 Dostanic, I., Schultz Jel, J., Lorenz, J. N. & Lingrel, J. B. The alpha 1 isoform of Na,K-ATPase regulates cardiac contractility and functionally interacts and co-localizes with the Na/Ca exchanger in heart. *The Journal of biological chemistry* **279**, 54053-54061, doi:10.1074/jbc.M410737200 (2004).
- 188 Pavlovic, D., Fuller, W. & Shattock, M. J. Novel regulation of cardiac Na pump via phospholemman. *Journal of molecular and cellular cardiology* **61**, 83-93, doi:10.1016/j.yjmcc.2013.05.002 (2013).
- 189 Despa, S., Lingrel, J. B. & Bers, D. M. Na(+)/K(+)-ATPase alpha2-isoform preferentially modulates Ca²⁺(+) transients and sarcoplasmic reticulum Ca²⁺(+) release in cardiac myocytes. *Cardiovascular research* **95**, 480-486, doi:10.1093/cvr/cvs213 (2012).
- 190 Shattock, M. J. *et al.* Na⁺/Ca²⁺ exchange and Na⁺/K⁺-ATPase in the heart. *The Journal of physiology* **593**, 1361-1382, doi:10.1113/jphysiol.2014.282319 (2015).
- 191 James, P. F. *et al.* Identification of a specific role for the Na,K-ATPase alpha 2 isoform as a regulator of calcium in the heart. *Molecular cell* **3**, 555-563 (1999).
- 192 Tian, J. & Xie, Z. J. The Na-K-ATPase and calcium-signaling microdomains. *Physiology* **23**, 205-211, doi:10.1152/physiol.00008.2008 (2008).
- 193 Liu, L., Zhao, X., Pierre, S. V. & Askari, A. Association of PI3K-Akt signaling pathway with digitalis-induced hypertrophy of cardiac myocytes. *American journal of physiology. Cell physiology* **293**, C1489-1497, doi:10.1152/ajpcell.00158.2007 (2007).
- 194 Geering, K. FXYD proteins: new regulators of Na-K-ATPase. *American journal of physiology. Renal physiology* **290**, F241-250, doi:10.1152/ajprenal.00126.2005 (2006).
- 195 Palmer, C. J., Scott, B. T. & Jones, L. R. Purification and complete sequence determination of the major plasma membrane substrate for cAMP-dependent protein kinase and protein kinase C in myocardium. *The Journal of biological chemistry* **266**, 11126-11130 (1991).
- 196 Bogaev, R. C. *et al.* Gene structure and expression of phospholemman in mouse. *Gene* **271**, 69-79 (2001).
- 197 Wetzell, R. K. & Sweadner, K. J. Phospholemman expression in extraglomerular mesangium and afferent arteriole of the juxtaglomerular apparatus. *American journal of physiology. Renal physiology* **285**, F121-129, doi:10.1152/ajprenal.00241.2002 (2003).
- 198 Feschenko, M. S. *et al.* Phospholemman, a single-span membrane protein, is an accessory protein of Na,K-ATPase in cerebellum and choroid plexus. *The Journal of neuroscience : the official journal of the Society for Neuroscience* **23**, 2161-2169 (2003).
- 199 Walaas, S. I., Czernik, A. J., Olstad, O. K., Sletten, K. & Walaas, O. Protein kinase C and cyclic AMP-dependent protein kinase phosphorylate phospholemman, an insulin and adrenaline-regulated membrane phosphoprotein, at specific sites in the carboxy terminal domain. *The Biochemical journal* **304 (Pt 2)**, 635-640 (1994).
- 200 Han, F., Bossuyt, J., Despa, S., Tucker, A. L. & Bers, D. M. Phospholemman phosphorylation mediates the protein kinase C-dependent effects on Na⁺/K⁺ pump function in cardiac myocytes. *Circulation research* **99**, 1376-1383, doi:10.1161/01.RES.0000251667.73461.fb (2006).
- 201 Khafaga, M. *et al.* Na(+)/K(+)-ATPase E960 and phospholemman F28 are critical for their functional interaction. *Proceedings of the National Academy of Sciences of the United States of America* **109**, 20756-20761, doi:10.1073/pnas.1207866109 (2012).
- 202 Pavlovic, D., Fuller, W. & Shattock, M. J. The intracellular region of FXYD1 is sufficient to regulate cardiac Na/K ATPase. *FASEB journal : official publication of the Federation of*

- American Societies for Experimental Biology* **21**, 1539-1546, doi:10.1096/fj.06-7269com (2007).
- 203 Silverman, B. *et al.* Serine 68 phosphorylation of phospholemman: acute isoform-specific activation of cardiac Na/K ATPase. *Cardiovascular research* **65**, 93-103, doi:10.1016/j.cardiores.2004.09.005 (2005).
- 204 Zhang, X. Q. *et al.* Phospholemman overexpression inhibits Na⁺-K⁺-ATPase in adult rat cardiac myocytes: relevance to decreased Na⁺ pump activity in postinfarction myocytes. *Journal of applied physiology* **100**, 212-220, doi:10.1152/jappphysiol.00757.2005 (2006).
- 205 Bossuyt, J. *et al.* Isoform specificity of the Na/K-ATPase association and regulation by phospholemman. *The Journal of biological chemistry* **284**, 26749-26757, doi:10.1074/jbc.M109.047357 (2009).
- 206 Lifshitz, Y., Lindzen, M., Garty, H. & Karlisch, S. J. Functional interactions of phospholemman (PLM) (FXD1) with Na⁺,K⁺-ATPase. Purification of alpha1/beta1/PLM complexes expressed in *Pichia pastoris*. *The Journal of biological chemistry* **281**, 15790-15799, doi:10.1074/jbc.M601993200 (2006).
- 207 Wang, X. *et al.* Phospholemman modulates the gating of cardiac L-type calcium channels. *Biophysical journal* **98**, 1149-1159, doi:10.1016/j.bpj.2009.11.032 (2010).
- 208 Moorman, J. R. *et al.* Unitary anion currents through phospholemman channel molecules. *Nature* **377**, 737-740, doi:10.1038/377737a0 (1995).
- 209 Moorman, J. R., Palmer, C. J., John, J. E., 3rd, Durieux, M. E. & Jones, L. R. Phospholemman expression induces a hyperpolarization-activated chloride current in *Xenopus* oocytes. *The Journal of biological chemistry* **267**, 14551-14554 (1992).
- 210 Morales-Mulia, M., Pasantes-Morales, H. & Moran, J. Volume sensitive efflux of taurine in HEK293 cells overexpressing phospholemman. *Biochimica et biophysica acta* **1496**, 252-260 (2000).
- 211 Despa, S., Tucker, A. L. & Bers, D. M. Phospholemman-mediated activation of Na/K-ATPase limits [Na]_i and inotropic state during beta-adrenergic stimulation in mouse ventricular myocytes. *Circulation* **117**, 1849-1855, doi:10.1161/CIRCULATIONAHA.107.754051 (2008).
- 212 Wang, J. *et al.* Phospholemman and beta-adrenergic stimulation in the heart. *American journal of physiology. Heart and circulatory physiology* **298**, H807-815, doi:10.1152/ajpheart.00877.2009 (2010).
- 213 Presti, C. F., Jones, L. R. & Lindemann, J. P. Isoproterenol-induced phosphorylation of a 15-kilodalton sarcolemmal protein in intact myocardium. *The Journal of biological chemistry* **260**, 3860-3867 (1985).
- 214 Presti, C. F., Scott, B. T. & Jones, L. R. Identification of an endogenous protein kinase C activity and its intrinsic 15-kilodalton substrate in purified canine cardiac sarcolemmal vesicles. *The Journal of biological chemistry* **260**, 13879-13889 (1985).
- 215 Sweadner, K. J. & Feschenko, M. S. Predicted location and limited accessibility of protein kinase A phosphorylation site on Na-K-ATPase. *American journal of physiology. Cell physiology* **280**, C1017-1026 (2001).
- 216 Bell, J. R. *et al.* Characterization of the phospholemman knockout mouse heart: depressed left ventricular function with increased Na-K-ATPase activity. *American journal of physiology. Heart and circulatory physiology* **294**, H613-621, doi:10.1152/ajpheart.01332.2007 (2008).
- 217 Bossuyt, J., Ai, X., Moorman, J. R., Pogwizd, S. M. & Bers, D. M. Expression and phosphorylation of the na-pump regulatory subunit phospholemman in heart failure. *Circulation research* **97**, 558-565, doi:10.1161/01.RES.0000181172.27931.c3 (2005).
- 218 Fuller, W., Eaton, P., Bell, J. R. & Shattock, M. J. Ischemia-induced phosphorylation of phospholemman directly activates rat cardiac Na/K-ATPase. *FASEB journal : official publication of the Federation of American Societies for Experimental Biology* **18**, 197-199, doi:10.1096/fj.03-0213fje (2004).

- 219 Pavlovic, D. *et al.* Nitric oxide regulates cardiac intracellular Na⁺ and Ca²⁺ by modulating Na/K ATPase via PKCepsilon and phospholemman-dependent mechanism. *Journal of molecular and cellular cardiology* **61**, 164-171, doi:10.1016/j.yjmcc.2013.04.013 (2013).
- 220 Song, J. *et al.* Serine 68 of phospholemman is critical in modulation of contractility, [Ca²⁺]_i transients, and Na⁺/Ca²⁺ exchange in adult rat cardiac myocytes. *American journal of physiology. Heart and circulatory physiology* **288**, H2342-2354, doi:10.1152/ajpheart.01133.2004 (2005).
- 221 Wang, J. *et al.* Regulation of in vivo cardiac contractility by phospholemman: role of Na⁺/Ca²⁺ exchange. *American journal of physiology. Heart and circulatory physiology* **300**, H859-868, doi:10.1152/ajpheart.00894.2010 (2011).
- 222 Neubauer, S., Newell, J. B. & Ingwall, J. S. Metabolic consequences and predictability of ventricular fibrillation in hypoxia. A ³¹P- and ²³Na-nuclear magnetic resonance study of the isolated rat heart. *Circulation* **86**, 302-310 (1992).
- 223 Tani, M. & Neely, J. R. Role of intracellular Na⁺ in Ca²⁺ overload and depressed recovery of ventricular function of reperfused ischemic rat hearts. Possible involvement of H⁺-Na⁺ and Na⁺-Ca²⁺ exchange. *Circulation research* **65**, 1045-1056 (1989).
- 224 Pogwizd, S. M., Sipido, K. R., Verdonck, F. & Bers, D. M. Intracellular Na in animal models of hypertrophy and heart failure: contractile function and arrhythmogenesis. *Cardiovascular research* **57**, 887-896 (2003).
- 225 Verdonck, F., Volders, P. G., Vos, M. A. & Sipido, K. R. Intracellular Na⁺ and altered Na⁺ transport mechanisms in cardiac hypertrophy and failure. *Journal of molecular and cellular cardiology* **35**, 5-25 (2003).
- 226 Verdonck, F., Volders, P. G., Vos, M. A. & Sipido, K. R. Increased Na⁺ concentration and altered Na/K pump activity in hypertrophied canine ventricular cells. *Cardiovascular research* **57**, 1035-1043 (2003).
- 227 Despa, S., Islam, M. A., Weber, C. R., Pogwizd, S. M. & Bers, D. M. Intracellular Na⁺ concentration is elevated in heart failure but Na/K pump function is unchanged. *Circulation* **105**, 2543-2548 (2002).
- 228 Undrovinas, A. I., Maltsev, V. A. & Sabbah, H. N. Repolarization abnormalities in cardiomyocytes of dogs with chronic heart failure: role of sustained inward current. *Cellular and molecular life sciences : CMLS* **55**, 494-505 (1999).
- 229 Fuller, W., Parmar, V., Eaton, P., Bell, J. R. & Shattock, M. J. Cardiac ischemia causes inhibition of the Na/K ATPase by a labile cytosolic compound whose production is linked to oxidant stress. *Cardiovascular research* **57**, 1044-1051 (2003).
- 230 Boguslavskiy, A. *et al.* Cardiac hypertrophy in mice expressing unphosphorylatable phospholemman. *Cardiovascular research* **104**, 72-82, doi:10.1093/cvr/cvu182 (2014).
- 231 El-Armouche, A. *et al.* Phospholemman-dependent regulation of the cardiac Na/K-ATPase activity is modulated by inhibitor-1 sensitive type-1 phosphatase. *FASEB journal : official publication of the Federation of American Societies for Experimental Biology* **25**, 4467-4475, doi:10.1096/fj.11-184903 (2011).
- 232 Semb, S. O. *et al.* Reduced myocardial Na⁺, K⁺-pump capacity in congestive heart failure following myocardial infarction in rats. *Journal of molecular and cellular cardiology* **30**, 1311-1328 (1998).
- 233 Allen, P. D., Schmidt, T. A., Marsh, J. D. & Kjeldsen, K. Na,K-ATPase expression in normal and failing human left ventricle. *Basic research in cardiology* **87 Suppl 1**, 87-94 (1992).
- 234 Mirza, M. A. *et al.* Phospholemman deficiency in postinfarct hearts: enhanced contractility but increased mortality. *Clinical and translational science* **5**, 235-242, doi:10.1111/j.1752-8062.2012.00403.x (2012).
- 235 Correll, R. N. *et al.* Overexpression of the Na⁺/K⁺ ATPase alpha2 but not alpha1 isoform attenuates pathological cardiac hypertrophy and remodeling. *Circulation research* **114**, 249-256, doi:10.1161/CIRCRESAHA.114.302293 (2014).

- 236 Brooker, G., Harper, J. F., Terasaki, W. L. & Moylan, R. D. Radioimmunoassay of cyclic AMP and cyclic GMP. *Advances in cyclic nucleotide research* **10**, 1-33 (1979).
- 237 Harper, J. F. & Brooker, G. Femtomole sensitive radioimmunoassay for cyclic AMP and cyclic GMP after ²O acetylation by acetic anhydride in aqueous solution. *Journal of cyclic nucleotide research* **1**, 207-218 (1975).
- 238 Williams, C. cAMP detection methods in HTS: selecting the best from the rest. *Nature reviews. Drug discovery* **3**, 125-135, doi:10.1038/nrd1306 (2004).
- 239 Sprenger, J. U. & Nikolaev, V. O. Biophysical techniques for detection of cAMP and cGMP in living cells. *International journal of molecular sciences* **14**, 8025-8046, doi:10.3390/ijms14048025 (2013).
- 240 Förster, T. Zwischenmolekulare Energiewanderung und Fluoreszenz. *Annalen der Physik* **437**, 55-75, doi:10.1002/andp.19484370105 (1948).
- 241 Piston, D. W. & Kremers, G. J. Fluorescent protein FRET: the good, the bad and the ugly. *Trends in biochemical sciences* **32**, 407-414, doi:10.1016/j.tibs.2007.08.003 (2007).
- 242 Shrestha, D., Jenei, A., Nagy, P., Vereb, G. & Szollosi, J. Understanding FRET as a research tool for cellular studies. *International journal of molecular sciences* **16**, 6718-6756, doi:10.3390/ijms16046718 (2015).
- 243 Zhang, J., Campbell, R. E., Ting, A. Y. & Tsien, R. Y. Creating new fluorescent probes for cell biology. *Nature reviews. Molecular cell biology* **3**, 906-918, doi:10.1038/nrm976 (2002).
- 244 Frings, S., Seifert, R., Godde, M. & Kaupp, U. B. Profoundly different calcium permeation and blockage determine the specific function of distinct cyclic nucleotide-gated channels. *Neuron* **15**, 169-179 (1995).
- 245 Willoughby, D. & Cooper, D. M. Organization and Ca²⁺ regulation of adenylyl cyclases in cAMP microdomains. *Physiological reviews* **87**, 965-1010, doi:10.1152/physrev.00049.2006 (2007).
- 246 Rochais, F. *et al.* Negative feedback exerted by cAMP-dependent protein kinase and cAMP phosphodiesterase on subsarcolemmal cAMP signals in intact cardiac myocytes: an in vivo study using adenovirus-mediated expression of CNG channels. *The Journal of biological chemistry* **279**, 52095-52105, doi:10.1074/jbc.M405697200 (2004).
- 247 Adams, S. R., Harootunian, A. T., Buechler, Y. J., Taylor, S. S. & Tsien, R. Y. Fluorescence ratio imaging of cyclic AMP in single cells. *Nature* **349**, 694-697, doi:10.1038/349694a0 (1991).
- 248 Zaccolo, M. *et al.* A genetically encoded, fluorescent indicator for cyclic AMP in living cells. *Nature cell biology* **2**, 25-29, doi:10.1038/71345 (2000).
- 249 Nikolaev, V. O., Bunemann, M., Hein, L., Hannawacker, A. & Lohse, M. J. Novel single chain cAMP sensors for receptor-induced signal propagation. *The Journal of biological chemistry* **279**, 37215-37218, doi:10.1074/jbc.C400302200 (2004).
- 250 Nikolaev, V. O., Gambaryan, S., Engelhardt, S., Walter, U. & Lohse, M. J. Real-time monitoring of the PDE2 activity of live cells: hormone-stimulated cAMP hydrolysis is faster than hormone-stimulated cAMP synthesis. *The Journal of biological chemistry* **280**, 1716-1719, doi:10.1074/jbc.C400505200 (2005).
- 251 Perera, R. K. *et al.* Microdomain switch of cGMP-regulated phosphodiesterases leads to ANP-induced augmentation of beta-adrenoceptor-stimulated contractility in early cardiac hypertrophy. *Circulation research* **116**, 1304-1311, doi:10.1161/CIRCRESAHA.116.306082 (2015).
- 252 Howie, J. *et al.* Substrate recognition by the cell surface palmitoyl transferase DHHc5. *Proceedings of the National Academy of Sciences of the United States of America* **111**, 17534-17539, doi:10.1073/pnas.1413627111 (2014).
- 253 Lewis, C. J., Gong, H., Brown, M. J. & Harding, S. E. Overexpression of beta 1-adrenoceptors in adult rat ventricular myocytes enhances CGP 12177A cardiostimulation: implications for 'putative' beta 4-adrenoceptor pharmacology. *British journal of pharmacology* **141**, 813-824, doi:10.1038/sj.bjp.0705668 (2004).

- 254 Tulloch, L. B. *et al.* The inhibitory effect of phospholemman on the sodium pump requires its palmitoylation. *The Journal of biological chemistry* **286**, 36020-36031, doi:10.1074/jbc.M111.282145 (2011).
- 255 Jia, L. G. *et al.* Hypertrophy, increased ejection fraction, and reduced Na-K-ATPase activity in phospholemman-deficient mice. *American journal of physiology. Heart and circulatory physiology* **288**, H1982-1988, doi:10.1152/ajpheart.00142.2004 (2005).
- 256 Chen, L. S., Lo, C. F., Numann, R. & Cuddy, M. Characterization of the human and rat phospholemman (PLM) cDNAs and localization of the human PLM gene to chromosome 19q13.1. *Genomics* **41**, 435-443, doi:10.1006/geno.1997.4665 (1997).
- 257 Louch, W. E., Sheehan, K. A. & Wolska, B. M. Methods in cardiomyocyte isolation, culture, and gene transfer. *Journal of molecular and cellular cardiology* **51**, 288-298, doi:10.1016/j.yjmcc.2011.06.012 (2011).
- 258 Calebiro, D. *et al.* Persistent cAMP-signals triggered by internalized G-protein-coupled receptors. *PLoS biology* **7**, e1000172, doi:10.1371/journal.pbio.1000172 (2009).
- 259 Lomas, O. *et al.* Adenoviral transduction of FRET-based biosensors for cAMP in primary adult mouse cardiomyocytes. *Methods in molecular biology* **1294**, 103-115, doi:10.1007/978-1-4939-2537-7_8 (2015).
- 260 Leroy, J. *et al.* Spatiotemporal dynamics of beta-adrenergic cAMP signals and L-type Ca²⁺ channel regulation in adult rat ventricular myocytes: role of phosphodiesterases. *Circulation research* **102**, 1091-1100, doi:10.1161/CIRCRESAHA.107.167817 (2008).
- 261 Mika, D., Richter, W., Westenbroek, R. E., Catterall, W. A. & Conti, M. PDE4B mediates local feedback regulation of beta(1)-adrenergic cAMP signaling in a sarcolemmal compartment of cardiac myocytes. *Journal of cell science* **127**, 1033-1042, doi:10.1242/jcs.140251 (2014).
- 262 Shattock, M. J. Phospholemman: its role in normal cardiac physiology and potential as a druggable target in disease. *Current opinion in pharmacology* **9**, 160-166, doi:10.1016/j.coph.2008.12.015 (2009).
- 263 Fischmeister, R., Castro, L., Abi-Gerges, A., Rochais, F. & Vandecasteele, G. Species- and tissue-dependent effects of NO and cyclic GMP on cardiac ion channels. *Comparative biochemistry and physiology. Part A, Molecular & integrative physiology* **142**, 136-143, doi:10.1016/j.cbpb.2005.04.012 (2005).
- 264 Rivet-Bastide, M. *et al.* cGMP-stimulated cyclic nucleotide phosphodiesterase regulates the basal calcium current in human atrial myocytes. *The Journal of clinical investigation* **99**, 2710-2718, doi:10.1172/JCI119460 (1997).
- 265 Madhani, M. *et al.* Phospholemman Ser69 phosphorylation contributes to sildenafil-induced cardioprotection against reperfusion injury. *American journal of physiology. Heart and circulatory physiology* **299**, H827-836, doi:10.1152/ajpheart.00129.2010 (2010).
- 266 Liu, L. & Askari, A. Beta-subunit of cardiac Na⁺-K⁺-ATPase dictates the concentration of the functional enzyme in caveolae. *American journal of physiology. Cell physiology* **291**, C569-578, doi:10.1152/ajpcell.00002.2006 (2006).
- 267 Liu, L. *et al.* Role of caveolae in signal-transducing function of cardiac Na⁺/K⁺-ATPase. *American journal of physiology. Cell physiology* **284**, C1550-1560, doi:10.1152/ajpcell.00555.2002 (2003).
- 268 Tian, J., Gong, X. & Xie, Z. Signal-transducing function of Na⁺-K⁺-ATPase is essential for ouabain's effect on [Ca²⁺]_i in rat cardiac myocytes. *American journal of physiology. Heart and circulatory physiology* **281**, H1899-1907 (2001).
- 269 Warriar, S. *et al.* Beta-adrenergic- and muscarinic receptor-induced changes in cAMP activity in adult cardiac myocytes detected with FRET-based biosensor. *American journal of physiology. Cell physiology* **289**, C455-461, doi:10.1152/ajpcell.00058.2005 (2005).
- 270 Horackova, M. & Byczko, Z. Differences in the structural characteristics of adult guinea pig and rat cardiomyocytes during their adaptation and maintenance in long-term cultures: confocal microscopy study. *Experimental cell research* **237**, 158-175, doi:10.1006/excr.1997.3775 (1997).

- 271 Xiang, Y. K. Compartmentalization of beta-adrenergic signals in cardiomyocytes. *Circulation research* **109**, 231-244, doi:10.1161/CIRCRESAHA.110.231340 (2011).
- 272 Baillie, G. S. *et al.* beta-Arrestin-mediated PDE4 cAMP phosphodiesterase recruitment regulates beta-adrenoceptor switching from Gs to Gi. *Proceedings of the National Academy of Sciences of the United States of America* **100**, 940-945, doi:10.1073/pnas.262787199 (2003).
- 273 Beca, S. *et al.* Phosphodiesterase type 3A regulates basal myocardial contractility through interacting with sarcoplasmic reticulum calcium ATPase type 2a signaling complexes in mouse heart. *Circulation research* **112**, 289-297, doi:10.1161/CIRCRESAHA.111.300003 (2013).
- 274 Malecot, C. O., Bers, D. M. & Katzung, B. G. Biphasic contractions induced by milrinone at low temperature in ferret ventricular muscle: role of the sarcoplasmic reticulum and transmembrane calcium influx. *Circulation research* **59**, 151-162 (1986).
- 275 Jurevicius, J., Skeberdis, V. A. & Fischmeister, R. Role of cyclic nucleotide phosphodiesterase isoforms in cAMP compartmentation following beta2-adrenergic stimulation of ICa,L in frog ventricular myocytes. *The Journal of physiology* **551**, 239-252, doi:10.1113/jphysiol.2003.045211 (2003).
- 276 Yan, C., Miller, C. L. & Abe, J. Regulation of phosphodiesterase 3 and inducible cAMP early repressor in the heart. *Circulation research* **100**, 489-501, doi:10.1161/01.RES.0000258451.44949.d7 (2007).
- 277 Lohmann, S. M., Fischmeister, R. & Walter, U. Signal transduction by cGMP in heart. *Basic research in cardiology* **86**, 503-514 (1991).
- 278 Zoccarato, A. *et al.* Cardiac Hypertrophy Is Inhibited by a Local Pool of cAMP Regulated by Phosphodiesterase 2. *Circulation research* **117**, 707-719, doi:10.1161/CIRCRESAHA.114.305892 (2015).
- 279 Song, J. *et al.* Overexpression of phospholemman alters contractility and [Ca(2+)](i) transients in adult rat myocytes. *American journal of physiology. Heart and circulatory physiology* **283**, H576-583, doi:10.1152/ajpheart.00197.2002 (2002).

7. Acknowledgements

It was a great honor and absolute pleasure to work with my supervisor and excellent guide Prof. Viacheslav Nikolaev, who supported and encouraged me giving best strategies throughout this exciting project. I would also like to thank him for giving me opportunities to develop my own ideas and motivating me with alternative experimental approaches. I very much appreciate having you as mentor during the past three years, Slava.

I would like to express my sincere gratitude to all members of my thesis committee, Prof. Blanche Schwappach, Prof. Walter Stühmer and Prof. Michael Shattock for inspiring thoughts about my work and vivid discussions in the time of our committee meetings. I am very grateful to Prof. Dörthe Katschinski and Prof. Susanne Lutz for accepting to be on my examination board and commenting on my thesis.

Part of the ideas for this dissertation stem from my co-supervisor Prof. Michael Shattock, whose enthusiasm always gave me the strength at the right time and made me learn and profit from my mistakes. It was an extremely enriching experience to work with him and his colleagues. I would like to address my genuine gratitude to him, Dr. Davor Pavlovic and Dr. Andrii Boguslavskyi at the Rayne Institute for all the support through the 'London-phase' of my project. At this point, I would also like to extend many thanks to Dr. William Fuller and Dr. Jacqueline Howie for their advice and assistance in generating the Rb-data in Dundee.

I am gratefully indebt to Prof. Julia Gorelik and Dr. Peter Wright for their cooperation and huge help in producing valuable MI-data.

I owe very special thanks to my teammates; Karina Schlosser for excellent technical support and always an open ear for me, as well as Tobias Goldak without whose help most of the experiments would not be possible. Julia Sprenger, Ruwan Perera and Konrad Götz were the best colleagues and friends one could imagine during my PhD time, thank you all for warmly welcoming me and helping me in all kinds of problems.

I surely want to thank the 'IRTG1816 family' and all its members, the administrative staff as well as each student. We shared so many unforgettable moments during the retreats, lunches and numerous events which gave me much more reason to think that 'research can be fun'. Therefore I would like to thank especially Prof. Dörthe Katschinski for making the IRTG possible.

Finally, I would like to say that I am extremely lucky in having such wonderful parents and sisters who were so patient and have supported me in every way possible. I would like to thank my family and my husband Mahmut for their endless encouragements and for making every thesis related life circumstance easier.